Inhibitors of Apoptosis Proteins (IAPs) as Targets for Anti-Cancer Treatment

Thesis

Daniele Lecis

Degree in Biotechnology

Inhibitors of Apoptosis Proteins (IAPs) as Targets for Anti-Cancer Treatment

This thesis is presented to

The Open University for the Degree of Doctor of Philosophy

Discipline: Life and Biomolecular Sciences

Date of submission: February, 2015

Affiliated Research Centre:

Fondazione IRCCS Istituto Nazionale dei Tumori, Milan (Italy)

Director of studies: Dr. Domenico Delia

External supervisor: Prof. Henning Walczak

DATE of SUBMISSION: 21 JANUARY 2015
DATE of AWARD: 27 APRIL 2015

ProQuest LLC.
789 East Eisenhower Parkway
P.O. Box 1346
Ann Arbor, MI 48106 – 1346

TABLE OF CONTENTS

1. ABSTRACT

Smac mimetics (SMs) constitute a class of compounds that target the inhibitor of apoptosis proteins (IAPs) and enhance the cytotoxic activity of several drugs. In our work, we built and characterized a library of about 140 SMs and focused on SM83 due to its high affinity for the targets, cytotoxic activity and good pharmacokinetic profile. *In vivo*, SM83 reduced in monotherapy the primary tumor growth of two triple negative breast cancer xenografts. Furthermore, SM83 treatment, alone or in combinations with TRAIL-armed $CD34^{+}$cell, resulted in the reduction of spontaneous lung metastasis formation. Mechanistically, by depleting cIAP1, SM83 affects the expression of the tumor genes and inhibits the metastasis-promoting gene Snai2, thus preventing cancer cell motility.

Moreover, we tested SM83 as a standalone in ascites cancer models and described an *in vivo* anti-tumor effect against cancer cell lines that are intrinsically resistant to SM treatment *in vitro*. In the *in vivo* settings, SM83, in fact, triggered an inflammation event of the host, characterized by macrophage secretion of TNF, IL-1β and interferon-γ (IFNγ), and rapidly killed floating tumor cells within the ascites by a non-apoptotic mechanism. Of note, SM83 treatment caused the massive accumulation of neutrophils within the ascites and tumor nodules, which, however, was not responsible for cancer cell killing.

Finally, we described the capability of SM83 to enhance the cytotoxic activity of camptothecin especially in human epithelial cells expressing oncogenic KRAS. The increased sensitivity of these premalignant cells is caused by an ERK2-dependent up-regulation of NOXA. Of note, oncogenic KRAS fails to sensitize a panel of isogenic cancer cell lines with wild type and mutated KRAS, and we demonstrated that this unresponsiveness could be reverted by concomitant inhibition of AKT. Therefore, our

work suggests that the activation of AKT is capable of counterbalancing the potential pro-death stimulus triggered by oncogenic KRAS.

2. INTRODUCTION

2.1. The apoptotic machinery

Apoptosis is a form of cell death regulated by an evolutionarily conserved molecular program (Degterev and Yuan, 2008). It is a fundamental process in the development of multicellular organisms and, due to its pivotal role, the deregulation leads to a number of diseases (Favaloro *et al*, 2012). Apoptosis is triggered with high specificity and efficiency in physiological conditions to induce suicide of excessive or misplaced cells in order to allow the correct development of the tissues (Clarke, 1990). Moreover, cell death can be induced by a plethora of both intra- and extra-cellular insults such as oxidative stress, DNA damages and inflammation that, when irremediable, activate the apoptotic machinery (Wong, 2011).

2.1.1. Pathways involved in apoptosis regulation

The apoptotic pathway is commonly divided in extrinsic and intrinsic, according to whether the pro-death stimulus is originated from the microenvironment and soluble factors outside the cells or by intracellular faults, respectively (Fulda and Debatin, 2006; Galluzzi *et al*, 2012). Even though these pathways are tightly interlinked and controlled by many common mediators, nonetheless it is conventionally accepted that the extrinsic apoptosis is initiated by the interaction between the death ligands of the tumor necrosis factor (TNF) superfamily and their cognate receptors (Newsom-Davis *et al*, 2009). When sufficiently stimulated, several adaptor proteins are recruited in concert to the intracellular portions of the TNF-receptor (TNF-R) family members leading to the formation of the death inducing signaling complex (DISC) (Scaffidi *et al*, 1998; Sprick *et al*,

2000). This in turn activates the cysteine-dependent aspartate-directed proteases, or caspases, which are responsible for the execution of the apoptotic process by cleaving several substrates and finally resulting in cell dismantling. The DISC activates the apical caspase-8 and -10 (Barnhart *et al*, 2003; Dickens *et al*, 2012a; Ganten *et al*, 2004), which start the whole apoptotic process and are therefore called initiator caspases. These proteases then cleave other members of the same family that propagate the pro-death signal and are therefore called effector caspases (especially caspase-3 and -7). In a few cell types, the activation of the extrinsic pathway is sufficient to lead to cell death because caspase-8 activates enough caspase-3 to result in irreversible damage. These cells are usually referred to as "type I" cells (Barnhart *et al*, 2003; Jost *et al*, 2009). Contrarily, "type II" cells need the involvement of the mitochondria to efficiently activate apoptosis in a process often called mitochondrial amplification that is initiated by caspase-8-mediated cleavage of Bcl-2 homology domain 3 (BH3) interacting-domain death agonist (Bid) (Kantari and Walczak, 2011). Cleaved, or truncated (t), Bid then activates Bcl-2-associated X protein (Bax) and Bcl-2 homologous antagonist/killer (Bak), two pro-apoptotic Bcl-2 family members, which lead to mitochondrial outer membrane permeabilization (MOMP) (Green and Kroemer, 2004). This is considered a "point of no return" of programmed apoptosis. MOMP allows the release into the cytosol of the cytochrome c that, together with the initiator caspase-9 and apoptotic protease activating factor 1 (Apaf-1), forms the apoptosome (Dickens *et al*, 2012b; Reubold and Eschenburg, 2012), a pro-death platform leading again to caspase-3 and -7 activation (Li *et al*, 1997; Zou *et al*, 1997).

In absence of an extrinsic stimulus, mitochondrial death can be initiated directly by an intrinsic apoptotic event such as DNA damage, endoplasmic reticulum stress and

oxidative stress. Mitochondria therefore play a pivotal role in the apoptosis process and represent the site where cell fate is determined (Galluzzi *et al*, 2012). In fact, many anti- (Bcl-2, Bcl-xL, Mcl) and pro-apoptosis (Bim, p53 up-regulated modulator of apoptosis/PUMA and NOXA) proteins localize here and the balance between them strictly determines the final outcome (Ploner *et al*, 2008; Wong, 2011). A schematic view of the programmed cell death pathway is shown in figure 1.

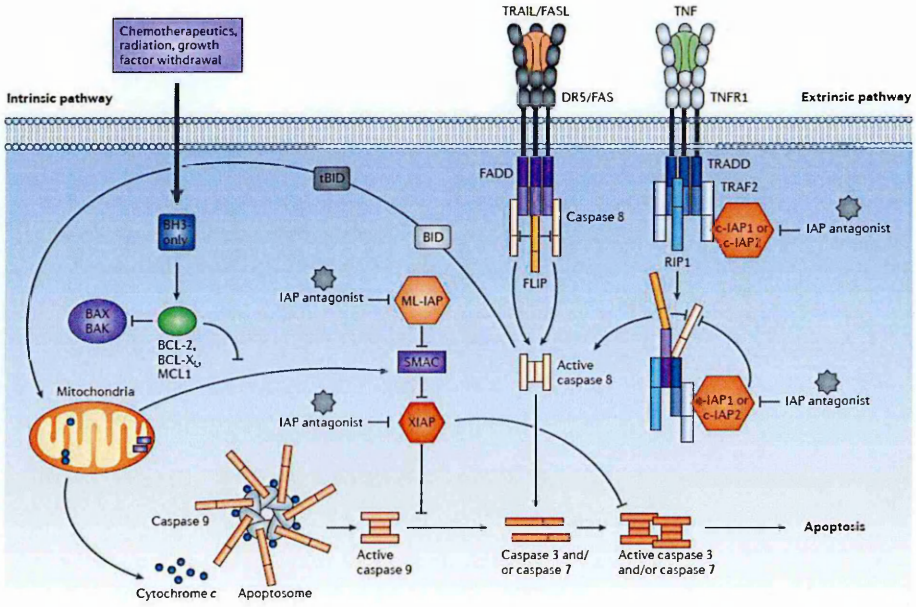

Figure 1. Overview of the diverse pathways resulting in cell death. (Fulda and Vucic, 2012). The apoptotic pathway can be initiated either by external or internal stimuli. The extrinsic pathway is triggered by death ligands that bind to the cognate receptors and cause the recruitment of the DISC. This complex is responsible for the activation of the initiator caspases, which in turn cleave and switch on the effector caspases. The extrinsic can converge to the intrinsic pathway by involving the mitochondria through tBid. Mitochondria are in fact rich in both pro- and anti-apoptotic proteins, whose balance determines cell fate. When mitochondria undergo MOMP, the apoptosome is formed and activates the initiator caspase-9 amplifying the apoptotic process. On the other hand, the intrinsic pathway can be stimulated by internal insults such as oxidative

stress, DNA damage and endoplasmic reticulum stress.

Despite the many diverse events that can activate programmed cell death and the different mechanisms involved, the consequence of an apoptotic process is extremely similar in all settings. Caspases in fact proteolytically cleave a number of substrates including the nuclear lamin, inhibitor of caspase activated DNase (ICAD) and especially poly-ADP ribose polymerase (PARP), which, when cleaved, is universally exploited as a marker for accomplished apoptosis (Nosseri *et al*, 1994). Typical morphological changes follow these biochemical events and include blebbing, cell contraction, nuclear fragmentation, chromatin condensation and chromosomal DNA fragmentation as shown in figure 2 (Degterev and Yuan, 2008). These features can be exploited to distinguish apoptotic cells by the ones dying from diverse types of death such as necrosis, necroptosis and autophagy (Degterev and Yuan, 2008; Galluzzi *et al*, 2015).

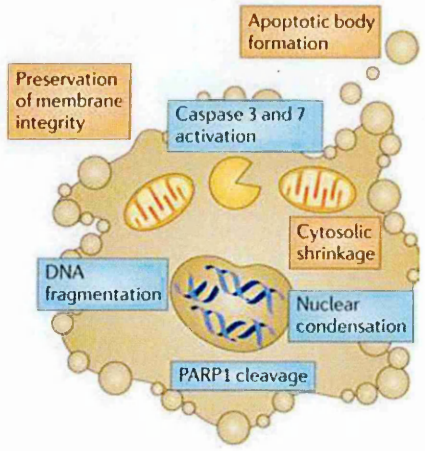

Figure 2. Morphological features of the apoptotic cells. Modified from Lamkanfi, 2011. When cells undergo an apoptotic process caused by activation of effector caspases, they are characterized by common morphological features such as DNA fragmentation, cell shrinkage, nuclear condensation and formation of apoptotic bodies. Cleavage PARP is commonly used as marker of apoptosis.

2.1.2. Role of apoptosis in cancer

Due to its crucial role in the control of several aspects of cell life, aberrant regulation of apoptosis can lead to numerous diseases. In particular, pathological resistance to apoptosis is a hallmark of cancer cells (Hanahan and Weinberg, 2011; Igney and Krammer, 2002) and a main issue in clinical treatment (Fulda and Vucic, 2012), as traditional chemotherapeutic compounds work by inducing cancer cell death. Unfortunately, malignant cells develop many mechanisms which can prevent the apoptotic process at several steps, prolong cancer cell lifespan (Lehman *et al*, 1993) and protect cancer cells from an unfavorable environment (Fernandez *et al*, 2000) characterized by low oxygen content (Maione *et al*, 2012), nutrients and poorly vascularized. Increased resistance to death also results in genetic instability and the accumulation of gene mutations caused by aberrant cell cycle checkpoints (Bishop *et al*, 2000). This, together with the capacity to grow in the absence of growth factors and anchorage to the extracellular matrix (ECM), the ability to survive without hormones and evade from the immune surveillance, supports tumor progression and the spread of the primary tumors by metastasis to distal organs (Liu *et al*, 2006; Yawata *et al*, 1998) and at the same time frustrates cancer treatment.

As already mentioned, mitochondria play a pivotal role in the apoptosis pathway and it is therefore not surprising that cancer cells are characterized by aberrant expression of many apoptosis-related mitochondrial proteins especially belonging to the Bcl-2 family members (Figure 3). These can be divided in anti-apoptotic proteins (Bcl-2, Bcl-xL, Bcl-W, Mcl-1 and A1) that display sequence homology in all BH1-BH4 domains, promote cell

survival and are over-expressed in about half of the tumors (Tekedereli *et al*, 2013), and pro-apoptotic factors. The latter are divided in multidomain, such as Bax and Bak, and BH3-only proteins, which are further divided in activators of Bax/Bak, i.e. Bim and Bid, and sensitizers that neutralize the effect of the anti-apoptosis members (Lomonosova and Chinnadurai, 2008). This is the case, for example, of Bcl2-associated agonist of cell death (Bad), Bcl-2-interacting killer (Bik), Bcl-2-modifying factor (Bmf), NOXA, and Puma, which are often down-regulated or aberrantly controlled in tumors.

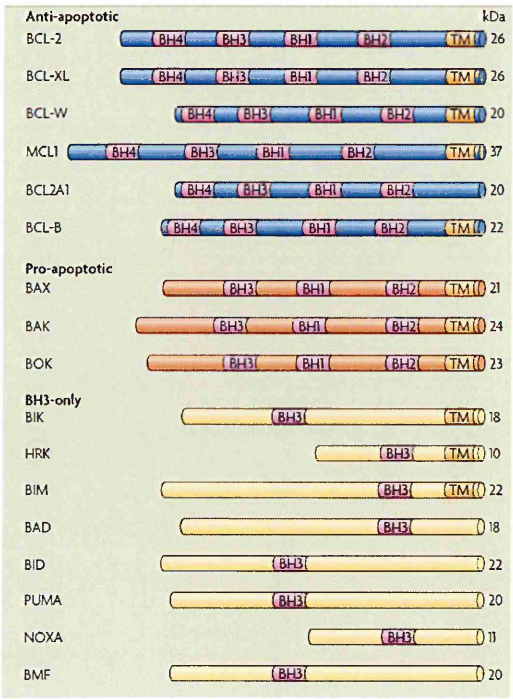

Figure 3. Members of the Bcl-2 family. (Taylor *et al*, 2008)**.** Bcl-2 family members are divided in anti-apoptotic proteins characterized by the presence of all BH1-BH4 domains, pro-apoptotic multi-domain and BH3-only proteins. The latter are further divided in activators of Bax/Bak and sensitizers that neutralize the anti-apoptotic Bcl-2 members.

Receptors belonging to the TNF-R superfamily (TNF-RS) display an important function in cancer surveillance (Cretney *et al*, 2002; Finnberg *et al*, 2008; Grosse-Wilde *et al*, 2008), but are often de-regulated in cancer cells. Moreover, decoy receptors unable to transmit

the death signal are also present and could compete with the other receptors, likely sequestering the ligands and therefore protecting cells from the pro-death stimuli (Riccioni *et al*, 2005). Interestingly, many cancer cells express normal and even higher levels of death receptors, but are still resistant to death-ligand activation of apoptosis. This observation suggests the presence of further downstream resistance mechanisms. This is the case, for example, of cellular FLICE (FADD-like IL-1β-converting enzyme)-inhibitory protein (c-FLIP) that displays high homology with caspase-8 and competes with it for the intracellular receptor domains (Xiao *et al*, 2002). This event has been shown to protect cells from the extrinsic apoptotic pathway because caspase-8 cannot be activated anymore even in the presence of high levels of TRAIL, TNF and Fas, and apoptosis is therefore hindered. Moreover, it has been demonstrated that tumors also develop the capacity to exploit the presence of death receptors using their signaling to enhance the cancer cell tumorigenic features (Chopra *et al*, 2013; Fingas *et al*, 2010; Ishimura *et al*, 2006; Trauzold *et al*, 2006). For example, oncogenic KRAS has been shown to switch the pro-death stimulus of TRAIL-R into an inducer of cell migration and invasion (Hoogwater *et al*, 2010).

Importantly, tumor cells - through the mutation, amplification and over-expression of oncogenes - strongly activate some pro-survival pathways that can counterbalance the environmental or chemical pro-death signals. In accordance to this, the AKT/ phosphatidylinositol 4,5-bisphosphate 3-kinase (PI3K) and mitogen-activated protein kinases (MAPK) pathways are often triggered by activating mutations (Cancer Genome Atlas Network, 2012; Wood *et al*, 2007) or continue stimulation of up-stream receptors such as the epidermal growth factor (EGF)-receptor (EGFR) (Yarom and Jonker, 2011). In this way, cancer cells switch off the pro-death cascades and trans-activate several genes

that promote tumorigenesis.

The nuclear factor kappa-light-chain-enhancer of activated B cells (NF-kB) pathway is usually activated in tumors and controls the transcription of many genes that increase cancer aggressiveness and favor cell survival. Cytokines and chemokines (Shakhov *et al*, 1990), cell adhesion molecules (Bunting *et al*, 2007), stress response genes (Xu *et al*, 2007), cell receptors (Thornburg and Raab-Traub, 2007), growth factors (Au *et al*, 2005), ligands (Saha *et al*, 2006) and regulators of apoptosis (Kreuz *et al*, 2001; Stehlik *et al*, 1998; You *et al*, 1997) are all NF-kB targets. In our work, we focused on the inhibitor of apoptosis proteins (IAPs), which both regulate and are targets of the NF-kB pathway as well as prevent apoptosis.

2.2. The inhibitor of apoptosis protein (IAP) family

All human IAP members are characterized by the presence of a conserved region within their sequence with high homology to baculovirus proteins (Duckett *et al*, 1996). As baculoviruses exploit these domains to block caspases and thus prevent the apoptotic cascade triggered by the host cells (Crook *et al*, 1993), IAPs were originally considered mainly apoptosis negative regulators. Nonetheless, later works have clearly shown that this definition is extremely simplistic as IAPs control several cell features and mechanisms (Rothe *et al*, 1995), whilst their effect on caspases is only a prerogative of 2-3 members of the family and probably is important in limited settings (Choi *et al*, 2009; Eckelman *et al*, 2006).

2.2.1. IAPs and their conserved domains

So far, eight members of the IAP family have been identified (Srinivasula and Ashwell, 2008) according to the presence of one or three conserved baculoviral IAP repeat (BIR) domains of about 70 aminoacids (Figure 4), important for protein-protein interactions and homologous to the baculoviral domains. The BIR domains can be classified into two types, I and II, where only type II can interact to caspases, while type I is responsible for the binding with other proteins such as TNF-R-associated factor (TRAF) 1 and 2 (Gyrd-Hansen and Meier, 2010). Type II BIRs display a conserved groove that can be occupied by the IAP binding motif (IBM). This sequence is composed by a tetramer that is conserved not only in caspases, but also in the IAP antagonist second mitochondria-derived activator of caspases (SMAC) (Srinivasula *et al*, 2001). Among the IAPs, only X-linked IAP (XIAP) is considered a direct inhibitor of caspases and it has been shown to interact with caspase-9 through its BIR3 domain, preventing its activation, whilst it sequesters both activated caspase-3 and -7 in the region containing the BIR2 and the upstream linker region (Chai *et al*, 2001; Datta *et al*, 2000; Riedl *et al*, 2001). However, the anti-caspase activity of other IAPs, such as cellular IAP1 (cIAP1) and cIAP2, is still controversial. Some groups suggested their capability to regulate caspases by favoring their degradation (Choi *et al*, 2009), but the evidence of a physical interaction with them is still lacking.

Besides the BIR domains, XIAP, cIAP1, cIAP2, Livin and insulin-like peptide 2 (ILP2) also display a really interesting new gene (RING) domain endowed with E3 ubiquitin-ligase activity. Through their RINGs, IAPs ubiquitinate numerous substrates (Cheung *et al*, 2008) causing not only their proteasome-dependent degradation, but also regulating several signaling cascades (Gerlach *et al*, 2011). Caspases themselves are substrates of some IAPs that could therefore block apoptosis also by reducing their levels (Choi *et al*, 2009; Gillissen *et al*, 2013; Suzuki *et al*, 2001). Finally, cIAP1 and cIAP2 contain a caspase

recruitment domain (CARD), whose role has not been fully understood yet, but seems to be responsible for the inhibition of RING dimerization and prevention of cIAP1 activation (Lopez *et al*, 2011).

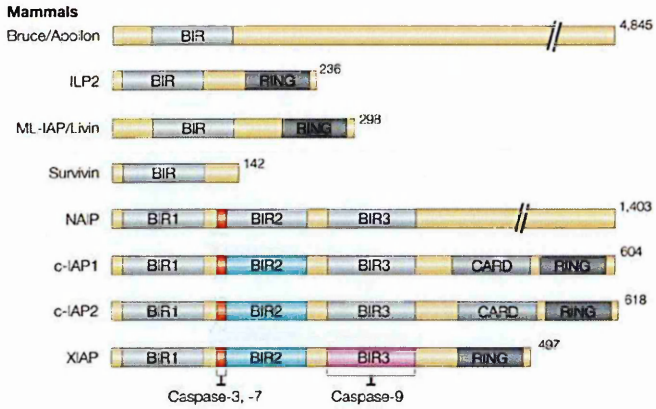

Figure 4. Members of the IAP family and their conserved domains. Modified from Riedl and Shi, 2004. The IAP family is constituted by 8 members, characterized by the presence of a conserved BIR domain.

2.2.2. The regulatory activity of IAPs in signaling cascades: MAPK and NF-kB

IAPs, and in particular cIAP1 and cIAP2, have been described as components of the TNF-R complex where they contribute to TNF signaling (Haas *et al*, 2009). The TNF-R superfamily members are characterized by the presence of a cysteine rich domain (CRD), repeated up to six times in the extracellular region of these transmembrane receptors (Branschadel *et al*, 2010).

In the intracellular region, some of them (e.g. TNF-R1, CD95, TRAIL-R1 and TRAIL-R2) display the conserved death domains (DD) (Lavrik *et al*, 2005) necessary for death induction (Figure 5). Despite what the name would suggest, the death receptors such as TNF-R1 usually induce gene transcription more readily than cell death (Wajant *et al*, 2003), by activating the MAPK pathway and stimulating the activity of the transcription

factors belonging to the NF-κB family (Varfolomeev *et al*, 2012). These pathways result in the rapid expression of several pro-survival proteins such as cFLIP (Kreuz *et al*, 2001) that counteract the possible killing effect of TNF. Accordingly, TNF often becomes toxic when cells are stimulated by this death ligand in the presence of inhibitors of protein translation (Autelli *et al*, 2005) such as cycloheximide (CHX).

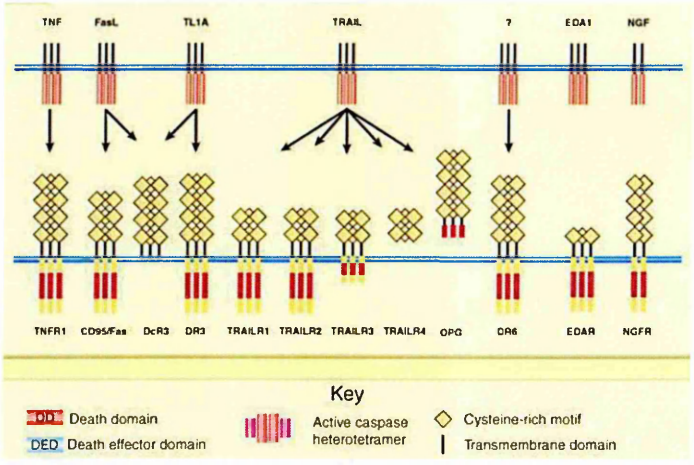

Figure 5. Death ligands and death receptors. Modified from Lavrik *et al*, 2005. The death ligands bind to and stimulate several receptors, which are constituted by a cysteine-rich extracellular domain. The vast majority is also characterized by cytosolic death domains. The few receptors that lack the DD are unable to trigger an apoptotic event after ligand stimulation.

Mechanistically, when TNF binds to TNF-R1, the receptors form a trimer and its intracellular portion recruits the receptor interacting protein 1 (RIP1) and TNF-R1-associated death domain (TRADD), which in turn serves as a scaffold for TRAF2 bound to cIAP1 and cIAP2 (Emmerich *et al*, 2011; Walczak, 2011). The latter IAPs catalyze the formation of several ubiquitin chains that further stabilize the signaling receptor complex and allow the recruitment of the NF-kB essential modulator (NEMO) and inhibitor of NF-kB (IkB) kinase (IKK), and TNF-associated kinase (TAK)/ transforming growth factor (TGF)-beta-activated kinase 1-binding protein (TAB) complexes, triggering the activation of

canonical NF-kB and MAPK pathways, respectively (Figure 6).

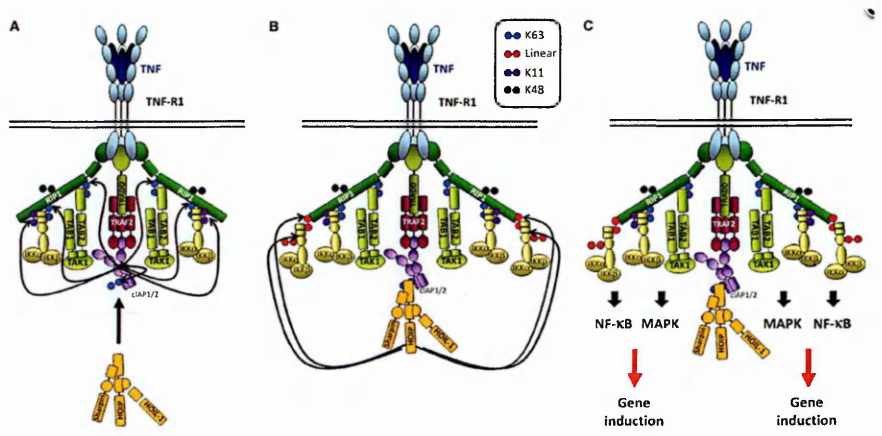

Figure 6. Model of the tumor necrosis factor-receptor signaling complex. (Walczak, 2011). The binding of TNF to TNF-R1 causes the trimerization of the receptor that recruits RIP1 and TRADD through its intracellular portion. TRADD in turn serves as a scaffold for TRAF2 that is bound to cIAP1 and cIAP2. The IAPs then catalyze the formation of several ubiquitin chains that stabilize the complex and allow the recruitment of NEMO and IKK, and TAK/TAB complexes, activating canonical NF-kB and MAPK pathways. cIAP1 and cIAP2 also favor the recruitment the receptor of HOIL-1, HOIP and Sharpin which prolong NF-kB activation.

Another complex made of heme-oxidized IRP2 ubiquitin ligase 1 (HOIL-1), HOIL-1-interacting protein (HOIP) and SHARPIN, and called linear ubiquitin chain assembly complex (LUBAC) is recruited to the TNF-R1 complex thanks to the ubiquitin chains formed by cIAP1 and cIAP2. This event is not essential for TNF-mediated signaling, but it strengthens and prolongs its effect (Gerlach *et al*, 2011; Ikeda *et al*, 2011; Tokunaga *et al*, 2011).

2.2.3. NF-kB: canonical and non-canonical pathways

As described above, IAPs regulate various signaling pathways that result in the transactivation of a plethora of genes. Accordingly, XIAP, cIAP1 and cIAP2 regulate the

activity of the transcription factors belonging to the NF-kB pathway (Zarnegar *et al*, 2008). Five members of this family are known: RelA (p65), RelB, CRel, NF-kB1 (p105/p50) and NF-kB2 (p100/p52). NF-kB1 and NF-kB2 do not contain a transactivation domain and therefore need to interact with the other members of this family to regulate the transcription of target genes. The NF-kB pathway is generally divided into "canonical" and "non-canonical" depending on the stimulus that causes the initial trigger and the mediators involved (Perkins, 2007).

The best characterized inducer of the canonical pathways is TNF that, upon binding to the TNF-R1, mediates the formation of complex I made of TRADD, TRAF2, TRAF5, cIAP1 and cIAP2 (Emmerich *et al*, 2011). In this setting, cIAP1-mediated ubiquitylation of the diverse components, in particular of RIP1 (Bertrand *et al*, 2008), allows the recruitment of the LUBAC, of the TAK1/TAB2/TAB3 and IKKγ/IKKα/IKKβ complexes. IKKβ is responsible for the ubiquitination and degradation of the IkB resulting in the release of NF-kB, which can then move from the cytosol to the nucleus where it trans-activates the target genes. In this process, cIAP1 and cIAP2 are fundamental for the up-stream activation of this pathway and consequently protect cells from the cytotoxic effect of TNF.

The non-canonical NF-kB pathway is mainly stimulated by CD40L, B cell activating factor (BAFF) and (TNF-related weak inducer of apoptosis) TWEAK, and relies on the apical NF-κB inducing kinase (NIK), which in turn activates IKKα (Demchenko *et al*, 2010; Razani *et al*, 2010). IKKα then is responsible for NF-kB2 phosphorylation that causes its ubiquitination and proteasome-mediated processing into the mature p52 form. Importantly, NIK levels are constitutively kept low by continuous ubiquitination by cIAP1 and cIAP2 (Zarnegar *et al*, 2008), with consequent degradation. Contrary to the canonical

one, this pathway is therefore inhibited by cIAP1 and cIAP2 (Figure 7).

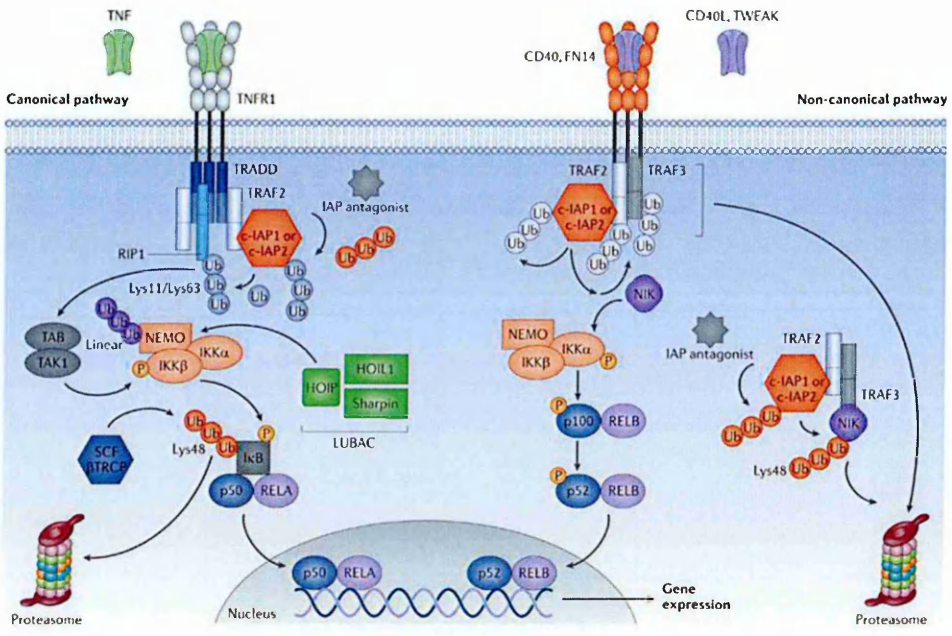

Figure 7. Schematic representation of the canonical and non-canonical NF-kB pathways. (Fulda and Vucic, 2012). The NF-kB pathway is usually divided in canonical and non-canonical. The canonical one is stimulated by several death ligands such as TNF and is promoted by the assembly of a cytosolic complex on the receptors. TRADD, RIP1 and TRAF2 are recruited and allow the activity of cIAP1 and 2, which in turn produce a net of ubiquitins that stabilize the complex and allow the signaling mediated by NEMO/IKKs which phosphorylate NF-kB1, which is then activated and moves to the nucleus. Here, it trans-activate the target genes by interacting with other members of the NF-kB family. The involvement of the LUBAC can enhance and stabilize this signaling pathway. The non-canonical pathway is activated by other ligands such as BAFF, CD40L and TWEAK, and it is promoted by the apical kinase NIK, which phosphorylates and activates IKKα. The expression of the target genes is mainly controlled by p52 and RelB.

2.2.4. IAPs in the regulation of immunity

The first response of the immune system to infection and tissue injury is mediated by the innate immune pattern recognition receptors (PRRs) superfamily members, which

sense various stress signals and activate the inflammatory response. In fact, these receptors detect the presence of conserved microbial components and activate the MAPK and NF-kB signaling pathways, which lead to the transcription of various mediators of inflammation (e.g. cytokines, chemokines, adhesion molecules, acute phase proteins and antimicrobial peptides). cIAP1, cIAP2 and XIAP, by their ubiquitinating activity, have been shown to regulate these pathways both at the receptor and downstream levels, thus regulating nucleotide-binding oligomerization domain-containing protein (NOD)1/2, toll-like receptors (TLRs), retinoic acid-inducible gene 1 (RIG-I) and pro-inflammatory cytokines signaling, including TNF (Estornes and Bertrand, 2014). Of note, at the site of infection, TNF further modulates the inflammatory response by stimulating the production of other cytokines and chemokines and cells of the immune system.

2.3. IAPs and their role in cancer

Due to their capability to promote resistance against cell death and control many survival pathways, it is not surprising that several cancer types have been reported to aberrantly express IAPs, which could also play a role in patients' prognosis (Che *et al*, 2012; Hundsdoerfer *et al*, 2010; Miura *et al*, 2011; Yang *et al*, 2012). IAPs are therefore considered potential targets in clinical treatment and much effort has been put into the development of IAPs-antagonizing small compounds (Fulda, 2014b).

2.3.1. Aberrant expression of IAPs in cancer cells

IAPs are over-expressed in many cancer types, where they often play a role in progression and resistance to therapy, and in some instances affect prognosis. This is the case, for example, of acute myeloid leukemia (AML), in which lower XIAP levels

correlate with longer survival (Tamm *et al*, 2000). In contrast, other works showed no correlation between XIAP expression and remission rate and overall survival (Carter *et al*, 2003). Indeed, over-expression of both XIAP and survivin was reported to be associated with a particularly poor prognostic impact and the same conclusion was made by a three-gene expression signature including cIAP2 that accurately predict poor overall survival (Ibrahim *et al*, 2012). Moreover, high levels of XIAP, cIAP1 and cIAP2 are found in chronic myeloid leukemia (CML), while melanoma-IAP (ML-IAP) and XIAP high levels have been related to poor prognosis and worse response to therapy in acute lymphocytic leukemia (ALL) (Fulda, 2014a).

Importantly, many tumor types often bear the 11q21-q23 amplification, in which both cIAP1 and cIAP2 are found. This is the case, for example, of esophageal carcinoma, hepatocellular carcinoma, cervical cancer, liver cancer, medulloblastoma, glioblastoma, non-small-cell lung cancer (NSCLC), small cell lung cancer and pancreatic cancer in which these IAPs are therefore expressed at high levels. In clear contrast, SMAC and XIAP-associated factor 1 (XAF-1), two well-characterized IAP-antagonizing proteins, are often down-regulated in cancer and their levels inversely correlate with prognosis (Fulda, 2014a).

2.3.2. Mutations affecting members of the IAP family

Despite the increased expression of IAPs due to gene amplification, active trans-activation and post-translational events, the IAPs are sometimes found mutated in tumors. For example, the (11;18)(q21;q21) translocation occurs frequently in mucosa-associated lymphoid tissue (MALT) lymphoma. This event results in the fusion of the BIR domains of cIAP2 with the paracaspase MALT1 (Rosebeck *et al*, 2011). The cIAP2–MALT1

fusion protein constitutively activates the NF-κB signaling pathway in this type of tumor (Darding *et al*, 2011). Moreover, in multiple myeloma (MM), a tumor type characterized almost always by the aberrant activation of the NF-kB pathway (Annunziata *et al*, 2007; Demchenko *et al*, 2010), cIAP1 and cIAP2 are often deleted, resulting in the constitutive activation of the non-canonical NF-κB pathway through stabilization of NIK.

2.3.3. Controlling migration and invasion: the effect on metastasis

IAPs are therefore responsible for the increased tumor aggressiveness by protecting cancer cells from apoptosis, modulating the microenvironment through the expression of cytokines and aberrantly increasing the activation of many pro-survival pathways. Altogether, these mechanisms promote tumor growth in harsh conditions and hamper therapy efficacy. Moreover, growing evidence shows that IAPs control migration, invasion and metastasis (Mehrotra *et al*, 2010), even if data are still controversial. On the one hand, XIAP has been reported to increase cell motility in a caspase-independent manner by physical interaction via its RING domain with the Rho guanosine diphosphate (GDP) dissociation inhibitor (RhoGDI). Wild type, but not H467A-mutated, XIAP promotes cell migration and it is associated to reduced RhoGDI activity as well as enhanced polymerization of actin (Liu *et al*, 2012). XIAP was reported to modulate also the activities of Raf-1, focal adhesion kinase (FAK) and FAK-related non kinase, stabilizing the α(5)-integrin-associated focal adhesion complex (Kim *et al*, 2010). Finally, XIAP protects cells from anoikis and, in complex with survivin, promotes cancer cell invasion and eventually metastasis by engaging an NF-kB-dependent expression of fibronectin (Mehrotra *et al*, 2010), without the morphological features of epithelial to mesenchymal transition (EMT).

Furthermore, high levels of cIAP1 have been related to increased motility, even if in

normal conditions its CARD domain inhibits cell migration by preventing RING dimerization (Lopez *et al*, 2011). Finally, the targeting of IAP proteins by means of specific compounds was shown to interfere with TRAIL-mediated invasion and metastasis in a cholangiocarcinoma model (Fingas *et al*, 2010).

In clear contrast, a number of other studies support the notion that IAPs can even suppress migration and invasion. Accordingly, XIAP, cIAP1, cIAP2 and ML-IAP were reported to cause the degradation of Raf-1 (Dogan *et al*, 2008) and Ras related C3 botulinum toxin substrate (Rac1), thereby modulating the MAPK signaling pathway and cell migration. Consistently, down-regulation of XIAP or cIAP1 resulted in stabilization of Rac1 and increased cell motility associated with elongated morphology (Oberoi *et al*, 2011; Tchoghandjian *et al*, 2013).

2.4. Targeting IAPs: Smac mimetics

The IAP family members play an important role in cancer progression and treatment failure and are therefore considered an attractive target for cancer chemotherapy (Fulda, 2014b). The observation that the XIAP natural antagonist, SMAC, interacts with the BIR domains of the IAPs through the defined region IBM inspired a class of protein-protein interaction (PPI) inhibitors called Smac mimetics (SMs), designed to target especially the BIR3 of XIAP (Figure 8).

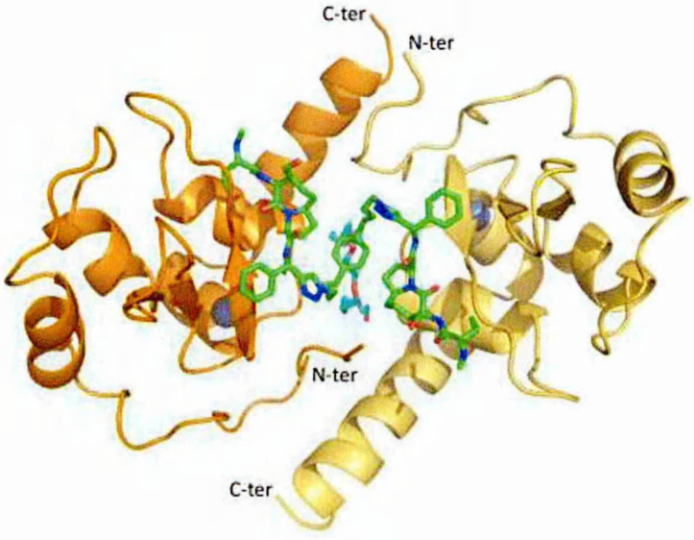

Figure 8. X-Ray structure of XIAP BIR3 dimer in complex with SM83. Modified from Cossu *et al*, 2012. SMs target the BIR domain of XIAP by interacting with a conserved groove present in the BIR domains of several IAPs.

2.4.1. A physiological (X)IAP natural antagonist: SMAC

SMAC is a pro-apoptotic protein, which is usually localized within the mitochondrial membranes. Upon an apoptotic stimulus, SMAC is released with cytochrome c into the cytosol (Du *et al*, 2000) where it undergoes maturation through dimerization and cleavage of the N-terminal region of 55 aminoacids, which allows the exposures of the tetrapeptide IBM constituted by the alanine-valine-proline-isoleucine (AVPI) sequence (Liu *et al*, 2000; Wu *et al*, 2000). This region can interact with the groove present in the BIR domains of the IAPs and in particular the BIR3 (Srinivasula *et al*, 2001), and to a lesser extent the BIR2, of XIAP, causing the displacement of caspase-3, -7 and -9, and therefore counteracting the anti-apoptotic function of the IAPs. Moreover, SMs were shown to reduce the levels of cIAP1 and cIAP2 (Petersen *et al*, 2007; Varfolomeev *et al*, 2007; Vince *et al*, 2007), but neither of XIAP nor Livin, by inducing their auto-ubiquitination followed by proteasomal-dependent degradation. Interestingly, SMAC also caused XIAP

ubiquitination, without affecting its levels (Yang and Du, 2004).

2.4.2. Targeting XIAP BIRs with SMAC-mimicking peptidic compounds

In an attempt to mimic the pro-apoptotic activity of SMAC, several groups have synthesized small synthetic peptides covering the first 7-8 aminoacids of the N-terminal region of matured SMAC (Fulda *et al*, 2002). These molecules were fused to cell-permeabilizing peptides and showed to be able to bypass the mitochondrial blockage and sensitize either *in vitro* and *in vivo* the cancer cells to TRAIL or chemotherapeutic drug treatments such as cisplatin, taxol, etoposide, paclitaxel and doxorubicin (Arnt *et al*, 2002; Yang *et al*, 2003). Later works have shown that the first 4 aminoacids are necessary and sufficient for the interaction with the BIR domains and that dimeric compounds are much more effective than the monomeric in targeting IAPs. Moreover, the aminoacid sequence was modified to increase the affinity towards the BIR domains (Li *et al*, 2004), focusing in particular on the BIR3 of XIAP. The resulting peptides interact with recombinant XIAP and displace caspases, and induce cell death in a caspase-dependent manner especially in combination with TRAIL.

2.4.3. Chemical modification of SMs: non-peptidic molecules

Having proved that small peptides mimicking the N-terminal region of SMAC can efficiently target IAPs, several groups modified the original peptidic sequence of the IBM to enhance the affinity for the target, permeability and pharmacological properties (Oost *et al*, 2004; Sun *et al*, 2004; Sun *et al*, 2006). For example, valine and proline were fused to form a scaffold constituted by a ring with increased rigidity (Sun *et al*, 2007), the alanine was modified by methylation to increase permeability (Sun *et al*, 2006) and several modifications were introduced to increase the molecular stability while containing

the molecular weight. Importantly, two classes of compounds were designed, monomeric (Seneci *et al*, 2009) and dimeric (Lecis *et al*, 2012), the latter synthesized by the chemical tethering of two AVPI-mimicking SMs.

Even though monomeric SMs were thought to be more "drug-like" due to their low molecular weight and thus respecting the "Lipinski's rules", dimeric SMs have been shown to be much more effective both *in vitro* and *in vivo*, killing sensitive cancer cells with much lower EC50s (Fulda, 2014b). The reason for this enhanced activity has not been fully understood yet, but it is speculated that dimeric compounds might interact simultaneously with two BIR domains within the same XIAP molecule (Cossu *et al*, 2009b; Cossu *et al*, 2012), therefore stabilizing the interaction with the target and displacing caspases more efficiently. Furthermore, dimeric compounds are more effective in causing the depletion of cIAP1 and cIAP2 (Varfolomeev *et al*, 2007). The vast majority of IAP-antagonizing peptide-mimetics have been designed to target XIAP BIR3 (Figure 9), but in few cases combinatorial library screenings were performed to select BIR2-specific compounds that showed *in vitro* and *in vivo* activity (Schimmer *et al*, 2004).

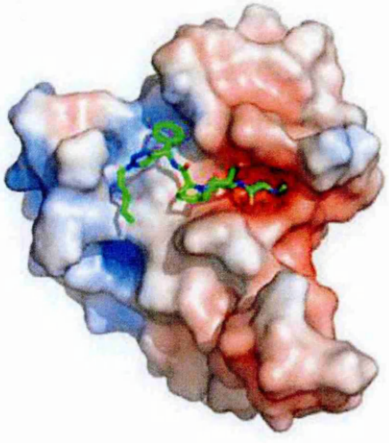

Figure 9. Model of SM83 interaction with the BIR3 groove of XIAP. Modified from Cossu *et al*, 2012. One residue of the dimeric SM83 compound enters the groove in the BIR domain of XIAP.

2.4.4. Mechanism of action of SM

As already mentioned, SMs were specifically designed to target XIAP and displace caspases, thus favoring the apoptotic cascade triggered by other compounds. SMs were therefore considered essentially as cancer cell sensitizers to chemotherapeutic drugs. Surprisingly, about 10-15% of cancer cell lines are efficiently killed *in vitro* by SMs as standalones (Petersen *et al*, 2007) with low nanomolar EC50s, depending on the molecules used. In 2007, three independent works showed that the cytotoxic effect of the SMs in monotherapy does not depend on their activity against XIAP, but it stems from a rapid SM-dependent depletion of cIAP1 and cIAP2 and subsequent autocrine TNF-mediated killing (Petersen *et al*, 2007; Varfolomeev *et al*, 2007; Vince *et al*, 2007). It was shown that cIAP1 and cIAP2 undergo a self-ubiquitination event after administration of different SMs, and this is followed by a proteasome-dependent degradation in a matter of a few minutes. SM interaction with cIAP1 and cIAP2 causes a conformational change (Figure 10) that allows cIAP1 dimerization and the exposure of the RING domain (Dueber *et al*, 2011; Feltham *et al*, 2011), which is normally inhibited by the CARD domain (Lopez *et al*, 2011). This event occurs in all treated cells, but in sensitive cancer cells it is sufficient to trigger a TNF-dependent apoptosis event. In fact, some cancer cell lines constitutively express high levels of TNF, which, after SM administration, is further increased. In fact, TNF is a target of the NF-kB pathway that, as already described, is regulated by cIAP1 and cIAP2. When these IAPs are depleted, NIK is stabilized and activates the non-canonical NF-kB pathways, causing a further increase of TNF expression (Varfolomeev *et al*, 2007). This ligand then stimulates the TNF receptors, which, in absence of cIAP1 and cIAP2, are no longer able to activate the NF-kB and MAPK pro-survival pathways and therefore recruit the formation of complex II, in which caspase-8 is

activated (Gaither *et al*, 2007). Studies on sensitive cell lines, such as the breast carcinoma MDA-MB231, the ovarian cancer SKOV3 and the rabdomyosarcoma Kym-1 demonstrated that caspase-8 silencing, IKK inhibition or blockage of TNF *de novo* expression and secretion can prevent SM toxicity (Varfolomeev *et al*, 2007).

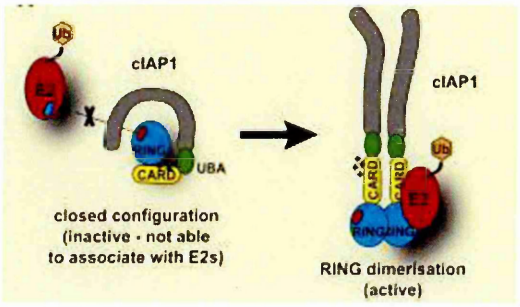

Figure 10. Model describing the conformational modification that occurs when cIAP1 is activated. (Lopez *et al*, 2011). The RING domain of cIAP1 is usually blocked through an intra-molecular interaction with the CARD domain. When a SM hits the BIR domain of cIAP1, it causes a rapid morphological modification that allows the dimerization of the RING with the same domain of another cIAP1 molecule, and its exposure and activation.

The majority of cell lines do not respond to SM administration in monotherapy and the reason for this resistance is not fully understood. It has been demonstrated that other pathways, such as the one controlled by PI3K can confer resistance to SM treatment and that cells can also acquire resistance (Petersen *et al*, 2010). In fact, when both cIAP1 and cIAP2 are depleted and the NF-kB pathway is activated, cIAP2 rebounds quickly because it is a target of the non-canonical NF-kB pathway. Importantly, upon SM treatment the degradation of cIAP2 was shown to be cIAP1-dependent (Darding *et al*, 2011). Therefore, after an initial effect on the cIAPs, cIAP2 is quickly replaced by newly-synthesized protein and, due to the absence of cIAP1, cannot be degraded anymore, conferring resistance and unresponsiveness to SMs (Darding *et al*, 2011). In fact, although less effective in

controlling some molecular pathways, cIAP2 however displays some common features with cIAP1 and redundant activities and its presence is sufficient to confer resistance to SM treatment.

Importantly, also cells that are extremely sensitive to SMs *in vitro*, often acquire resistance *in vivo*. Although this event has not been fully understood yet, the expression levels of leucine-rich repeats and immunoglobulin-like domains protein 1 (LRIG-1) could mediate it, at least in part (Bai *et al*, 2012). Interestingly, also the opposite effect can be observed *in vivo*, i.e. cells refractory to SM treatment *in vitro* become partially sensitive *in vivo* and SM administration results in the inhibition of primary tumor growth in animal xenografts (Lecis *et al*, 2013). Even in this case, the precise mechanisms have not been dissected, but it is likely that the cytokines expressed by the microenvironment might interact with the SMs becoming toxic for the tumor.

2.4.5. Regulation of the ripoptosome: decision between apoptosis and necroptosis

Exploiting SM-dependent depletion of cIAP1 and cIAP2, two independent groups described a novel platform, called ripoptosome (Feoktistova *et al*, 2011; Tenev *et al*, 2011), constituted by RIP1, Fas-associated protein with death domain (FADD), and caspase-8, which activates cell death independently of death receptor activation, contrary to complex II. The ripoptosome is inhibited by cIAP1, cIAP2 and cFLIP and can activate both caspase-dependent and -independent cell death (Vince *et al*, 2012). The latter is usually referred to as necroptosis and relies on RIP3 and mixed-lineage kinase domain-like protein (MLKL), and RIP1 kinase activity as its inhibitor necrostatin-1 can prevent it. Ripoptosome, depending on the cellular settings, can activate both apoptosis and

necroptosis, which mutually control each other (Dickens *et al*, 2012b; Oberst *et al*, 2011). Accordingly, chemical inhibition of caspases and in particular of caspase-8 can strongly activate a necroptotic event (Wu *et al*, 2011), especially in cells such as the macrophages (Muller-Sienerth *et al*, 2011). In fact, caspase-8 and RIP1 mutually inhibit each other as genetically demonstrated by the means of knock-out mice (Dillon *et al*, 2014).

2.4.6. Hybrid SMs

Dimeric Smac mimetics are usually synthesized as homodimeric compounds in which the same monomer is tethered by a chemical linker resulting in a symmetric molecule. In a few cases, molecules were modified in order to link the two monomers at different positions, therefore forming asymmetric molecules (Servida *et al*, 2010). Further studies have also been undertaken to establish the effect of different linkers on the efficacy of these compounds (Lecis *et al*, 2012).

Moreover, we and others have also produced heterodimeric compounds with the aim to link two different monomeric SMs, one highly affine for the BIR3 and the other with increased affinity for BIR2, in an attempt to stabilize the intramolecular interaction with two different BIR domains. Furthermore, to exploit the ubiquitinase activity of IAPs and target specific proteins to proteasomal degradation, SM compounds were also linked to all-trans retinoic acid (ATRA), a cellular retinoic acid binding protein (CRABP-II) ligand, in order to cause the ubiquitination and down-regulation of this receptor and result in the inhibition of cancer cell proliferation (Itoh *et al*, 2012). A similar approach was used to increase the delivery of IAP-antagonizing compounds to cancer cells. In this case, monomeric SMs have been linked to the sigma-2 ligand to target pancreatic and ovarian tumor (Garg *et al*, 2014; Hashim *et al*, 2014; Zeng *et al*, 2013), in which the sigma-2

receptor is over-expressed, or to integrin inhibitors. In both circumstances, the aim was to enhance the molecular uptake of the SM (Mingozzi *et al*, 2014). For this purpose, we recently described the conjugation of SMs with nano-conjugates (Seneci *et al*, 2014). Finally, in an attempt to enhance the cytotoxic activity, we have also linked a monomeric SM to procaspase activating compound (PAC)-1, a Zn chelator described as a direct activator of caspase-3 (our unpublished data). The idea is therefore to simultaneously activate the apoptotic machinery by direct activation of caspases and simultaneously prevent their inhibition by the IAPs.

2.5. SMs in anti-cancer treatment

Given the crucial role of IAPs in favoring aggressiveness of cancer and resistance to therapy, the discovery of SMAC-based compounds raised great enthusiasm in cancer therapy. As already mentioned SMs are very rarely cytotoxic in monotherapy and have therefore been tested in combination with a plethora of other drugs (Greer *et al*, 2011). Despite the fact that preliminary pre-clinical experiments showed little toxicity for non-transformed cells, *in vivo* experiments and the first clinical trials revealed some side-effects and unwanted toxicity caused especially by immune system activation and cytokine production (Amaravadi *et al*, 2011; Infante *et al*, 2014; Sikic *et al*, 2011). Much effort is thus currently being made to comprehend the mechanisms responsible for this toxicity and to possibly modify the molecules in order to prevent the undesired effects.

2.5.1. SMs in combination therapy

Since the description of the first SMs, they have been shown to enhance the activity of diverse compounds and potently activate apoptosis by blocking IAPs. Due to the

crucial role of IAPs in preventing TRAIL-mediated toxicity, the SMs were proposed particularly in combination with the death ligands belonging to the TNF family (Dai *et al*, 2009; Lecis *et al*, 2010; Lu *et al*, 2011; Metwalli *et al*, 2010; Vogler *et al*, 2009). Whereas TNF and FasL are not considered good candidates for clinical purposes due to systemic toxicity and acute hepatotoxicity respectively, great expectation was raised on the employment of TRAIL. In melanoma (Lecis *et al*, 2010), head and neck (Raulf *et al*, 2014), breast (Foster *et al*, 2009), pancreatic (Vogler *et al*, 2009) and many other cancer models, genetic and chemical inhibition of XIAP was shown to sensitize cells to TRAIL treatment, in some cases also employing mouse xenografts.

2.5.1.2. TRAIL and its application in anti-cancer treatment

TRAIL is a ligand of the TNF family, which can both activate apoptosis and trigger various signaling pathways by interacting with its cognate receptors TRAIL-R1/death receptor (DR4), TRAIL-R2/DR5. Moreover, three decoy receptors have been described TRAIL-R3/decoy receptor (DcR1), TRAIL-R4/DcR2 and the soluble osteoprotegerin (OPN) that bind TRAIL ligand but are unable to trigger apoptosis (Walczak, 2011). TRAIL seems to play a physiological role in controlling cancer, as knock-out (KO) of TRAIL-R promotes susceptibility to tumor and metastasis development (Cretney *et al*, 2002; Grosse-Wilde *et al*, 2008). TRAIL has been shown to kill cancer cells whilst sparing normal tissues (Walczak *et al*, 1999). Nonetheless, later work and the first clinical trials dampened the initial enthusiasm by reporting that TRAIL-based treatments have a very modest effect in curing tumors (Falschlehner *et al*, 2009; Yang *et al*, 2010).

Several hypotheses have been made to explain the limited efficacy *in vivo*. The first is that TRAIL has an extremely short half-life and it is therefore rapidly eliminated (Wang,

2008); the reaching of clinically active concentrations is therefore extremely arduous. Furthermore, soluble TRAIL (sTRAIL) seems to efficiently activate only the TRAIL-R1 (Muhlenbeck *et al*, 2000) and therefore its efficacy is reduced when this receptor is poorly expressed in cancer cells. To overcome these issues, many approaches have been proposed such as the design of modified TRAIL molecules or the use of agonist antibodies. First of all, TRAIL has been cloned with tags that increase its stability and allow its trimerization such as leucine zipper-TRAIL (lzTRAIL) (Ganten *et al*, 2004; Walczak *et al*, 1997) and isoleucine zipper TRAIL (izTRAIL) (Ganten *et al*, 2006). Stabilized complexes of ligands can in fact enhance the activation of the receptors both *in vitro* and *in vivo*. Moreover, several humanized agonist antibodies against TRAIL-R1 or TRAIL-R2 are currently tested in phase I/II clinical trials advanced solid tumors (Falschlehner *et al*, 2009).

Another method to increase the efficacy of TRAIL consists in the exploitation of a gene therapy-based approach in which cells are engineered to express a membrane-bound form of TRAIL (mTRAIL). mTRAIL can activate both TRAIL-R1 and TRAIL-R2 (Muhlenbeck *et al*, 2000), and due to its continuous expression by mTRAIL-bearing cells, it results in increased stability and concentration within the tumor, where these cells seem to accumulate. So far, mesenchymal stem cells transduced with lentiviruses bearing the sequence for mTRAIL (Luetzkendorf *et al*, 2010) and $CD34^+$ transfected with adenoviruses have been employed (Carlo-Stella *et al*, 2006). These approaches demonstrated that mTRAIL reduces growth of primary colon cancer and multiple myeloma *in vivo* (Lavazza *et al*, 2010), and inhibit spontaneous formation of lung cancer in a breast xenograft model (Rossini *et al*, 2012). Interestingly, and in agreement with a recent paper describing a soluble trimerized version of TRAIL, the effect of mTRAIL seems more directed at tumor-

associated vasculature than at the tumor itself (Wilson *et al*, 2012). The reason has not been fully understood yet and the expression of TRAIL-Rs does not seem to be correlated with cell sensitivity to TRAIL treatment. In fact, TRAIL-Rs are expressed also in normal tissues and tumor cells, but these cells are not killed by TRAIL treatment. Nonetheless, the destruction of the neo-vasculature reduces the growth of the primary tumors and causes the formation of large necrotic areas within the solid tumors (Lavazza *et al*, 2010; Rossini *et al*, 2012).

TRAIL and receptor agonists are therefore currently tested in clinical trials in combination with diverse compounds, e.g. paclitaxel, carboplatin, gemcitabine, cisplatin, bortezomib, pemetrexed, doxorubicin, FOLFIRI, rituximab, avastin and capacitabine to try to increase their efficacy (Falschlehner *et al*, 2009). A high percentage of patients showed partial response and stable disease, a promising result given that most tumor patients enrolled in these clinical studies had already been unsuccessfully treated.

2.5.1.3. SMs in association to traditional chemotherapy

Besides having been tested in combination with TRAIL, SMs have also been combined with traditional chemotherapeutic drugs (Probst *et al*, 2010) and radiation, and shown to induce apoptotic and also necroptotic death (Laukens *et al*, 2011; Steinhart *et al*, 2013). Recent reports have shown that SMAC can induce an inflammatory type of tumor cell death (Emeagi *et al*, 2012) and SMs cancer cell killing in monotherapy is known to be TNF-dependent. Nonetheless, the role of the cytokines and in particular of TNF in combination therapy is still a matter of debate as there are many reports showing that the SM/chemotherapy combination kills cells in a NF-kB (Berger *et al*, 2011; Stadel *et al*, 2011) and TNF-dependent manner (Laukens *et al*, 2011; Probst *et al*, 2010), while others

present a diametrically opposite conclusion (Allensworth *et al*, 2013; Eschenburg *et al*, 2012; Greer *et al*, 2011).

Despite the diverse speculated mechanisms of activity, all these works agreed that SMs could increase the *in vitro* activity of many classes of compounds. *In vivo*, as already mentioned, SM treatment could take advantage of cytokines and TNF produced by the host (Lecis *et al*, 2013). Accordingly, SMs have been shown to synergize with compounds activating the innate immunity (Jinesh *et al*, 2012), such as 5' cytosine-phospho-guanine (CpG) and polyinosinic-polycytidylic acid/poly(I:C), causing a "perfect cytokine storm" (Beug *et al*, 2014).

2.5.2. Testing SMs in clinical trials

An enormous amount of pre-clinical data supports the employment of SMs in combination therapy and hence five different IAP antagonists combined with paclitaxel, daunorubicin, cytarabine, or gemcitabine are currently tested in phase I/II clinical trials for solid and hematologic malignancies. Monovalent GDC-0917/CUDC-427 (Genentech, Inc./Curis), LCL161 (Novartis) and AT-406 (Ascenta Therapeutics) can be administered orally, while bivalent compounds such as HGS1029 (Aegera Therapeutics/Human Genome Sciences) and TL32711 (TetraLogic Pharmaceuticals) require intravenous administration. Completed phase I trial for safety and pharmacologic properties demonstrated that SMs are usually well tolerated, even if inducing an increase of cytokines in patients (Fulda, 2014b).

Recently, the clinical trial testing of CUDC-427 was suspended due to the death of a patient because of liver failure. Even though the patient's treatment had been discontinued one month before death and that no sign of liver toxicity was found in other

patients making this event most likely not attributable to SM treatment, nonetheless it caused alarm regarding the possible risks of SMs. In line with this, it has been recently shown that SM-triggered cytokine release stems from the inhibition of XIAP and, to avoid this, the new compound Birinapant has been designed with reduced affinity for XIAP, but still conserving the same effect on cIAP1 and cIAP2. The efficacy of this compound was shown to be independent of TNF and more tolerability was suggested (Allensworth *et al*, 2013; Condon *et al*, 2014), in agreement with a role of XIAP inhibition in cytokine toxicity (Wong *et al*, 2014).

Compound	Combination	Cancer type	Status	Phase I/II	Trial
LCL-161	None	Solid tumors	Completed	Phase I	NCT01098838
LCL-161	Paclitaxel	Solid tumors	Recruiting	Phase I	NCT01240655
LCL-161	Paclitaxel	Breast cancer	Recruiting	Phase II	NCT01617668
AT-406	None	Solid tumors, lymphomas	Recruiting	Phase I	NCT01078649
AT-406	Daunorubicin, cytarabine	AML	Terminated	Phase I	NCT01265199
HSG1029	None	Solid tumors	Completed	Phase I	NCT00708006
HSG1029	None	Lymphoid malignancies	Terminated	Phase I	NCT01013818
TL32711	None	Solid tumors	Active, not recruiting	Phase I/II	NCT01188499
TL32711	GEM	Solid tumors	Recruiting	Phase I	NCT01573780
TL32711	None	Solid tumors, lymphomas	Completed	Phase I	NCT00993239
TL32711	None	AML	Recruiting	Phase I/II	NCT01486784
TL32711	5-Aza	MDS	Not yet recruiting	Phase I/II	NCT01828346
TL32711	None	Ovarian, peritoneal cancer	Recruiting	Phase II	NCT01681368
GDC-0152	None	Solid tumors	Completed	Phase I	NCT00977067
CUDC-427	None	Solid tumors, lymphomas	Recruiting	Phase I	NCT01908413

Abbreviations: AML, acute myeloid leukemia; GEM, gemcitabine; MDS, myelodysplastic syndrome; 5-Aza, 5-azacytidine.

Table 1. Clinical trials with IAP antagonists. (Fulda, 2014b). 5 different SMs are being currently tested in several clinical trials for solid and hematological malignancies.

2.6. Cancer and oncogenes

It has already been mentioned that IAPs are aberrantly expressed and even mutated in a number of different cancer types. Multiple myeloma for example is known not be particularly affected by mutations involving the NF-kB pathway (Annunziata *et al*, 2007; Keats *et al*, 2007), IAPs included. Nonetheless, also the other cancer types are all variably characterized by aberrant IAP expression, suggesting a general mechanism of cancer resistance more than a peculiar feature of a specific tumor type. In line with this

observation, SM efficacy is not associated to a particular cancer and this class of compounds has therefore been employed in models of many different malignancies (Fulda and Vucic, 2012). Furthermore, cancer cells sensitive to SMs in monotherapy belong to various cancer types and, although the triple negative breast carcinoma cell line MDA-MB231 is probably the most employed to test the efficacy of the IAP-antagonizing molecules, also ovarian cancer SKOV3, rabdomyosarcoma Kym1 and several lung cancer cell lines have been shown to be killed by SMs as standalones (Varfolomeev *et al*, 2007). Therefore, in our work, we did not focus on a particular cancer type, but we employed *in vitro* and *in vivo* models deriving from several different tumors and normal tissues as controls along with premalignant models. When possible, to study the effect of a specific mutation on drug resistance, we took advantage of isogenic pairs of cell lines with knock-in (KI) and knock-out mutations in the oncogene of interest. This technique constitutes a powerful tool to study the effect of a specific mutation independently from the genetic environment (Arena *et al*, 2007) and is therefore exploited to study the capacity of a gene to affect drug resistance (Di Nicolantonio *et al*, 2008), gene expression, aggressiveness, and to identify drugs particularly effective in a certain genetic setting. This is the case, for example, of the so-called "synthetic lethality", which renders cancer cells bearing a particular mutation sensitive (Farmer *et al*, 2005), while normal wild type cells remain completely resistant to a drug.

2.6.1. Exploiting the synthetic lethal effect in pharmacology

Most of the chemotherapeutic agents currently used in clinics have low therapeutic indices and therefore narrow therapeutic windows. This results in high toxicity for patients when effective anti-tumor concentrations are reached or poor efficacy when the concentration of the drug is maintained low due to excessive toxicity. The perfect drug

should in theory target a specific protein or a pathway essential only for cancer cell viability and not present or not essential in normal cells. This is the case, for example, of fusion proteins that sometimes are caused by chromosome translocations (Rosebeck *et al*, 2011) and result in the expression of a protein not expressed in normal cells and so representing a potential specific target. Unfortunately, this event is infrequent and rarely provides a drug-able target for therapy. On the contrary, it is more recurrent that a particular protein becomes more important in cancer cells compared to normal cells and could therefore be exploited as a pharmacological target (Farmer *et al*, 2005). Sometimes, cancer cells depend so much on a protein that this becomes essential, while it is dispensable in normal cells. This phenomenon is often referred to oncogene (Roulston *et al*, 2013) and non-oncogene addiction (Chaturvedi *et al*, 2011).

An opportunity in cancer treatment is also represented by the so-called synthetic lethality. Two genes are considered synthetic lethal when the mutation of either gene alone is viable, but not the mutation of both of them. This effect was initially described in yeasts and is frequently caused by loss-of-function mutations. Only rarely, it can be associated to gain-of-function events (Kaelin, 2005). New drugs have therefore been designed to target a particular pathway essential for cancer cells due to the simultaneous mutation impairing parallel pathways (Weidle *et al*, 2011). The same compound spares healthy tissues because they can rely on the alternative pathway that is not functional in cancer cells. This is the case of PARP inhibitors, which become toxic only in the presence of breast cancer susceptibility genes-1 (BRCA1) mutations (Farmer *et al*, 2005). Cancer cells bearing BRCA1 mutations in fact depend on PARP to repair DNA damages, while normal cells can employ both alternative pathways going through BRCA1 or PARP.

2.6.2. Colorectal cancer

Colorectal cancers (CRC) are among the most widespread cancer types and are characterized by low survival rates especially in advanced stage patients. Several multidrug combinations are used to treat colorectal cancer employing oxaliplatin, 5-FU and the camptothecin (CPT) analogue irinotecan (Meyerhardt and Mayer, 2005). Moreover, cetuximab and panitumumab, two antibodies blocking the EGFR, are approved in combination with chemotherapy for metastatic CRC and as maintenance therapy in chemorefractory tumors. Receptor tyrosine kinases such as EGFR, through the activation of the downstream guanosine triphosphate (GTP)ases, regulate several pro-survival pathways such as the ones regulated by the MAPKs and PI3K. Cetuximab activity stems from the blockage of these pathways even if mutations or amplification of KRAS are often associated to unresponsiveness and acquired resistance (Misale *et al*, 2012). Of note, about 40% of CRCs display mutated KRAS, the most frequent in codon 12 and 13, and resulting in constitutive hyperactivation.

2.6.2.1. Oncogenic KRAS

KRAS is a 21 KDa protein that plays a pivotal role in cell signal transduction belonging to the RAS subfamily, which comprises several other small GTPases endowed with GTP-hydrolyzing activity. In unstimulated conditions, GTPases bind to GDP and are unable to trigger the down-stream signaling processes. RAS proteins therefore require GTP to be activated and undergo rapid cycles of activation and inactivation that are essential for physiological signaling (Pylayeva-Gupta *et al*, 2011). Because the cascades regulated by RAS stimulate cell growth and division, amongst many other cellular effects, aberrant signaling can ultimately lead to cancer transformation. The 3 human RAS genes (HRAS, KRAS, and NRAS) encoding for 4 Ras isoforms (KRAS exists in two alternatively-

spliced variants) are among the most prevalent drivers of human cancer, with KRAS being mutated in about 20%-25% of all human tumors and up to 90% in certain cancer types e.g. pancreatic cancer (Eser *et al*, 2014). In these settings, KRAS activates several down-stream effectors leading to the stimulation of the RAF/MAPK/ERK kinase (MEK)/extracellular signal-regulated kinase (ERK) and PI3K pathways. Despite oncogenic KRAS being often associated with poorer prognosis, it can also result in synthetic lethality (Steckel *et al*, 2012; Weidle *et al*, 2011). In fact, the presence of constitutively active KRAS sensitizes cancer cells to MEK and BCL-xL (Corcoran *et al*, 2013) or RAF inhibition (Lamba *et al*, 2014), TRAIL (Huang *et al*, 2011), 5-FU and oxaliplatin (de Bruijn *et al*, 2010). Nonetheless, KRAS activation is usually associated with reduced capacity to undergo apoptosis and increased resistance to chemotherapy by activating several pro-survival pathways (Di Nicolantonio *et al*, 2010; Hata *et al*, 2014; Tao *et al*, 2014) that often cause the upregulation of anti-apoptotic factors such as the members of the IAP family members (Hadj-Slimane *et al*, 2010; Moller *et al*, 2014).

2.6.3. Breast cancer classification

Breast cancer is a heterogeneous disease, with many subtypes displaying distinct biological features and leading to different treatment responses and clinical outcomes. Traditional classification made according to biological characteristics (tumor size, lymph node involvement, histological grade, patient's age, estrogen Receptor/ER, progesterone receptor/PR and human epidermal growth factor receptor 2/HER2 status) is now associated to gene expression microarray studies that identify distinct molecular tumor classes.

Approximately 75% of breast cancers are positive for ER and/or PR. ER-responsive

genes encode proteins typical of luminal epithelial cells and therefore ER-positive tumors are termed "luminal". Further studies have divided this group in two luminal-like subclasses (Yersal and Barutca, 2014).

2.6.3.1. Luminal A breast cancer

The luminal A is the most common subtype. It represents about half of all breast cancers and is generally associated to good prognosis. These tumors usually show low histological grade, a degree of nuclear pleomorphism and mitotic activity, and include special histological types (i.e., tubular, invasive cribriform, mucinous and lobular). The luminal A subclass is characterized by high levels of ER, expression of cytokeratin CK8 and CK18 and lower levels of proliferation-related genes. Despite the fact that relapse rate of patients belonging to this group is significantly lower than other subtypes, recurrence may occur in bone, whereas liver, lung and central nervous system metastases involve less than 10% of patients. Treatment is mainly based on hormonal therapy.

2.6.3.2. Luminal B breast cancer

Luminal B tumors cover about 15%-20% of all breast cancers and are more aggressive than luminal A subtype. Luminal B tumors are characterized by higher histological grade, proliferative index and recurrence rate. This results in worse prognosis and lower survival rates after relapse compared to subtype A.

2.6.3.3. Basal-like breast cancer

The basal-like subtype comprises from 8% to 37% of all breast cancers and is associated with high histological grade, mitotic and proliferative indices, poor tubule formation and inner necrotic or fibrotic zones. This type of tumor is characterized by pushing borders, lymphocytic infiltrate and medullary features. About 80% of basal-like

tumors are triple-negative, expressing no PR and ER, and with HER2 not amplified. Most of these tumors are infiltrating ductal tumors, extremely aggressive and with high capacity to form brain and lung metastasis. Claudin-low breast cancer is one of the triple-negative subtypes characterized by poor clinical outcome, low expression of genes involved in tight junctions and cell-cell adhesions including claudins, occludin and E-cadherin, but high expression of EMT genes and displaying stem cell-like features.

2.6.3.4. Metastasis and the epithelial to mesenchymal transition process

Cancer metastasis is the major issue in cancer therapy because it is responsible for around 90% of cancer deaths even though the dissemination of the primary tumor is an extremely inefficient process (Chiang and Massague, 2008). In fact, only a small fraction of cancer cells, less than 0.01% in experimental animal models, will form metastases. Accordingly, cancer cells can be found also in the bloodstream of patients that will not develop metastases.

To disseminate from the primary tumor, cancer cells invade the surrounding tissues as single cells (Giampieri *et al*, 2009) or clumps (Friedl and Gilmour, 2009). Environmental conditions determine whether single cells will move by elongated-mesenchymal or rounded-amoeboid migration (Sahai and Marshall, 2003). The intravasation process in which invading cells cross the blood vessel walls and enter the circulation is the first step of metastasis formation. Few cells survive the stress and the immune cells of the bloodstream, finally attach to endothelial walls, extravasate and start proliferating in the stroma. If these micrometastases efficiently survive in the new environment, they eventually grow into clinically detectable macrometastases. Therefore, attachment to the endothelium is not sufficient for metastasis formation, but cancer cells also need growth

signals and the appropriate environment to invade a target tissue (Reymond *et al*, 2013).

EMT is a physiological step of early embryonic development. It is characterized by cell-cell adhesion reduction and acquisition of motility, together with the appearance of mesenchymal markers. This process seems to play a role in allowing the detachment of cancer cells from primary tumors even if its importance is still controversial. During the EMT, cells express a number of E-cadherin repressors such as Twist-1, Twist-2, ZEB-1, ZEB-2, Snail and Slug that bind to the E-boxes at the CDH1 (E-cadherin) promoter. The loss of E-cadherin is an essential step of EMT (Acloque *et al*, 2008) that, in this way, reduces the intercellular adhesion junctions therefore increasing cell detachment.

2.6.4. Ovarian cancer ascites

Ovarian carcinomas are characterized by the formation of ascites especially at advanced stages. Ascites are formed by the mechanical constriction exerted by the tumor and is characterized by the peritoneal increase of fluid production and decreased absorption. Ovarian cancers rarely spread by metastasis outside the peritoneum and ascites themselves are often the cause of death (Lengyel, 2010). The ascitic fluid is rich in soluble factors that constitute the cross-talk between cancer, stromal and inflammatory cells, and support tumor development. This microenvironment also promotes immunosuppression and favors tumor escape from the immune system, although the ascitic fluid is usually enriched in immune cells such as macrophages.

Macrophages are plastic cells that can be classically activated (M1) and 'alternatively' activated (M2) (Sica and Mantovani, 2012). Tumor-associated macrophages are classified as M2 macrophages and produce immunosuppressive cytokines such as interleukin-10 (IL-10). In contrast, M1 macrophages produce pro-inflammatory cytokines including

interferon-γ (IFNγ) and IL-12. M1, but not M2, macrophages can elicit an effective antitumor response. Importantly, the NF-kB pathway controls the plasticity of macrophages.

3. AIM OF STUDY

Resistance to cell death is a hallmark of cancer cells and is responsible for unresponsiveness to therapy and tumor progression. Several findings support the notion that IAPs play a pivotal role in conferring resistance to apoptosis by blocking caspases and stimulating several pro-survival pathways. A chance to target the IAPs is now offered by the SM compounds, which are currently tested in a number of clinical trials and widely employed in pre-clinical studies. SMs rapidly deplete cIAP1 and cIAP2, and prevent the activity of XIAP in blocking caspases but few cancer cell lines are killed by SM treatment in monotherapy. There is therefore the need to identify new drugs that can be successfully combined to enhance their cytotoxic activity. Furthermore, it is fundamental to fully understand the mechanisms of SM activity in order to predict the cancer settings where they are likely to be more effective, and avoid side effects and toxicity.

The aim of this study is therefore to characterize new SMs compounds that we have developed in collaboration with the University of Milan, focusing on SM83, in particular. We describe its capability to interact with the known SM targets and to be effective both *in vitro*, killing sensitive cell lines, and *in vivo*, reducing the growth of both solid tumors and cancer ascites. Importantly, we also study the effect of SM83 treatment on metastasis formation and begin to explain the mechanisms responsible for the anti-metastatic effect observed. Finally, we look for genetic lesions that favor the efficacy of SM83 treatment in combination with other drugs and identify a cancer mechanism able to counteract the potentially pro-death stimulus of oncogenic KRAS.

4. MATERIALS AND METHODS

4.1. Reagents

SMs were synthesized at the CISI institute as recently described (Manzoni *et al*, 2012), dissolved in dimethylsulfoxide (DMSO) (Sigma-Aldrich) to obtain a 10 mM solution and stored at -20°C. Recombinant TNF (Emmerich *et al*, 2011) and TRAIL (Ganten *et al*, 2006) were produced by the University of Milan and the UCL respectively, London using two plasmids encoding for tagged human TNF and TRAIL kindly provided by Prof. Henning Walczak. Recombinant human TWEAK was kindly provided by Prof. Harald Wajant (Salzmann *et al*, 2013). Mouse bearing cancer ascites and IGROV-1 were treated with commercial TRAIL purchased by Enzo Life Sciences. TNF blockers Infliximab (Schering-Plough) and Enbrel (Wyeth Pharmaceuticals) were kindly provided by Prof E Berti (Ospedale Policlinico Maggiore). Double strand break inducer neocarzinostatin (Sigma-Aldrich), topoisomerase inhibitors etoposide (Teva) and camptothecin (Sigma-Aldrich) were used in combination therapy with SM83.

The antibodies targeting the following proteins were used in western blot experiments: NIK, NF-kB1, NF-kB2, cleaved PARP, cleaved caspase-3, cleaved caspase-9, LRIG-1, Snai2, Beclin-1, LC3B, total RAS, ERK1/2 and phospho-ERK1/2 Thr202/Tyr204, AKT and phospho-AKT (Cell Signaling Technology), cIAP1 (R&D Systems), cIAP2 and XIAP (BD Biosciences), caspase-8 (Enzo Life Sciences), NOXA (CalBiochem), Mcl1 (Santa Cruz Biotechnology), actin and vinculin (Sigma-Aldrich), and RIP1 (Ab Frontier).

Transient ectopic expression of KRAS G13D was achieved by transduction of the employed cells with viral particles collected from conditioned medium of packaging cells HEK293FT (Life Technologies), transfected with Lipofectamine 2000 and ViraPower

(Life Technologies) and the pINDUCER20 inducible lentiviral vector kindly provided by Stephen Elledge (Howard Hughes Medical Institute). Cells efficiently transduced were selected with 500 µg/ml G418 (Life Technologies). Pan-caspase inhibitor z-VAD(OMe)-FMK was purchased by BIOMOL, RIP1 inhibitor Necrostatin-1 from Enzo Life Sciences. MEK inhibitors PD98059 and UO126 were purchased from CalBiochem, PI3K inhibitor LY294002, IKK inhibitor BAY 11-7082 and transcription inhibitor cycloheximide from Sigma-Aldrich, AKT inhibitor Triciribine from Selleckem.

4.2. Fluorescence polarization-based binding assay

4.2.1. XIAP BIR3 cloning, expression and purification

The cDNA sequence coding for the human XIAP BIR3 domain (residue 241-356) cloned in pET28 vector (Novagen) was used to transform the Escherichia coli strain BL21. Protein expression was induced for 3 h at 37°C with isopropyl-b-D-thiogalactopyranoside (IPTG) to a final concentration of 1 mM in the presence of 100 µM zinc acetate (ZnAc). Bacteria were grown in 2YT medium plus kanamycin and harvested, resuspended in a buffer containing 50 mM Tris HCl pH 7.5, 200 µM NaCl and protease inhibitors, treated with 100 µg/ml lysozyme for 30 min in ice and then lysed by sonication. After elimination of debris by centrifugation, the recombinant protein was purified using Ni-NTA (His-trap FF crude, Ge-Healthcare) followed by gel filtration (Superdex 200, Ge-Healthcare). BIR3-His-tag was eluted with 250 mM imidazole and thereafter stored in 20 mM Tris HCl pH 7.5, 200 mM NaCl and 10 mM dithiothreitol (DTT).

4.2.2 Fluorescence polarization assay: XIAP BIR3 saturation and competitive binding experiments

Fluorescent polarization experiments were performed in black, flat-bottom 96-well microplates (Greiner Bio-One) and fluorescent polarization was measured by Ultra plate reader (Tecan). Fluorescent-labelled SMAC peptide [AbuRPF-K(5-Fam)-NH2] - fluorescein isothiocyanate (FITC)–SMAC, stocked in DMSO - to a final concentration of 5 nM and increasing concentration of BIR3 His-tag from 0 to 20 μM were added to an assay buffer. The final volume in each well was 120 μL, with the assay buffer consisting of 100 mM potassium phosphate, pH 7.5; 100 μg/mL bovine γ-globulin; 0.02% sodium azide. After a 15 min shaking at room temperature (RT), the plate was incubated for 3 h at room temperature. Fluorescence polarization was measured at an excitation and emission wavelengths of 485 nm and 530 nm respectively. The equilibrium binding graphs were constructed by plotting millipolarization units (mP) as function of the XIAP BIR3 concentration. Data were analyzed using Prism 5.02 software (Graphpad Software).

Dimers were evaluated for their ability to displace FITC–SMAC probe from recombinant protein. 5 nM of FITC–SMAC, XIAP BIR3 His-tag and serial dilutions of the dimers (concentrations ranging from 4 μM to 0.4 nM) were added to each well to a final volume of 120 μL in the assay buffer described above. The concentration of BIR3 His-tag used was 60 nM, able to bind more than 50% of the ligand in the saturation binding experiment. After being mixed for 15 min on a shaker and incubated 3 h at RT, fluorescent polarization was measured by Ultra plate reader (Tecan).

4.2.3. Cloning, expression and purification of human cIAP-1 BIR3

The sequence coding for cIAP-1 domain residues 245–357 was cloned in the

pET21(a) vector (Novagen) with a C-terminal 6xHis-tag and used to transform Escherichia coli strain BL21(DE3). The recombinant protein was purified using Ni-NTA (His-trap FFcrude, Ge-Healthcare), gel filtration (Superdex 200, Ge-Healthcare) and eluted in 20 mM Tris pH 8.0, 250 mM NaCl and 10 mM DTT.

4.2.4. Fluorescence polarization assay: cIAP1 BIR3 saturation and competitive binding experiments

FITC-SMAC to a final concentration of 2 nM and increasing concentration of BIR3 His-tag from 0 to 20 μM were added to the assay buffer described above. After a 15 min shaking, the plate was incubated for 3 h at RT. Fluorescence polarization was measured at an excitation and emission wavelengths of 485 nm and 530 nm respectively. The equilibrium binding graphs were constructed by plotting mP as function of the cIAP1 BIR3 concentration. Data were analyzed using Prism 5.02 software (Graphpad Software).

Dimers were evaluated for their ability to displace FITC–SMAC probe from recombinant protein. 2 nM of FITC–SMAC, cIAP1 BIR3 His-tag and serial dilutions of the dimers (concentrations ranging from 4 μM to 0.4 nM) were added to each well to a final volume of 120 μL in the assay buffer described above. The concentration of BIR3 His-tag used was 10 nM, able to bind more than 50% of the ligand in the saturation binding experiment. After being mixed for 15 min on a shaker and incubated 3 h at RT, fluorescent polarization was measured by Ultra plate reader (Tecan).

4.2.5. Cloning, expression and purification of human XIAP linker-BIR2–BIR3

A pET28 vector (Novagen) with the cDNA coding for human XIAP from residue 124 to 356 (linker-BIR2–BIR3), coding for BIR2 and BIR3 domains and the linker region

preceding BIR2, was used to transform Escherichia coli strain BL21. Protein expression was induced by IPTG to a final concentration of 1 mM and 100 µM zinc acetate (ZnAc) for 20 h at 20°C. Bacteria grown in 2YT medium plus kanamycin were harvested, resuspended in a buffer containing 50 mM Tris HCl Ph 7.5, 200 mM NaCl and protease inhibitors, treated with 100 µg/ml lysozyme for 30 min in ice and then lysed by sonication. After elimination of debris by centrifugation, the recombinant protein was purified using Ni-NTA (His-trap FFcrude, Ge-Healthcare) followed by gel filtration (Superdex 200, Ge-Healthcare). The linker-BIR2–BIR3-His-tag was eluted with 250 mM imidazole and thereafter stored in 20 mM Tris HCl pH 7.5, 200 mM NaCl and 10 mM DTT.

4.2.6. Fluorescence polarization assay: XIAP linker-BIR2–BIR3 saturation binding and competitive experiments

Fluorescent-labeled dimeric SMAC peptide SMAC-1F to a final concentration of 1 nM and increasing concentration of linker-BIR2– BIR3 His-tag from 0 to 2 µM were added to the assay buffer in a final volume of 120 µl. After a 15 min shaking, the plate was incubated for 3 h at RT. Fluorescence polarization was measured at an excitation and emission wavelengths of 485 nm and 530 nm respectively. The equilibrium binding graphs were constructed by plotting mP as function of the XIAP linker-BIR2–BIR3 concentration. Data were analyzed using Prism 5.02 software (Graphpad Software).

Dimers were evaluated for their ability to displace SMAC-1F probe from recombinant protein. 1 nM SMAC-1F, 3 nM XIAP linker-BIR2–BIR3 His-tag and serial dilutions of the dimers (concentrations ranging from 2 µM to 0.4 nM) were added to each well to a final volume of 120 µL in the assay buffer described above. After being mixed for 15 min on a shaker and incubated 3 h at RT, fluorescent polarization was measured by

Ultra plate reader (Tecan).

4.3. Cell cultures

The human breast adenocarcinoma MDA-MB231, the promyelocytic HL60 and the prostatic adenocarcinoma PC3 cell lines employed in the experiments performed to test the cytotoxic activity of the dimeric SMs were obtained from Interlab Cell Line Collection (ICLC, Genova, Italy). The cell lines were cultured in Roswell Park Memorial Institute (RPMI)-1640 medium supplemented with 2 mM L-glutamine, penicillin (100 U/mL)/streptomycin (100 µg/mL), 10% fetal bovine serum (FBS) (all from Sigma-Aldrich) at 37°C and 5% CO_2 in fully humidified atmosphere.

The breast cancer cell lines used for all the other experiments were kindly provided by Dr. Elda Tagliabue: MDA-MB231, MDA-MB468, T47D, MDA-MB453, BT549, SUM149 and SUM159. Ovarian carcinoma IGROV-1 cells were provided by Dr. Nadia Zaffaroni. The mouse sarcoma Meth A cell line was kindly provided by Dr. Mario Colombo, human mammary immortalized epithelial HME and MCF10A, and CRC DLD1, SW48, Lim1215, HCT116 cell lines were all kindly provided by Prof. Alberto Bardelli. HME isogenic pairs and MCF10A cell lines were cultured in Dulbecco's Modified Eagle's medium-F12 (DMEM-F12; Gibco), supplemented with 10% FBS (LONZA), 2 mM glutamine (LONZA), 20 ng/ml EGF (Immunological Science), 10 µg/ml insulin (Sigma), 500 µg/ml hydrocortisone (Sigma-Aldrich). SW48 and DLD1 isogenic pairs were cultured with DMEM (Gibco) supplemented with 10% FBS and 2 mM glutamine. Lim1215 isogenic pairs were cultured with RPMI (LONZA) supplemented with 10% FBS, 2 mM glutamine and 1 µg/ml insulin. HCT116 were cultured in RPMI, supplemented with 2 mM glutamine, sodium pyruvate (LONZA), and non-essential amino acids (LONZA).

4.4. Cell viability assay

MDA-MB231 and PC3 cells were seeded in 96-well flat bottom cell culture plates at a density of 5000 cells/well, while HL60 cells were seeded at a density of 10,000 cells/well in 100 µL of complete culture medium. MDA-MB231 and PC3 cells were allowed to adhere for 24 h before being treated for 96 h. Cells were treated with serial dilutions of SMs, ranging from 0.1 nM to 50 µM. To evaluate cell viability, 10 µL of WST-8 were added to each well. After 4 h of incubation at 37°C, the absorbance was measured at 450 nm using a microplate reader. The data were then expressed as a mean percentage of triplicates normalized to the untreated control. The experiments were repeated twice. The IC50, the concentration of compound capable of inhibiting the cell growth by 50%, was calculated using the GraphPad Prism 4 software.

To evaluate the cytotoxic activity of SM83 in combination with izTRAIL, IGROV-1 cells were counted and seeded in 6-well plates. The following day, cells were treated with the indicated concentrations of compounds and cultured for 3 days. At the end of the treatment, IGROV-1 cells were trypsinized and counted. Viability is expressed as a percentage of untreated cells.

Another technique to evaluate cell viability was by employment of CellTiter-Glo (Promega). In these experiments, cells were seeded in white optical 96-well plates and treated as indicated. At the end of the experiments, medium was discarded and 60 µl of reagent diluted 1:4 in phosphate-buffered saline PBS was added to each well. After 15 min of shaking at RT, luminescence was measured with a Tecan Ultra plate reader. Viability was shown as a percentage compared to untreated or mock treated cells.

4.5. Pharmacokinetic experiments of SM83

Pharmacokinetic experiments were performed by the Test Facility of NiKem Research, Baranzate (MI). Briefly: male CD-1 mice (Charles River Italy, Calco) were treated with SM83 by intraperitoneal (ip) admininistration and euthanized at eight time points (5, 15, 30, 60, 120, 240, 480 min and 24 h) under anesthesia with ethyl ether. For the intravenous (iv) route of administration, mice were treated with SM83 by iv injection and euthanized at eight time points (2, 10, 30, 60, 120, 240, 480 min and 24 h) under anesthesia with ethyl ether. Blood (about 500 µL) was collected in heparinized tubes, and centrifuged (3500 g, 15 min, 4°C). Plasma samples were stored at -80°C and later analyzed by LC–MS/MS (Premiere XE, Waters). The lowest limit of quantification (LLOQ) was 1 ng/mL.

4.6. Detection of proteins by western blot and dot blot

For western blot analysis, cells were trypsinized and harvested by centrifugation at 4500 rpm for 5 minutes at 4°C. After washing once with PBS, cells were lysed by boiling in 60-100 µl cell lysis buffer (125 mM Tris HCl pH 6.8, 5% sodium dodecyl sulfate/SDS) supplemented with 1 x complete protease inhibitors (Roche Diagnostics) and phosphatase inhibitors (Sigma-Aldrich), sonicated and centrifuged at 13000 rpm for 20 min at RT. Cleared supernatants were transferred to a new tube and frozen at -20°C. To determine the protein concentration of cell lysates, the bicinchonic acid (BCA)-containing protein assay was applied according to the manufacturer's instructions (QuantumMicro Protein, Euroclone). In a 96-well plate, 2 µl of lysate were incubated with 148 µl water and serial dilutions of bovine serum albumin (BSA) used as standard protein. BCA solution was added in a 1:1 ratio. After incubation at RT, absorbance was measured at 485 nm

using Ultra microplate reader (Tecan). Protein concentration was determined by interpolation with the curve obtained with the standard BSA.

Proteins were then separated according to their molecular weight using pre-cast 4-12% Bis-Tris NuPAGE gels (Life Techonolgies). Cell lysates were mixed with 4x reducing SDS-Sample buffer and heated for 10 min at 99°C. As a molecular weight standard, Page Ruler Plus Pre-Stained Protein Ladder (Euroclone) was used. The electrophoretic separation was achieved by applying a constant voltage in MES buffer. Proteins within the gels were then blotted onto PVDF membranes (Millipore) using the XCell II blot module (Life Technologies). Membranes were incubated with blocking buffer (4% non-fat milk dissolved in PBS plus tween 0.1%, PBS-T) for 30' and then incubated overnight with the indicated primary antibodies. Membranes were then washed 3 times in PBS-T and incubated 1 h with the appropriate horseradish peroxidase-conjugated secondary antibody (Sigma). After washing in PBS-T, proteins were detected by electrochemiluminescence (ECL) reaction, by exposure of films to the membranes after incubation with luminol-based chemiluminescent substrates (Pierce).

For dot blotting, ascitic fluid samples cleared of cells were spotted on PVDF membranes and let to dry. After saturation with non-fat dry milk-PBS, filters were hybridized with anti-HMGB-1 Ab (Abcam, 1:2000). High mobility group box 1 (HMGB-1) was then detected as for western blotting.

4.7. Gene knock-down by silencing and ectopic expression of KRAS

To achieve transient knock-down of target genes two different protocols were used. Human epithelial cells were transfected with indicated short interfering RNAs (siRNAs) using a reverse transfection protocol in which siRNAs (Qiagen) and RNAiMAX (Life

Technologies) were used. Two mixes were prepared: one containing 3.25 µl of RNAiMAX in 100 µl Optimem (GIBCO) and the other with 3.25 µl of siRNA (20 µM) stock in the same volume. The two mixes were incubated for 5 min at RT and then combined and left at RT for 30-40 min. Meanwhile, cells were trypsinized and counted. After the incubation, the siRNA/RNAiMAX mix was put in a culturing well and cells seeded on top. About 0.15 x 10^6 cells were cultured in a 6-well plate in a final volume of 2 ml medium without antibiotics. For transfection in 96-well plates, mixes were prepared with 0.25 µl siRNAs plus 0.25 µl RNAiMAX and 10^4 cells were seeded in 100 µl final volume.

Tumor cells were transfected with a similar protocol, employing the same regents and volumes. In this case, cells were seeded the day before the transfection and siRNA/RNAiMAX was added on top of the cells. After transfection, cells were incubated for 72 h before harvesting. If cells needed to be treated after transfection, drugs were added 48 h after transfection and viability or western blot analysis performed the day after. In each experiment, scramble siRNAs (siCtr) were used as control and siRNA targeting an essential gene (ubiquitin, UBB) served to evaluate the transfection efficiency.

To ectopically over-express mutated KRAS, the cDNA encoding the KRAS G13D was cloned in the pInducer20 lentiviral vector (kindly provided by Prof. Stephan Elledge) and used to produce lentiviral particles in HEK293FT packaging cells. Viruses were obtained by reverse transfection of HEK193FT cells following manufacturer's protocol and mixing pInducer20-KRAS G13D with the ViraPower packaging plasmid mix (Life Technologies) and the Lipofectamine2000 transfection reagent. After 24 h, medium was replaced with fresh medium that was collected after further 24 h and used to transduce HME and MCF10A cells. Cells having integrated the cDNA were selected by adding 500 µg/ml G418 (Sigma)

to the culturing medium. Transgene expression was stimulated by adding doxycicline (Dox, Sigma-Aldrich) to the medium for at least 48 h.

4.8. Preparation of TRAIL-armed CD34+ cells and co-culture with cancer cells

$CD34^+$ cells were purified from peripheral blood of consenting donors of allogeneic stem cells using the Auto-MACS device (Miltenyi Biotec, Bergisch-Gladbach, Germany, EU) and kindly provided by Prof. Carlo-Stella. Replication-deficient adenoviruses encoding the human TRAIL gene (mTRAIL) under the control of a CMV promoter were purchased from the Riken BioResource Center (Tsukuba). $CD34^+$ cells were plated at $2x10^6$/ml concentration in 1 ml of serum-free Iscove's modified Dulbecco's medium (IMDM) containing adenoviruses at a MOI of 200 plaque-forming units (pfu)/cell. After incubation at 37°C in 5% CO_2 for 2 h, cultures were supplemented with 1 ml IMDM plus FBS 20 % and BoosterExpress TM reagent (Gene Therapy Systems; final dilution 1:200) and incubated for 18 h, extensively washed in serum-containing medium and evaluated for transduction efficiency by flow cytometry, using an anti-TRAIL antibody (R&D).

For cytotoxicity experiments, TRAIL-armed CD34+ cells were co-cultured with the indicated cancer cell lines in a 1:1 ratio. Viability of cancer cells was measured by western blot detecting several markers of apoptosis, by the use of a fluorescent substrate of activated caspase-3/-7 or by AnnexinV/propidium iodide (PI) staining followed by flow cytometry gaited for $CD45^-$ cells to detect non-$CD34^+$ cells and therefore analyzing only the cancer cells.

4.9. *In vivo* experiments

Mice were maintained in laminar flow rooms keeping temperature and humidity constant. Mice had free access to food and water and were weighted twice a week. Experiments were approved by the Ethics Committee for Animal Experimentation of the Fondazione IRCCS Istituto Nazionale dei Tumori of Milan according to institutional guidelines and by the Italian Minister of Health, project INT_12_2011.

For the breast cancer xenograft models, non-obese diabetic/severe combined immunodeficiency disease (NOD/SCID) mice were engrafted in the left flank by subcutaneous (sc) injection of 200 µl physiological saline containing $5x10^6$ MDA-MB468 and MDA-MB231. At day 13, animals were randomized and divided in two groups. One group was treated with ip or iv injections with 5 mg/kg SM83, 5 times/week to a total of 13 (MDA-MB231) or 17 (MDA-MB468) injections. Tumor growth was monitored by caliper measurement 3 times a week. Mice were euthanized 6 h after the last injection for biochemical analysis of the primary tumor or two weeks later for detection of lung metastasis. In combination experiments with $CD34^+$ expressing mTRAIL, MDA-MB468 were injected sc in NOD/SCID and let grow for 2 weeks; mice were then treated 4 times with ip injections of 5 mg/kg SM83 and/or iv administration of 10^6 $CD34^+$ cells at day 14, 18, 21 and 25. Primary tumor growth was measured until day 18 and then nodules were collected for immunohistochemistry (IHC) analysis. NOD/SCID mice engrafted with 10^6 MDA-MB231 cells were treated with daily ip injections with 5 mg/kg SM83, 5 times/week starting at day 14, and received 2 iv injections/week of 10^6 CD34-TRAIL cells for two weeks (total of 4 injections) starting after 1 week of SM83 treatment. Mice were euthanized at day 46.

The *in vivo* effects of SM83 were tested using a human ovarian carcinoma ascites model obtained by ip injection of IGROV-1 cells into athymic nude mice. The cells had previously been adapted to grow ip and maintained by serial passages of ascitic cells. Nude mice develop hemorrhagic ascites and diffuse carcinomatosis and eventually die. In order to assess the effects of SMs on survival, mice were inoculated ip with $2.5x10^6$ cells in 0.2 ml saline and, starting the day after cell injection, injected ip with the compounds (dissolved in saline) at 5 mg/kg body weight, once daily for 5 days per week for 2 weeks (qdx5/wx2w). The animals were inspected and weighed daily. The progression of ascites was assessed from an increase in body weight (measured on day 17). For ethical reasons, they were killed before impending death, recognized by their suffering status and loss of reactivity to external stimuli. The day of killing was taken as the day of death for calculating the median survival time. The antitumour activity of treatments was expressed as the ratio of median survival time in treated mice to that of untreated control mice x100 (T/C%). To evaluate the effect of a single dose of SM83, 24 h after the injection of 5 mg/kg SM83 the ascitic fluid was collected, cells harvested by centrifugation, dissolved in PBS and counted. Cancer cell killing was also confirmed by evaluation of the levels of human CK18 in the plasma of engrafted animals. CK18 is in fact released by dying cells and was quantified by M65 enzyme-linked immunosorbent assay (ELISA) kit (Vinci-biochem) following manufacturer's protocol.

In the syngeneic ascites model, $2x10^5$ mouse Meth A cells were injected ip into immunocompetent BALB/c mice and treatment, starting 7 days later, consisted of five consecutive daily ip injections of SM83 at a dose of 5 mg/kg body weight. The progression of ascites was assessed from both an increase in body weight (measured on day 13) and overall survival, as calculated above. For survival analyses, the percent survivorship over

time was estimated using the two-sided Kaplan–Meier product method; differences between groups were compared using the log-rank test.

To deplete neutrophils, nude mice bearing IGROV-1 ascites were injected ip with the anti-Ly-6G antibody (clone 1A8; Affymetrix) 24 h before SM83 administration. In the Meth A model, mice were injected with 20 mg 1A8 antibody every second day, for 14 consecutive days, starting one day before SM83 treatment (day 7). The efficiency of polymorphonuclear leucocytes (PMNs) depletion in nude mice was tested by sampling the bone marrow (BM) 24 h after injection of the anti-Ly-6G antibody. Cells were double-stained with anti-CD11b/Ly-6G and cell populations were quantified by flow cytometry.

Primary tumors, lymph nodes and lungs were collected at the end of the experiments, dissected and lysed in 125 mM Tris HCl pH 6.8, 5% SDS for western blot analysis, formalin-fixed for paraffin inclusion (prepared by IHC facility of the Institute) and OCT-frozen for immunofluorescence (IF). IHC of mouse lungs were stained to detect MDA-MB231 cells by the facility of the institute using an anti-vimentin antibody (Dako). Primary tumors were also stained for the marker of cell proliferation KI67 and to detect the vasculature with the endothelial marker CD31 (data not shown), and by hematoxylin and eosin (H&E) stain.

4.10. Immunofluorescence

OCT-frozen primary tumors were cut in sections and laid onto poly-d-lysine–coated glasses, fixed in 4% paraformaldehyde (PFA) and permeabilized with PBS 0.1% Triton-X. Cells were then saturated 1 h with PBS BSA 2% and incubated with the anti-cleaved caspase-3 antibody diluted 1:400 in PBS BSA 1% for 2 h in a humidified chamber. Slides were then washed three times in PBS and incubated with a

(tetramethylrhodamine) TRITC-conjugated secondary anti-rabbit antibody (Life Technologies) for 45 min, washed again and mounted using coverslip with a drop of 4',6-Diamidino-2-phenylindole dihydrochloride (DAPI)-containing anti-fading mounting medium (ProLong Gold Antifade Mountant; Life Technologies).

Floating cells harvested from the ascites were prepared for double-marker immunofluorescence by centrifugation on slides using a cytospin cytocentrifuge. Briefly, acetone-fixed cells were re-hydrated in PBS and incubated 1 h with a primary antibody. Cells were then washed in PBS and incubated for 30 min with the appropriate Alexa Fluor 488-conjugated secondary antibody. After washing, slides were incubated for 30 min with another primary antibody, washed and incubated for 30 min with an Alexa Fluor 546-conjugated secondary antibody. The primary antibodies used were: rat anti-mouse CD11b mAb (1:200; BD Biosciences); rat anti-mouse Ly-6G mAb (1:200; BD Biosciences); and rabbit anti-HMGB-1 Ab (1:400; Abcam, Cambridge, UK). In some experiments, nuclei were stained with 40,6-diamidino- 2-phenylindole. Slides were mounted with Prolong medium (Life Technologies, Monza, Italy) and examined under a RADiance-2000 (Bio-Rad, Milan, Italy) Nikon-TE300 laser scanning confocal microscope (Nikon Instruments S.p.A, Florence, Italy).

4.11. Gene expression profiling

Primary tumors collected from MDA-MB231 NOD/SCID xenografts were collected 6 h after the last injection of SM83 and cut in pieces. One piece was lysed for RNA extraction using RNeasy Mini Kit (Qiagen) and then total RNA was retro-transcribed using SuperScript II Reverse Transcriptase kit (Life Technologies) and used for gene expression profiling (GEP) performed by the genomic unit facility using the Illumina HumanHT-

12_V4_0_R2 chip and results analyzed by the bioinformatic unit of the institute through R 2.15.2, packages: "lumi" and "limma" from Bioconductor. In this way, 50 genes were found significantly up-regulated and 15 down-regulated by SM83 treatment.

4.12. Wound healing-based migration assay

Wound healing experiments were performed using Culture-Insert in μ-Dish 35 mm (Ibidi). $2x10^4$ MDA-MB231 cells were transfected with an optimized reverse transfection protocol directly in the culture inserts in 12-well plates. After 72 h, inserts were removed, cells washed once to eliminate detached cells and multi-well plates put in a Cell-IQ instrument (CM-Technologies). Images were taken every hour for 24 h and analyzed with the provided software to measure the gap area. Data were then used to draw a sigmoidal curve with GraphPad Prism and determine the time necessary to close half of the wound area. In this way, 3 genes were selected, whose down-regulation significantly delayed the migration of MDA-MB231: Slug/Snai2, RING finger protein 144B (RNF144B) and (brain-derived neurotrophic factor) BDNF.

4.13. Cytokine quantification in ascitic fluid and cell culture medium

Conditioned medium of cell cultures and supernatant removed by centrifugation of the ascitic fluid collected from mice were stored at -80°C. Medium and ascitic fluid were then assayed for cytokines (human and murine TNF, and murine IL-1β, IL-4, IL-10, IFNγ and TGF-β through ELISA kits (Affymetrix) or used in blotting and in neutrophil assays.

4.14. Macrophage primary cultures and reporter gene assays

BM precursors were obtained from BALB/c and TLR4-KO mice and used to isolate

macrophages from the precursors by cultivation in RPMI medium 10% fetal calf serum containing 5 ng/ml macrophage colony-stimulating factor (MCSF). On day 5, the medium was replaced with fresh medium containing macrophage colony-stimulating factor. On day 7, adherent cells were harvested and phenotypically characterized by immunofluorescence using mAb to the macrophage markers CD11b and F4/80 (BD Biosciences). Up to 90% of the adherent population consisted of bone marrow-derived macrophages (BMDM). For *in vitro* experiments, $5x10^5$ BMDM were seeded in six-well plates, allowed to attach for 1 h at 37°C and then treated or not with 1 μM SM83. The release of TNF and IL-1β to the culture medium, after 3, 6 and 24 h, was evaluated using ELISA kits (Affymetrix). In viability experiments, $1x10^4$ cells were seeded in 96-well plates and exposed to serial dilutions of SM83 in the absence or presence of either 50 μM necrostatin-1 (Enzo Life Sciences) or 20 μM z-vad-fmk (Enzo Life Sciences). After 24 h, cells were examined morphologically by microscopy and tested for viability using the CellTiter-Glo (Thermo Scientific) assay. In other experiments, 10^4 RAW 264.7 macrophages (kindly provided by Dr. Sabina Sangaletti) were plated in 96-well plates, grown for 16 h and then treated or not with 1 μM SM83 for up to 24 h. The activation of the NF-kB promoter was assayed using the Dual-Luciferase Reporter Assay System (Thermo Scientific).

4.15. Spleen neutrophil preparation and assays

Neutrophils were obtained from BALB/c (wild-type) or TNF-R1-KO mice through immunomagnetic cell separation of a spleen cell suspension, using the Anti-Ly-6G MicroBead Kit (Miltenyi Biotec). Migration of neutrophils PMNs was tested using the Transwell system (Corning). Briefly, $5x10^5$ PMNs were placed in serum-free RPMI in the upper chamber of the Transwell insert. The lower chamber was filled with ascites

(1:20) or TNF in serum-free DMEM. PMNs were allowed to migrate for 24 h and then collected from the lower chamber. In some cases, experiments were performed by adding 100 mM HMGB-1 inhibitor glycyrrhizin (Sigma-Aldrich, St. Louis, MO, USA) to the top chamber.

4.16. High-throughput screening

The high-throughput screening was formerly performed in 2010 at the ICR. At day 1, 350 HeLa cells/well were seeded in 384-well white plates in 20 µl medium. At day 2, cells were treated with or without 100 nM SM83 followed by 3 Food and Drug Administration (FDA)-approved drug libraries at the final concentration of 1 µM. At day 3, plates treated with SM83 were further treated with 20 pg/ml izTRAIL and viability was tested at day 5 by CellTiter-Glo (Promega). Compound hits were selected due to their capability to enhance the cytotoxic activity of SM83/izTRAIL and then validated using the same HeLa cells employed in the screening. In validation experiments, SM83 and izTRAIL were administrated alone and in combination, also changing the schedule and pre-treating cells with SM83 24 h before izTRAIL or administrating these compounds simultaneously. On the basis of these results, validated hit compounds were tested in a panel of premalignant and cancer cell lines.

4.17. Detection of activated KRAS

Due to the lack of a specific antibody detecting the mutated form of KRAS, presence of oncogenic KRAS was determined indirectly by western blot of down-stream KRAS targets such as phosphorylated ERK1 and ERK2 or by RAS-GTP pull-down assay. In this case, 2.5 x 10^6 cells were seeded into 10 cm dishes. The next day, cells were incubated with and without 250 ng/ml of Dox. Cell lysis and RAS-GTP pulldown was performed: cells

were then lysed in 500 µl in ELB buffer (150mM NaCl, 50mM Hepes pH7, 5mM EDTA, 0,1% NP-40) supplemented with a cocktail of protease inhibitors. To fully detach lysed cells, they were scratched using a cell scraper and transferred into tubes for a 30-minute lysis at 4 °C on a rotator. Lysates were centrifuged at 13000 rpm for 30 min and cleared supernatants were transferred to a new tube. RAS-GTP was precipitated using beads coated with the Raf-1 Ras binding domain (RBD) recombinant protein. The following day, beads were washed 5 times with ELB buffer and precipitated protein complexes were eluted from the beads via boiling in SDS-Sample buffer for 10 minutes at 80°C. Proteins were separated by SDS-PAGE and analyzed by western blot. As control loading, proteins were stained by blue coomassie (Thermo Scientific Pierce).

5. RESULTS

5.1. Building the SM library

In 2007, we started a collaboration with the University of Milan aiming at the development of SM compounds. We designed and characterized several compounds. During my PhD studies, I focused on dimeric molecules and in particular on the SM83 compound. The novel dimeric compounds tested are covered by the patent WO/2013/124701 (PCT/IB2012/000297: 'Homo- and heterodimeric smac mimetic compounds as apoptosis inducers').

5.1.1. Quantification of SM affinity for the IAPs: a fluorescent polarization-based binding assay

In collaboration with the University of Milan, we built a library of about 140 novel SM compounds, both monomeric and dimeric, which were developed in order to increase the affinity for the BIR domains of XIAP, cIAP1 and cIAP2, but also to improve their pharmacokinetic features thus increasing the solubility, the ability to cross the biological membranes and also trying to reduce the molecular weight. In fact, small molecules are more likely to pass through the biological barriers and are usually characterized by increased bioavailability. All the newly synthesized compounds were tested to assess their purity (>98%) and then employed in cell-free assays to evaluate their affinity for the targets. Each SM was tested by the means of four tests with recombinant proteins containing the BIR3 and linkerBIR23 domains of XIAP, the BIR3 of cIAP1 (Table 2) and the BIR3 of cIAP2 (data not shown). In fluorescent polarization-based assays, we evaluated the capability of the new compounds to displace a fluorescent probe – monomeric when

testing the BIR3 alone, dimeric in the case of the linkerBIR23 of XIAP – from the recombinant proteins. Using serial dilutions of the SMs, it is possible to increasingly free the fluorescent probe and cause a reduction of the polarization that is measured as mP. This variation is detectable using a Tecan Ultra plate reader. By drawing a sigmoidal curve for each compound, we determined the concentration of the SM that displaced half of the probe, providing a quantification of the SM affinity for the recombinant receptor, i.e. the BIR domains.

Compound	XIAP-BIR3	cIAP1-BIR3	XIAP-lkBIR23
SM07[a]	80.7	12.6	3.3
SM12	293	<1 (0.6)	5.3
SM38	244	1.7	15.5
SM39	352	2.9	8.4
SM40	305	1.4	3.9
SM59[b]	41.2	<1 (0.7)	<1 (0.8)
SM74	181	1.4	5.9
SM75	179	3.8	3.2
SM76	157	3.5	2.3
SM83	25.4	5.4	<1 (0.8)
SM84	65.7	17.6	4.4
SM85	125	1.7	15.5
SM86	120	<1 (0.6)	16.2
SM87	37.5	<1 (0.7)	1.6
SM88	29.9	1.9	<1 (0.3)
SM107	26.7	2.6	<1 (0.8)
SM108	24.5	1.1	<1 (0.1)
SM109	26.0	1.5	<1 (0.2)
SM110	31.1	3.2	<1 (0.1)
SM111	31.2	1.5	<1 (0.1)
SM112	29.7	5.0	<1 (0.1)
SM131	24.9	<1 (0.9)	<1 (0.6)

Table 2. Affinities of dimeric SMs tested in fluorescent polarization-based assays. Affinities, expressed as concentration (nM) of dimeric SMs that can displace the 50% of the fluorescent probe (EC50) in binding assays, were evaluated using the recombinant proteins containing the BIR3 domain of XIAP, the BIR3 of cIAP1 or the region including the linker region upstream the BIR2, the BIR2 and the BIR3 domains. [a] Called Compound 3 elsewhere (Li *et al*, 2004); [b] Called SM-164 elsewhere (Sun *et al*, 2007).

In this experiment, we used also 2 standard compounds from other groups to compare our newly designed dimeric SMs to the ones already described in literature. These molecules were Compound 3 (Li *et al*, 2004; called SM007 by us) and SM-164 (Sun *et al*, 2007; SM59). Several of our SMs tested showed similar and even increased affinity towards the targets (Table 2), supporting the idea that the modifications introduced by us enhanced the binding affinity for the BIR domains and therefore potentially increased the efficacy of these compounds. This technique, already employed by us for the characterization of the monomeric SMs synthesized (Nikolovska-Coleska *et al*, 2004; Seneci *et al*, 2009), detected different binding potencies among our SMs and could easily be employed in the XIAP BIR3 assay. Unfortunately, in the case of the BIR domains of cIAP1, the affinities quantified were very similar to the sensitivity limit of this test, making the characterization of the diverse compounds extremely difficult.

5.1.2. *In vitro* toxicity of SMs

Only the SMs that showed an affinity for the expected targets were employed in viability assays to evaluate the cytotoxic activity using a panel of cancer cell lines. In fact, we wanted to focus only on the compounds that were target-specific, excluding the ones that could still be cytotoxic in cancer cells, but whose mechanism of action would have been difficult to predict. For this purpose, we selected the human triple negative breast carcinoma MDA-MB231, the promyelocytic leukemia HL-60 and the prostate adenocarcinoma PC-3 cell lines, which are known to display different sensitivities to SM treatments. Our dimeric SMs showed a nanomolar activity in MDA-MB231 and HL-60 cells, comparable to SM-164, while showing no or little effect in PC-3 cells (Table 3).

Compound	MDA-MB231	HL-60	PC-3
SM07[a]	*0.175*		
SM12	*3.28*		
SM38	*4.84*	7.39	>50
SM39	*3.32*		
SM40	*0.728*		
SM59[b]	0.039		
SM74			
SM75	*0.337*	0.128	>50
SM76	*1.60*		
SM83	0.055	0.071	>50
SM84	0.430		
SM85	*0.379*	0.935	>50
SM86	*0.567*		
SM87	*2.30*		
SM88	0.540		
SM107	45.4		
SM108	*10.6*		
SM109	46.9		
SM110	*0.582*		
SM111	10.7	20.6	>50
SM112	*1.28*		
SM131	>50		

Table 3. Toxicity of dimeric SMs. IC50 (μM) were measured in viability tests employing the human breast carcinoma MDA-MB231, acute promyelocytic leukemia HL-60 and prostate cancer PC-3 cell lines. [a] Called Compound 3 elsewhere (Li *et al*, 2004); [b] Called SM-164 elsewhere (Sun *et al*, 2007).

5.1.3. Characterization of SM83

On the basis of the capability to interact with the IAPs (5.1.1) and kill *in vitro* sensitive cancer cell lines (5.1.2), I decided to proceed with my studies focusing on the SM83 compound (Figure 11A). This molecule showed high affinity for the BIR domains of XIAP, cIAP1 (Table 2) and cIAP2 (data not shown) and was one of the most potent compounds in MDA-MB231 and HL-60 cytotoxic assays (Table 3). Furthermore, it showed good solubility making its use ideal for *in vitro* and *in vivo* experiments. Conversely, other SMs of the library such as SM74 were almost completely insoluble, and precipitated in the

medium and buffers used for cell culturing and mouse treatment. SM83 was then tested in pharmacokinetic tests to predict its employability *in vivo*, confirming that this compound is stable and soluble; it spreads *in vivo* reaching good concentrations in the plasma (Figure 11B) and crosses sufficiently the biological barriers despite the remarkable molecular weight (M.W.: 1409,54).

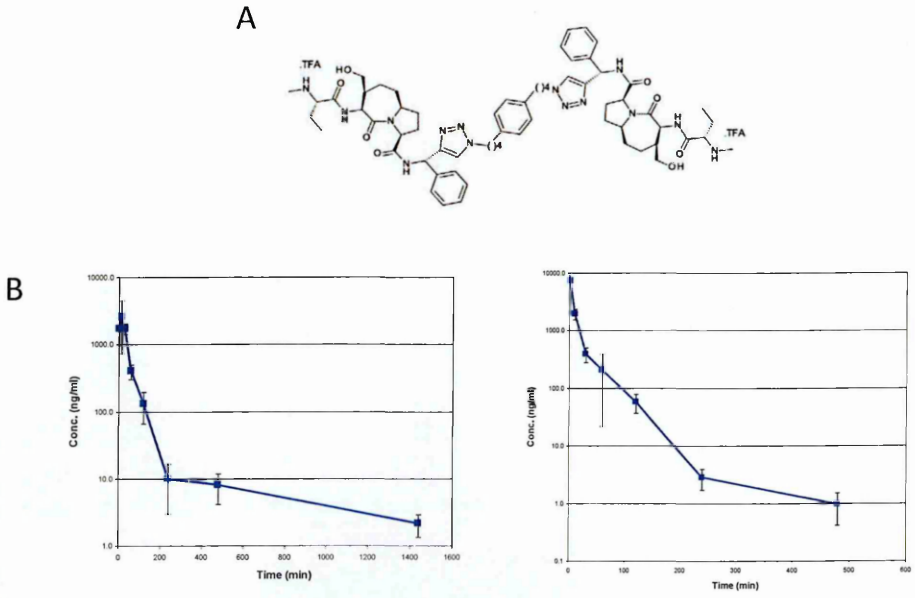

Figure 11. Molecular structure of SM83 and kinetic profiles of SM83. SM83 is a dimeric SM with nanomolar affinities for XIAP and cIAP1 (A). Mice were injected ip (2 mg/kg, left) or iv (5 mg/kg, right) with SM83 and the plasma levels of this SM were evaluated in time-course experiments (B).

5.2. Anti-tumor activity of SM83: the breast cancer model

5.2.1. Effect of SM83 treatment on IAPs

The interaction of SMs with the IAPs triggers the rapid proteasome-dependent degradation of cIAP1 and cIAP2 (Varfolomeev *et al*, 2007; Vince *et al*, 2007), while XIAP levels are usually not affected. Accordingly, SM83 rapidly depleted cIAP1 and cIAP2 in a

dose-dependent manner, without modifying the levels of XIAP (Figure 12, left). Importantly, many works showed that the SM-triggered degradation of cIAP2 is dependent on cIAP1 presence (Darding *et al*, 2011). In our experiments, cIAP2 is depleted by SM83 also in cells with down-regulated cIAP1 (Figure 12, right) suggesting a direct effect on cIAP2 and therefore the existence of different mechanisms by which diverse SMs deplete the cIAPs.

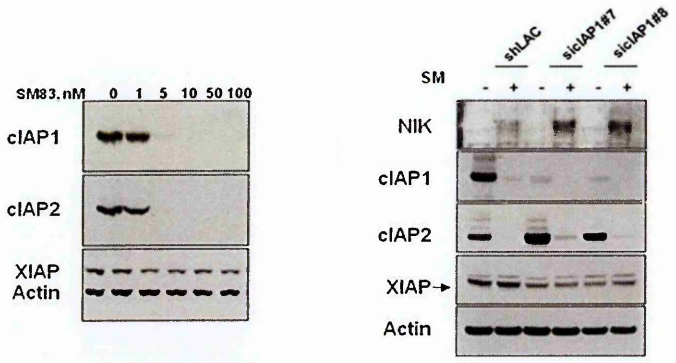

Figure 12. SM83 administration depletes cIAP1 and cIAP2 and allows the stabilization of NIK. MDA-MB231 cells were treated 3 h with SM83 at the indicated concentrations and western blot performed to detect the levels of SM targets cIAP1, cIAP2 and XIAP (left panel). MDA-MB231 cells were transfected with a non-targeting siRNA and with 2 different siRNAs specific for cIAP1 (right panel). After 72 h, cells were treated with 100 nM SM83 for 45 min and lysed. Western blot was performed to detect SM targets, as in the left panel, and NIK. Actin is shown as a loading control, the arrow indicates the specific XIAP band.

cIAP1 and cIAP2 constitutively ubiquitinate and cause the degradation of NIK (Varfolomeev *et al*, 2007; Vince *et al*, 2007); as expected, when they are depleted by SM83, NIK levels increase (Figure 12, right) and this protein activates the non-canonical NF-kB pathway resulting in cleavage of NF-kB2 p100 in p52 (Figure 13).

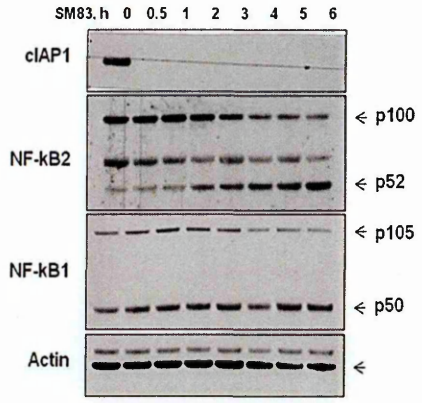

Figure 13. SM83-dependent depletion of cIAPs stimulates the activation of the non-canonical NF-kB pathway. MDA-MB231 cells were treated with 100 nM SM83 for the indicated time and harvested for western blot analysis. SM83 treatment causes the complete cIAP1 depletion already at the first time-point. The activation of the non-canonical NF-kB pathway is demonstrated by the cleavage of NF-kB2 from the p100 to the p52 form, while NF-kB1 (p105/p50), a transcription factor regulated by the canonical NF-kB pathway is not affected. Actin is shown as a loading control. Arrows indicate the specific bands.

5.2.2. Cytotoxic activity towards sensitive cancer cell lines

Initially designed to target XIAP and facilitate the apoptotic cascade triggered by other compounds (LaCasse *et al*, 2008), SMs were later shown to kill some cancer cell lines also in monotherapy (Petersen *et al*, 2007). It was demonstrated that the cell death strictly relies on the autocrine secretion of TNF that is further stimulated by SM administration and becomes toxic when cIAPs are depleted (Vince *et al*, 2007). In accordance with this mechanism, we observed that SM83 can kill some cancer cell lines also as a standalone and that its administration activates the apoptotic pathway triggered by caspase-8 (Figure 14).

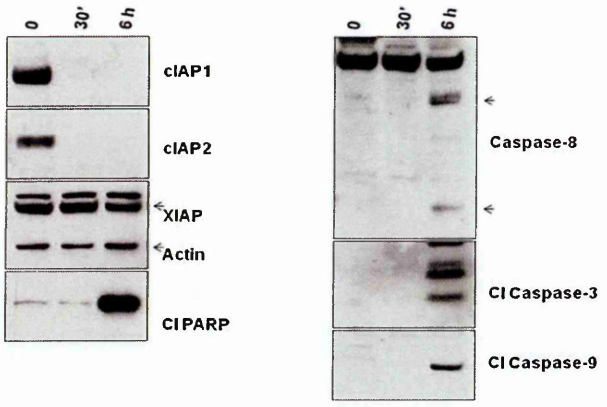

Figure 14. SM83 triggers a rapid apoptotic response in MDA-MB231 cells. MDA-MB231 cells were treated with 100 nM SM83 for the indicated time and harvested for western blot. SM83 rapidly depletes both cIAP1 and cIAP2 without affecting XIAP levels (left). The apoptotic activation is demonstrated by PARP (p89) and caspase-8 (p43/p41), -3 (p17/p19) and -9 (p37) cleavage (right). Actin is shown as a loading control. Arrows indicate the specific bands.

5.2.3. Combination of SM83 with TRAIL

SMs have been shown to kill a few cancer cell lines as standalones (Vince *et al*, 2007), but they can also be used to enhance the cytotoxic activity of other compounds (Probst *et al*, 2010). In particular, they synergize with the ligands of the TNF family such as TNF itself and TRAIL (Li *et al*, 2004). The latter combination is extremely interesting from a clinical point of view, because TRAIL treatment is well tolerated by patients and selectively kills cancer cells while sparing normal tissues. However, at the same time it is poorly effective *in vivo* due to short half-life and difficulty in reaching effective concentrations (Falschlehner *et al*, 2009). For this reason, we tested our SM83 *in vitro* in combination with soluble TRAIL as well as human $CD34^+$ expressing membrane-bound TRAIL (Lavazza *et al*, 2010). Our results clearly show that SM83 can enhance the cytotoxic activity of both sTRAIL and TRAIL-armed $CD34^+$ cells reducing the viability of both MDA-MB231 (Figure 15

left) and MDA-MB468 (Figure 15 right), by activating apoptosis (Figure 16).

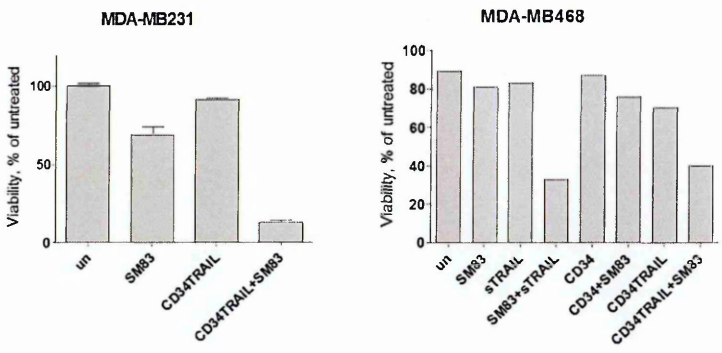

Figure 15. Viability of breast cancer cell lines treated with sTRAIL and TRAIL-armed CD34$^+$ cells in combination with SM83. MDA-MB231 (left) and MDA-MB468 (right) cells were treated with 50 ng/ml sTRAIL (izTRAIL) and/or CD34$^+$cells (ratio 1:1 with cancer cells) transduced with adenoviruses that allow the expression of membrane-bound TRAIL in combination with SM83 (50 nM for MDA-MB231, 100 nM MDA-MB468). Viability was measured by AnnV/PI staining after 24 h of treatment.

It is important to note that MDA-MB231 cells are sensitive to SMs in monotherapy, but MDA-MB468 cells are not, confirming that SMs can sensitize to other compounds also cancer cells intrinsically resistant to SMs. As expected, treatment with SM83 completely depleted cIAP1 and cIAP2, without affecting XIAP levels (Figure 16A), and resulted in the activation of an apoptotic event (Figure 16B and C). In fact, the cleavage of the initiator caspase-8 and the effector caspase-3 was clearly detectable especially in combination treatment by western blot, along with the accumulation of cleaved PARP. Employment of a fluorescence substrate of caspase-3/-7 further confirmed that MDA-MB231 are partially killed by SM83 and TRAIL-CD34$^+$ cells at the concentration used but the treatment becomes extremely more toxic when both SM83 and mTRAIL are administered (Figure 16C).

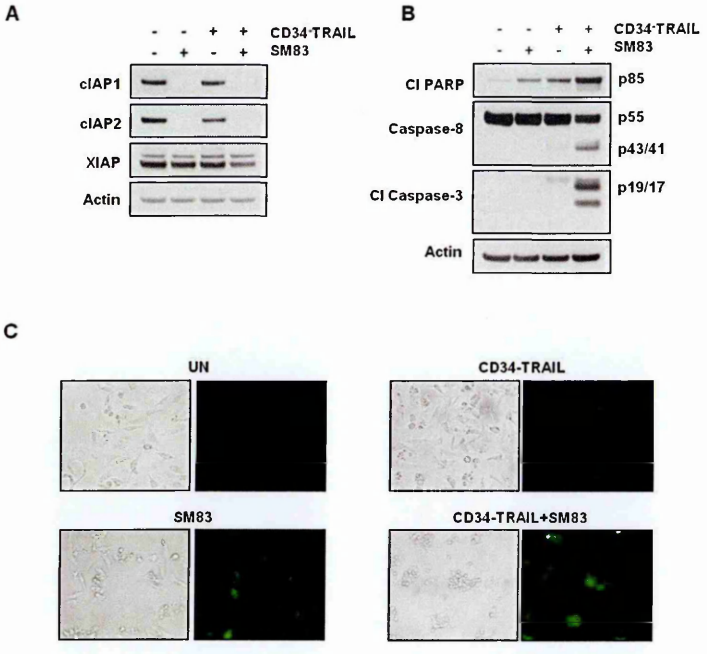

Figure 16. SM83 enhances the cytotoxic activity of mTRAIL by targeting the IAPs. MDA-MB231 cells were treated with 50 nM SM83 for 6 h with and without $CD34^+$ cells transduced with adenovirus carrying the sequence for membrane-bound TRAIL. Cells were then analyzed by western blot detecting SM targets cIAP1, cIAP2 and XIAP (A), and the markers of apoptosis cleaved PARP and caspase-3, and caspase-8 (B). Actin is shown as a loading control. Apoptosis was also evaluated using a fluorescent substrate of caspases -3 and -7 (C).

5.2.4. *In vivo* activity of SM83

To test the employability of SM83 also *in vivo*, we subcutaneously engrafted NOD/SCID mice with the triple negative breast cancer cell lines MDA-MB468 and MDA-MB231. Thirteen days after the inoculum, the animals were treated with ip daily injections of 5 mg/kg SM83 and primary tumors were measured with a caliper twice a week. The treatment resulted in a significant reduction of the primary tumor growth in both models (Figure 17A and B), meaning that SMs can be effective *in vivo* also against cancer cells that are *in vitro* resistant to the treatment. In fact, both MDA-MB231 and MDA-MB468 primary tumor volumes were reduced by about 50%. Importantly, the

inhibitory effect was independent from the administration route (ip vs iv) used (Figure 17C), and the primary tumors of treated mice started regrowing like the untreated ones after the interruption of the injections.

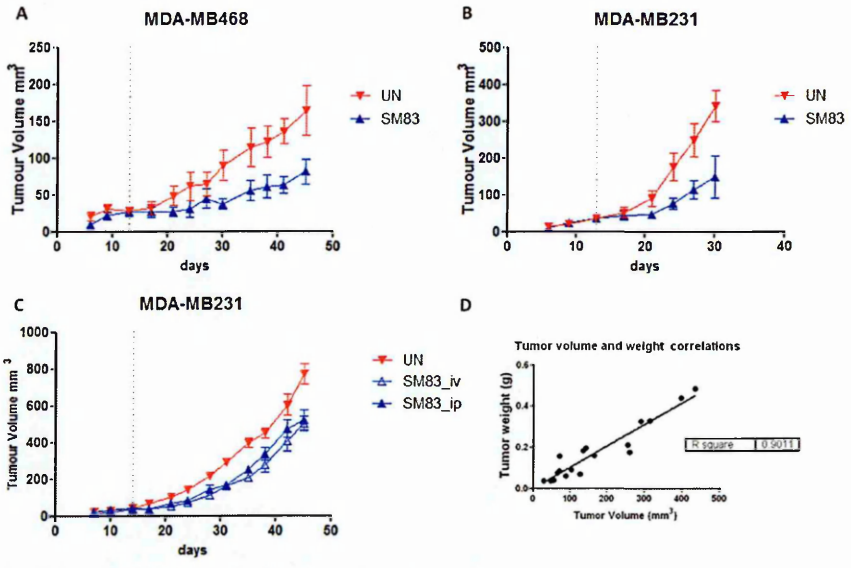

Figure 17. SM83 inhibits the primary tumor growth of human breast cancers in xenograft models. NOD/SCID mice were engrafted with $5x10^6$ MDA-MB468 (A) and MDA-MB231 (B). At day 13, animals were randomized and divided in two groups. One group was treated with daily ip injections of 5 mg/kg SM83 showing a reduction of primary tumor growth of about 50% compared to untreated animals in both models. The MDA-MB231 model was employed in an independent experiment (C) to compare the two different administration routes ip and iv confirming a similar efficacy of the treatment in both cases. Dash lines indicate the starting of the treatment. At the end of the experiment, animals bearing both MDA-MB468 and MDA-MB231 were euthanized and primary tumor collected and weighted, confirming a good correlation between the real tumor size and the one deduced by caliper measurement (D).

At the end of the experiment, mice were euthanized and primary tumors, lymph nodes and lungs collected. Primary tumors were weighted confirming a good correlation between the measurement of the tumor volume by caliper and its actual mass (Figure

17D). Furthermore, tumors were dissected and lysed for biochemical analysis and for RNA purification, and paraffin-embedded for IHC.

Protein lysates were then tested in western blots to detect the levels of SM83 targets and the markers of apoptosis. As expected, SM83 depleted cIAP1 (Figure 18) and cIAP2 (data not shown) also *in vivo* and, interestingly, also reduced the levels of XIAP (Figure 18). Conversely, despite the fact that tumors were collected 6 h after the last injection, little if any signs of activated apoptosis could be detected in western blots (Figure 18).

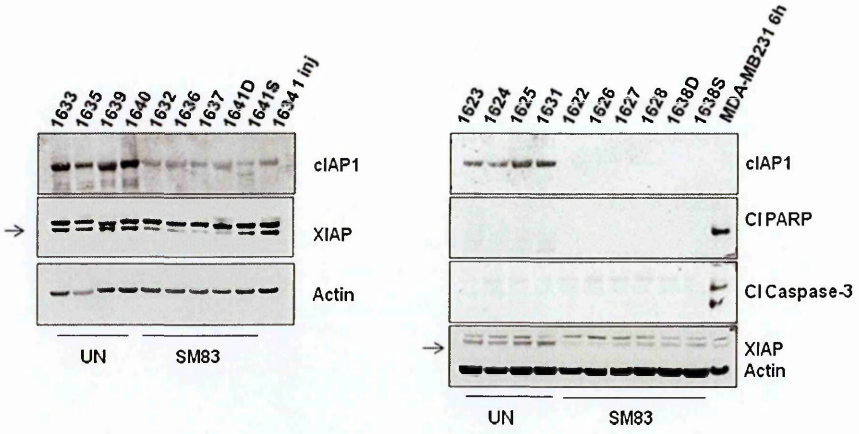

Figure 18. SM83 depletes cIAP1 in primary breast tumor xenografts. MDA-MB468 (left) and MDA-MB231 (right) primary tumors collected from animals treated as in figure 18A and B were collected 6 h after the last injections of SM83 and analyzed by western blot. Both models confirmed that SM83 depletes cIAP1 to undetectable levels while reducing XIAP only partially. No sign of apoptosis (cleaved PARP and caspase-3) was detectable in MDA-MB231 primary tumors. Actin is shown as a loading control. 1641D and 1641S, and 1638D and 1638S are primary tumors collected from the two flanks of the same animal (right and left, respectively). The mouse 1634 was treated with only one injection of SM83 6 h before tumor was collected. MDA-MB231 cells were treated *in vitro* with 100 nM SM83 for 6 h as a control of activated apoptosis.

As the absence of obvious apoptosis could be due to mechanisms of resistance

acquired after several treatments, we also collected tumors after one single SM83 injection and western blots were performed. Again, cleaved caspase-3 and reduction of caspase-8 were almost completely undetectable. Moreover, tumors were also OCT-embedded for caspase-3 immunofluorescence (figure 19 left). In this way, we observed that only few cells within the primary tumor undergo apoptosis, suggesting that the markers of apoptosis might be too faint to be detected in western blot, but also that SM83, despite maintaining an anti-cancer potential, is less efficient *in vivo* in inducing apoptosis at the doses used compared to the *in vitro* settings (Figure 19 right).

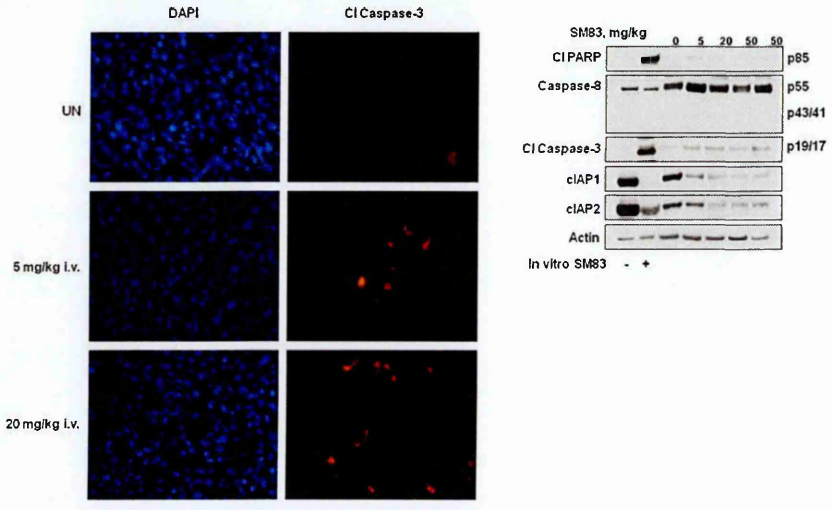

Figure 19. SM83 treatment activates a weak apoptotic event *in vivo*. Mice engrafted with MDA-MB231 cells were treated with one single injection of SM83 at the indicated doses. (Left) Primary tumors were collected and OCT-frozen 6 h after SM83 administration. Immunofluorescence reveals the activated form of caspase-3 showing that only few cells within the tumor are undergoing apoptosis. (Right) Primary tumors were collected from mice treated as in A and lysed for western blot. One single injection of SM83 was able to deplete cIAP1 and cIAP2 in a dose-dependent manner, but no signs of cleaved PARP, caspase-8 and -3 could be detected. MDA-MB231 treated 6 h *in vitro* with 100 nM SM83 are loaded as positive controls of activated apoptosis. Actin is shown as a loading control.

5.2.5. *In vivo* combination of SM83 with TRAIL-armed CD34$^+$ cells

After testing the *in vitro* activity of SM83 in monotherapy and in combination with TRAIL, and *in vivo* as standalone, the capacity of SM83 was also tested in order to increase the anti-tumor effect of TRAIL-armed CD34$^+$ cells in animal xenografts. For this, NOD/SCID mice engrafted with MDA-MB231 were treated with daily injections of 5 mg/kg SM83 plus 4 iv administrations with 10^6 TRAIL-armed CD34$^+$. Conversely, in the MDA-MB468 model, NOD/SCID mice were treated only 4 times with SM83 before the administration of TRAIL-armed CD34$^+$ cells.

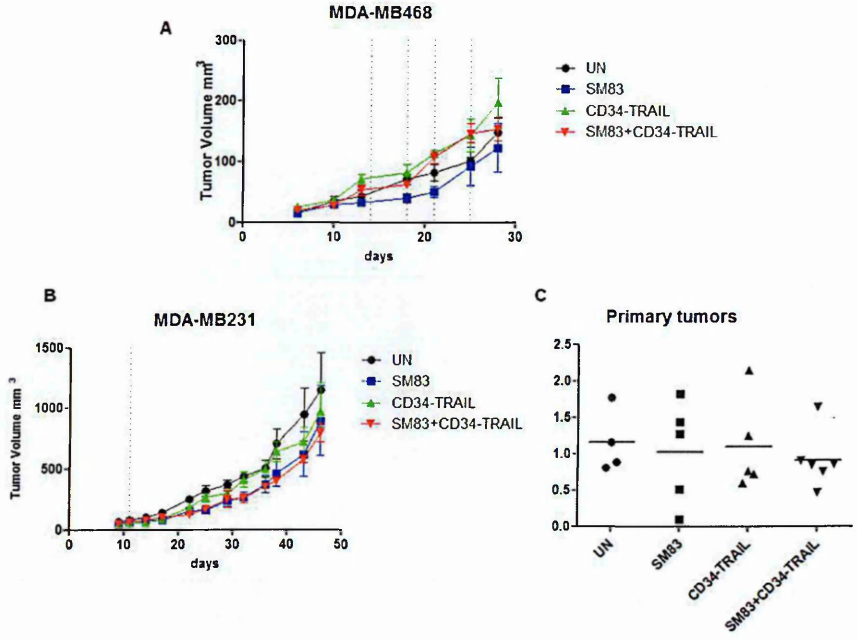

Figure 20. TRAIL-armed CD34$^+$ cells are ineffective against breast cancer primary tumors. NOD/SCID mice were engrafted with MDA-MB468 cells and treated 4 times with SM83 with or without CD34$^+$ cells expressing membrane-bound TRAIL (A). NOD/SCID mice were engrafted with MDA-MB231 cells and after 13 days treated with daily injections of 5 mg/kg SM83 plus 4 administrations of 10^6 TRAIL-armed CD34$^+$ cells (B). Two weeks after the last treatment, tumors were collected and weighted (g) revealing no significant difference among the animal groups (C).

In both cases, the outcome of the combination treatment on primary tumor was very modest and the reduction of tumor growth was only due to SM83 administration, while the combination with the TRAIL-CD34$^+$ cells had no effect (Figure 20). Again, after the interruption of the treatment, tumor started growing at the same rate in both treated and untreated animals, and tumor masses were similar in each group.

5.2.6. Anti-metastatic effect of SM83

MDA-MB231 cells spontaneously metastasize in immunosuppressed animals. Therefore, at the end of the *in vivo* experiment, lungs were collected and IHC stained to study a possible effect of SM83 treatment on lung metastasis. MDA-MB231 micro and macro-metastasis are easily detectable by IHC in the lung tissues because they express high levels of vimentin. Analysis of the number and size of the metastasis showed a significant reduction of spontaneous lung metastasis in animals treated with SM83. Of note, despite the fact that the combination with CD34$^+$ cells had no effect on primary tumors, it further increased the anti-metastatic effect of SM83 (Figure 21). Importantly, in an independent experiment, we tested the anti-metastatic effect of SM83 comparing two administration routes, i.e. intravenous and intraperitoneal injections (Figure 17C).

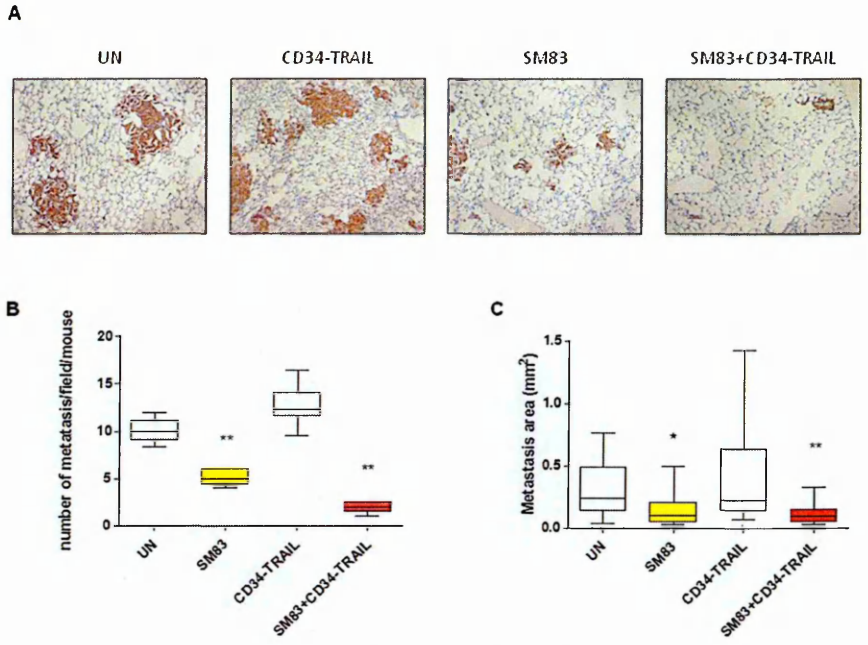

Figure 21. SM83 reduces spontaneous metastasis to the lungs. As MDA-MB231 cells are known to spontaneously metastasize to distal organs, lungs from mice of the experiments described in figure 20B were collected and paraffin-fixed. IHC of lungs with anti-vimentin revealed a reduction of the capability to form lung metastasis in animals treated with SM83 alone and in combination with TRAIL-armed $CD34^+$ cells (A). Analysis of the number (B) and size (C) of lung metastasis confirmed the anti-metastasis effect of SM83 treatment that was further increased in combination with TRAIL-armed $CD34^+$ cells. *p<0.05, **p<0.01

As for the effect on primary tumors, the different routes had the same effect on metastasis: both reducing in a significant fashion the number of lung metastasis (Figure 22). Of note, treatment with SM83 completely abrogated metastasis formation in some animals (Table 4).

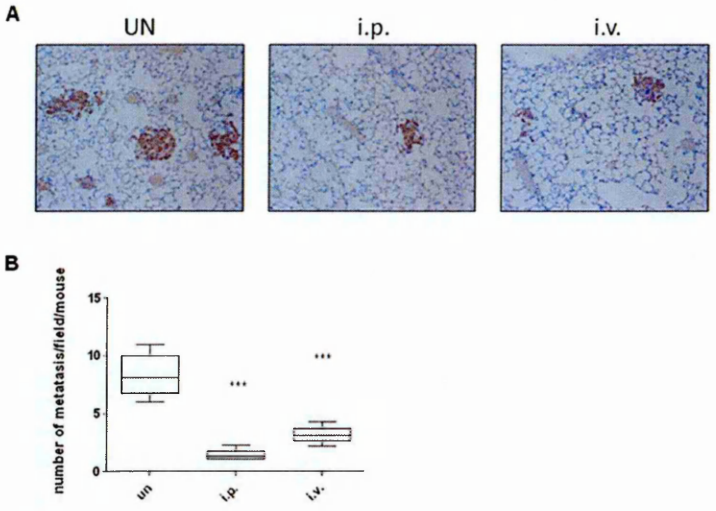

Figure 22. SM83 administration in monotherapy reduces the formation of lung metastasis independently of the administration route. Lungs collected from animals of the experiment 17C were collected and paraffin-embedded for IHC analysis with the anti-vimentin antibody to reveal lung metastasis (A). Analysis of the number of lung metastasis confirmed the anti-metastasis effect of SM83 treatment independently whether the compound was administered ip or iv (B). *** $P < 0.001$

Treatment	Metastasis-free mice
UN	0/7
SM83 i.p.	2/8
CD34-TRAIL	0/6
CD34-TRAIL + SM83	2/6
SM83 i.v.	3/6

Table 4. Summary of the various treatments of MDA-MB231 engrafted mice and number of the animals with no detectable lung metastasis. All NOD/SCID animals engrafted with MDA-MB231 cells developed detectable lung metastasis. A few animals treated with SM83, alone or in combination therapy, showed no metastasis formation, whilst treatment with TRAIL-$CD34^+$ did not prevent lung metastasis in any mice.

5.2.7. Modulation of tumor gene expression by IAPs

IAPs were initially thought to be essentially negative regulators of apoptosis, but it is

now clear that they are also apical modulators of several signaling pathways and control MAPK and NF-kB signaling. By causing the degradation of cIAP1 and cIAP2, and also targeting XIAP, SMs can thus influence the trans-activation of several genes. Therefore, we speculated that the anti-metastasis effect observed *in vivo* could be at least in part mediated by the inhibition of expression of genes involved in the metastatic process. For this reason, RNA was extracted from MDA-MB231 primary tumors collected in treated and untreated mice (Figure 17B), and gene expression analysis was performed. In this way, we identified 15 genes significantly down- and 50 up-regulated regulated by the treatment (Figure 23).

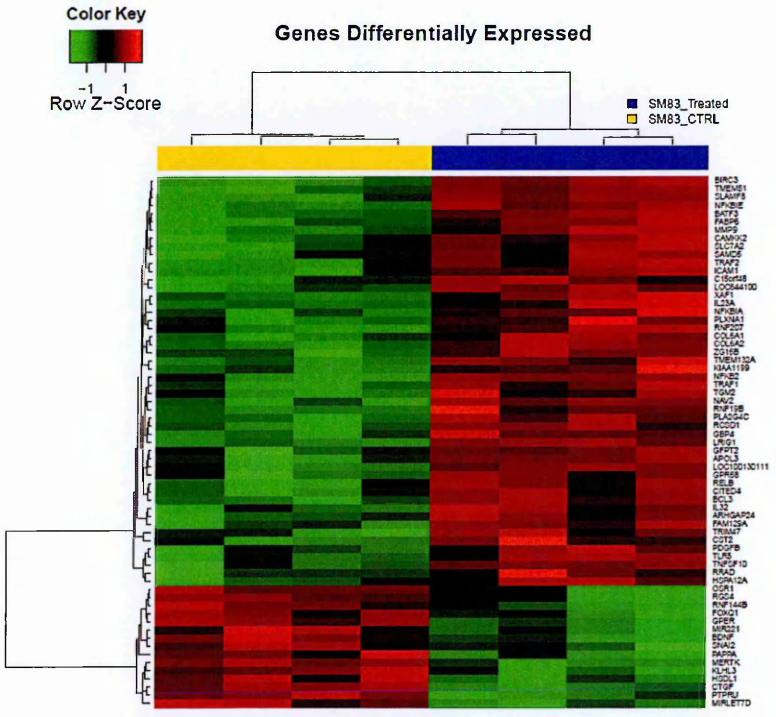

Figure 23. GEP of MDA-MB231 primary tumors collected 6 h after the last SM83 injection. Primary tumors of experiment as described in figure 17B were collected and lysed for RNA extraction. Gene expression profiles revealed that 65 genes were significantly modulated by SM83 treatment with 50 genes up-regulated and 15 down-regulated.

Many of the up-regulated genes are known targets of the NF-KB pathway (e.g. baculoviral IAP repeat containing 3/BIRC3, matrix metallopeptidase-9/MMP9, intercellular adhesion molecule 1/ICAM1) or are involved in its regulation (e.g. TRAF1, TRAF2, NFKBIA, NFKB2, RelB). To identify the genes responsible for the anti-metastasis effect of SM83, we individually knocked-down by siRNAs each of the genes down-regulated in the GEF. Transfected MDA-MB231 cells were then tested in proliferation experiments (data not shown) and wound-healing migration assays. In this way, we selected three genes, whose down-regulation prevents *in vitro* the motility of cancer cells: Snai2/Slug, RNF144B and BDNF (Table 5). As Snai2/Slug is a mediator of the EMT, a fundamental step in metastasis formation, we decided to focus on this gene.

	BDNF	SNAI2	RNF144B	PAPPA	KLHL3	PTPRU	FOXQ1	NT1	MERTK	GPER	CTGF	HSDL1	ANTIMIR221	RGS4	OSR1
T ½, h	19.69	17.71	14.21	11.67	11.04	10.54	9.697	8.78	8.45	8.403	8.348	7.444	7.034	6.09	5.117

Table 5. Effect of the silencing of the 15 genes selected by GEP on MDA-MB231 *in vitro* migration. The 15 genes shown to be down-regulated *in vivo* by SM83 treatment and identified by GEP (Figure 23) were silenced in MDA-MB231 cells that were then tested in wound healing assays. Wound area was measured every hour and values plotted to evaluate the time necessary to close half of the gap (T1/2, h). NT1 is a non-targeting siRNA used as control.

5.2.8. SM83 treatment reduces Snai2 levels *in vivo*

GEP of primary tumors treated with SM83 showed a reduction of the expression levels of Snai2; we then investigated whether there was a reduction also at the protein level. Tumors were thus analyzed by western blot that confirmed a significant reduction of Snai2 protein along with cIAP1 (Figure 24). Interestingly, MDA-MB468 tumors, which are poorly metastatic *in vivo*, showed Snai2 levels below the detection level, both in treated and untreated tumors.

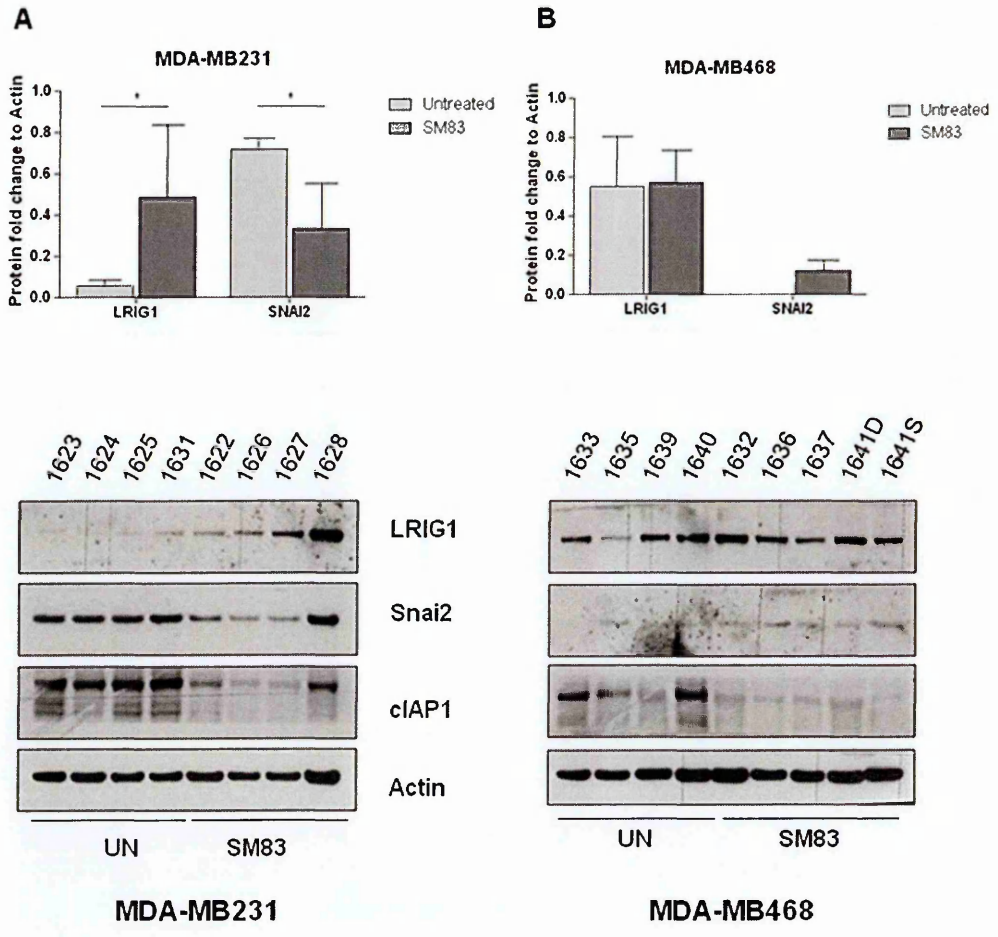

Figure 24. SM83 treatment reduces the levels of Snai2 protein in primary breast cancer xenografts. MDA-MB231 (A) and MDA-MB468 (B) primary tumors collected from experiments shown in figure 17B and 17A respectively were lysed for protein extraction and analyzed by western blot to detect Snai2 and LRIG1 levels, along with cIAP1. Actin is shown as a loading control. Upper panel show the densitometric analysis of the western blot shown in the lower panels. * $p<0.05$

5.2.9. cIAP1, but not cIAP2, depletion is responsible for Snai2 down-regulation

To investigate whether SM83 treatment is sufficient to reduce the levels of Snai2, MDA-MB231 cells were treated also *in vitro* for 6 h (Figure 25A) or in time-course experiments (Figure 25B). These experiments confirmed that the targeting of the IAPs reduces the levels of this protein. Furthermore, as SMs are known to target at least three

members of the IAP family – cIAP1, cIAP2 and XIAP – and cause the degradation of cIAP1 and cIAP2, we silenced these proteins in order to investigate whether their reduction is sufficient for Snai2 decrease (Figure 25A). By western blot, we observed that cIAP1 targeting, but not cIAP2, affects Snai2 levels suggesting that cIAP1 is the IAP responsible for sustaining the levels of this pro-metastasis gene. As SM83 treatment is toxic for MDA-MB231, we also checked that the reduction of Snai2 does not stem from an SM83-related cytotoxic effect by pre-treatment of the cells with inhibitors of apoptosis and necroptosis. As Snai2 levels are reduced in the same manner also in the presence of death blockers (Figure 25C), we concluded that this effect is due to cIAP1 targeting and not to a toxic side-effect. Moreover, to test whether cIAP1 regulates Snai2 only in a cell-type manner or whether this effect is reproducible also in other cells, a panel of breast cancer cells was treated with SM83. By western blot, we found that only few cell lines express high levels of Snai2, and SM83 administration reduces its levels also in BT-549 cells (Figure 25D).

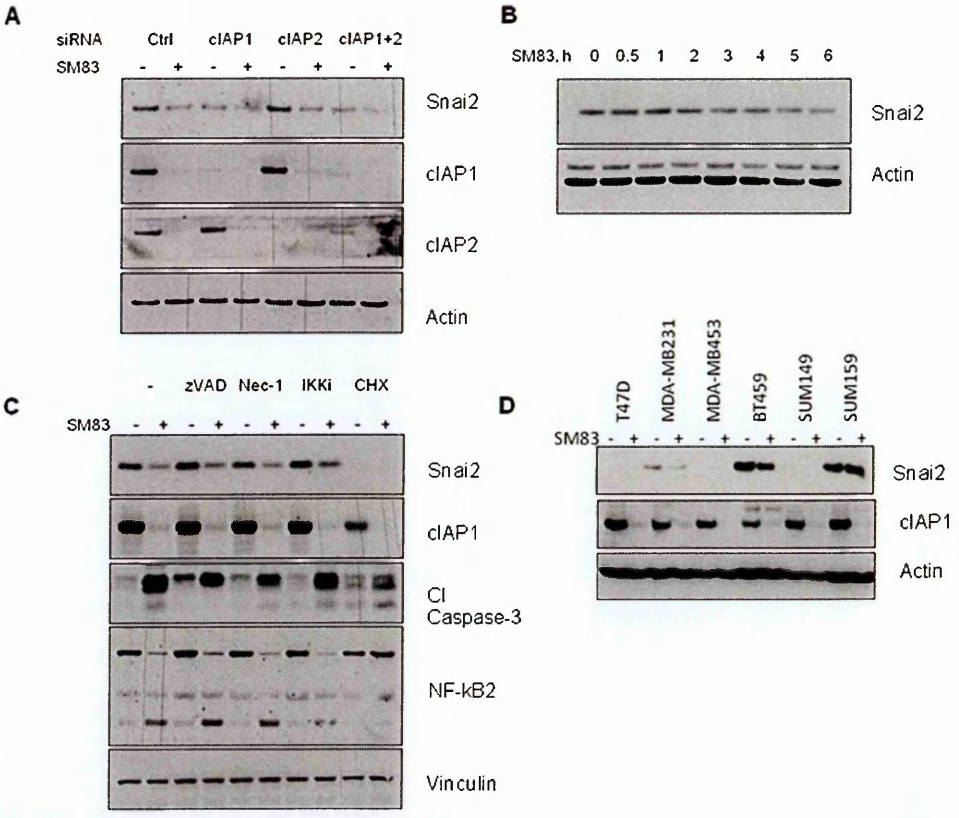

Figure 25. SM83-mediated depletion of cIAP1 down-regulates Snai2 levels. MDA-MB231 cells were transfected with siRNAs targeting cIAP1 and/or cIAP2 and treated with 100 nM SM83 for 6 h or left untreated. Western blot was performed to detect cIAP1, cIAP2 and Snai2 showing that cIAP1 silencing or depletion due to SM83 treatment reduces the levels of Snai2 (A). Time-course experiments showing the reduction of Snai2 after 100 nM SM83 administration (B). MDA-MB231 cells were pre-treated for 1 h with caspase inhibitor z-VAD, RIP1 inhibitor Nec-1, IKK inhibitor and the protein translation inhibitor CHX, and then treated with 100 nM SM83 for 6 h. Levels of Snai2 were studied whereas cIAP1, cleaved caspase-3 and NF-kB2 were detected to confirm the efficacy of IKKi, SM83 and zvad administration. Only prevention of the NF-kB pathway partially blocked the SM83-dependent down-regulation of Snai2 (C). The capacity of SM83 to reduce the levels of Snai2 was confirmed also in other human breast cancer cell lines (D). Actin and vinculin are shown as loading controls.

5.2.10. Activation of the non-canonical NF-kB pathway correlates with Snai2 reduction

cIAP1 and cIAP2 are known to negatively regulate the non-canonical while promoting the canonical NF-kB pathway. SM-mediated cIAP1 depletion thus results in the opposite effect, i.e. stimulation of the non-canonical NF-KB pathway and prevention of the activation of the canonical one. To understand which of these events is responsible for the reduction of Snai2, we silenced several mediators of the NF-kB pathways and stimulated MDA-MB231 cells with SM83. As expected, Snai2 was down-regulated by SM83 in cells transfected with a non-targeting siRNA, but depletion of NIK and NF-kB2 resulted in stabilization of Snai2, strongly suggesting that the activation of this pathway inhibits Snai2 expression (Figure 26A). Moreover, we treated the MDA-MB231 cells with TWEAK, a ligand of the TNF family, which preferentially activates the non-canonical NF-kB pathway. In accordance with SM83 treatment, TWEAK administration resulted in lower levels of Snai2 (Figure 26B). In clear contrast, TNF administration stimulated Snai2 levels (Figure 26C).

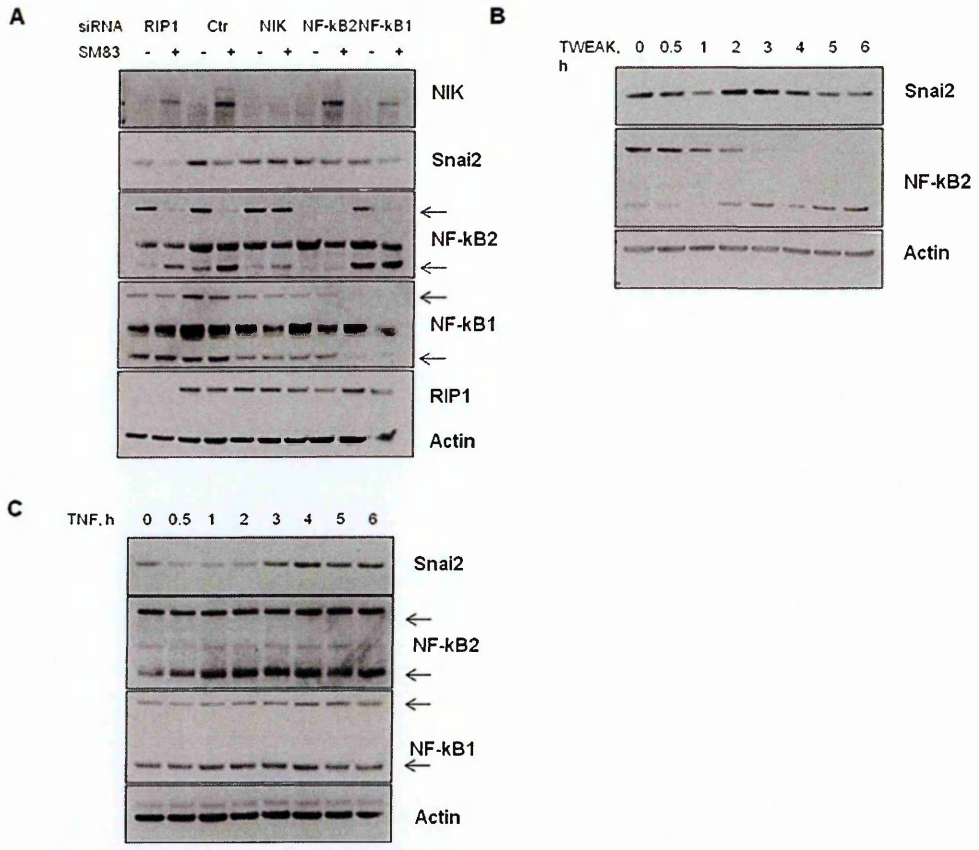

Figure 26. Snai2 down-regulation correlates with non-canonical NF-kB activation. MDA-MB231 cells were transfected with siRNA targeting several mediators and regulators of the NF-kB pathway. After 72 h, cells were treated with 100 nM SM83 for 6 h and harvested. Western blot revealed that prevention of the non-canonical NF-kB activation by down-regulation of NIK and NF-kB2, blocked SM83-mediated Snai2 down-regulation (A). The MDA-MB231 cell line was treated with 200 ng/ml TWEAK, a ligand that preferentially activates the non-canonical NF-kB pathway, in a time-course experiment. Western blot shows that TWEAK-mediated activation of the non-canonical NF-kB pathway correlates with the down-regulation of Snai2 (B). On the contrary, stimulation of the MDA-MB231 cells with 50 ng/ml TNF stimulated the expression of Snai2 (C). Actin is shown as a loading control.

5.3. Affecting the immune system: the ovarian model

Besides the investigation of SM83 activity in a model that is intrinsically sensitive to SM treatment such as the MDA-MB231 cell line, we also studied different models, using cell lines resistant to SMs *in vitro*. Furthermore, as SMs are known to modulate cancer microenvironment by causing the secretion of several cytokines, we tested the efficacy of SM83 in cancer ascites models, in which the environment greatly controls the tumor development and it is easy to detect cytokine levels and the number of cells, by collecting the ascitic fluid.

5.3.1. *In vitro* activity of SM83 against ovarian cancer cell lines

Despite SM83 showing a good cytotoxic activity in monotherapy towards few cancer cell lines such as MDA-MB231 and Kym-1, it is unable to trigger apoptosis in the vast majority of cancer cell lines. Nonetheless, as shown above, SM83 can enhance the *in vitro* activity of other compounds in combination therapy. Due to this property, ovarian carcinoma IGROV-1 cells, not affected by SM83 treatment as a standalone (Figure 27A), are killed in combination with TRAIL and this is caused by the activation of the apoptotic pathway as demonstrated by PARP cleavage (Figure 27B and C). To compare the *in vitro* capacity of SM83 to activate apoptosis in combination with TRAIL with a literature standard, IGROV-1 were also treated with SM-164 (SM59), showing almost the same cytotoxic activity in this model (Figure 27C).

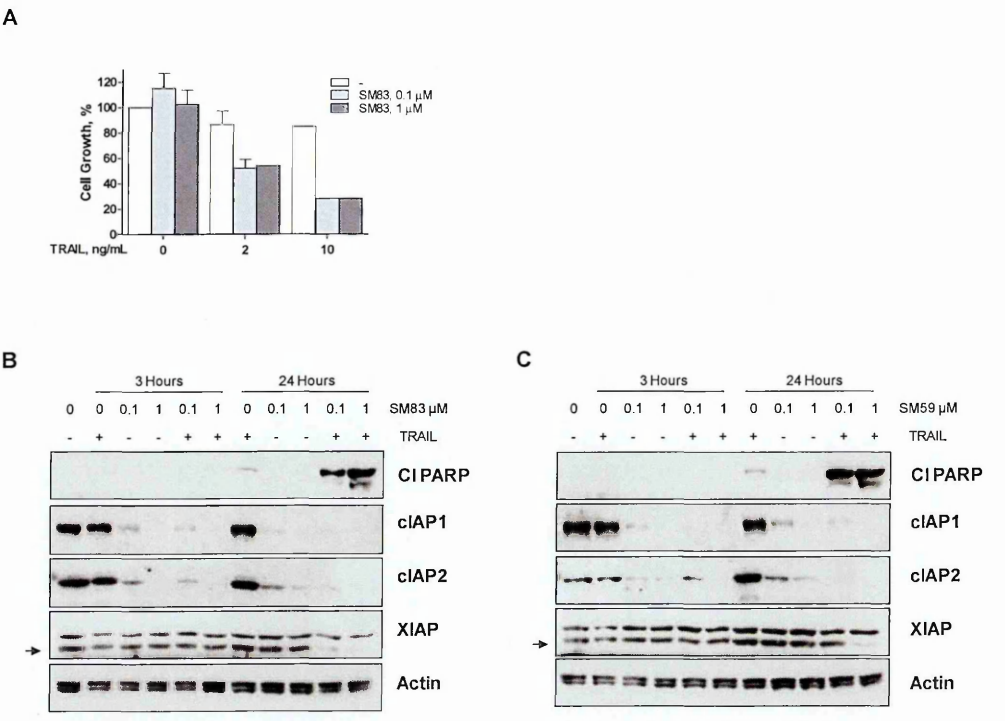

Figure 27. SM83 enhances the pro-apoptotic activity of TRAIL. (A) IGROV-1 cells were treated with 0.1 or 1 µM SM83 alone or in combination with 2 or 10 ng/mL TRAIL and cells counted after 72 h. Cell growth is expressed as a percentage relative to cells mock-treated with vehicle. Values are shown as mean with standard deviation (SD). Western blot analysis of XIAP, cIAP1, cIAP2 and cleaved PARP (Cl PARP) in IGROV-1 cells treated 3 or 24 h with 0.1 and 1 µM SM83 (B) or SM59 (C) in the absence or presence of 10 ng/mL TRAIL. Actin is detected as a loading control. Arrows show the specific XIAP band.

5.3.2. *In vivo* activity of SM83 in cancer ascites

IGROV-1 cells can grow both *in vitro* and *in vivo*, injected subcutaneously and in the peritoneum of immunosuppressed mice. In the latter case, tumor cells develop cancer ascites constituted by ascitic fluid heavily infiltrated with cells of the immune system such as macrophages and neutrophils, and floating cancer cells. Furthermore, tumor nodules develop in the inner side of the peritoneum wall. To investigate whether SM83 displays an anti-tumor effect also *in vivo*, ascites-bearing *nude* mice were daily injected with this

compound in monotherapy or in combination with TRAIL (Figure 28A). As a control of the efficacy of our compound, mice bearing IGROV-1 ascites were also treated with the SM-164 compound (Figure 28B).

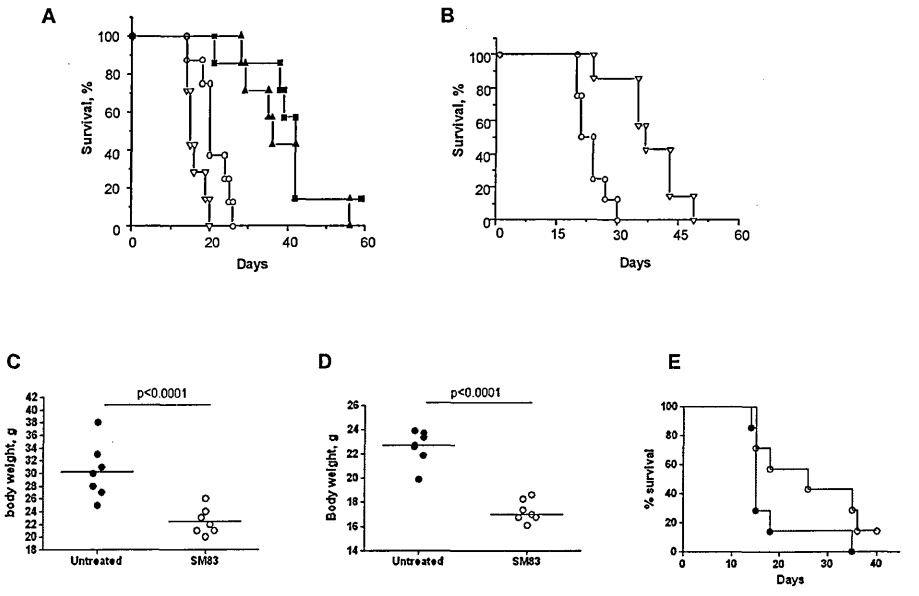

Figure 28. SMs increase the survival of mice engrafted bearing cancer ascites. (A) Nude mice were injected ip with IGROV-1 cells and left untreated (O) or treated 5 times a week, with 5 mg/kg SM83 (▲), 2.5 mg/kg TRAIL (▽), or with the same doses of SM83 and TRAIL together (■). Treatment lasted for 2 consecutive weeks and started the day after injection. Each treatment group contained 7 mice. Survival curve for SM83-treated mice and controls is shown. (B) Survival curve for SM59-treated and control mice. Untreated (O) or treated with SM59 (▽). (C) The formation of ascites was checked by monitoring body weight on day 17. BALB/c mice were injected with Meth A cells and, starting on day 7, were treated daily with 5 mg/kg SM83. (D) The formation of ascites was checked by monitoring body weight on day 13. The horizontal line represents the mean. (E) Survival curve for untreated (●) or mice treated with SM83 (O) starting from day 7.

Surprisingly and conversely to what was observed *in vitro*, SM83 treatment was effective also in monotherapy, reducing the mouse ascites volumes (Figure 28C) and

prolonging mouse survival (Figure 28A). The comparison with SM-164 showed little differences of activity between the two compounds (Figure 28B). Interestingly, the combination with TRAIL did not increase the efficacy of the treatment; once more supporting the idea that SMs can display different effects and mechanisms of activity *in vitro* and *in vivo*. To further assess whether the SM83 anti-tumor effect observed in IGROV-1 ascites was reproducible and not restricted to the model used, SM83 was used to treat immunocompetent BALB/c mice injected with syngenic Meth A cancer cells, which form ascites too. Even using this model, SM83 treatment reduced the ascites volume (Figure 28D) and increased mouse survival (Figure 28E).

5.3.3. SM83 rapidly kills the cancer cells within the ascites

To understand the mechanism of SM83 activity *in vivo*, mice bearing IGROV-1 ascites were injected once with SM83 and the ascitic fluid was collected at different time points. Detached tumor cells were counted, showing a striking decrease in SM83-treated mice at 24 h compared to the control of untreated mice, without appreciable changes at 3 or 6 h (Figure 29A). The autopsy revealed neither cancer cell peritoneal wall adhesion nor migration outside the peritoneum. Furthermore, a significant increase of human cytokeratin-18 was detected in the serum of mice treated for 24 h (Figure 29B). Since this protein is released from dying epithelial cells, this observation strongly supports the idea that SM83 treatment was reducing the number of human tumor cells within the ascites by killing them.

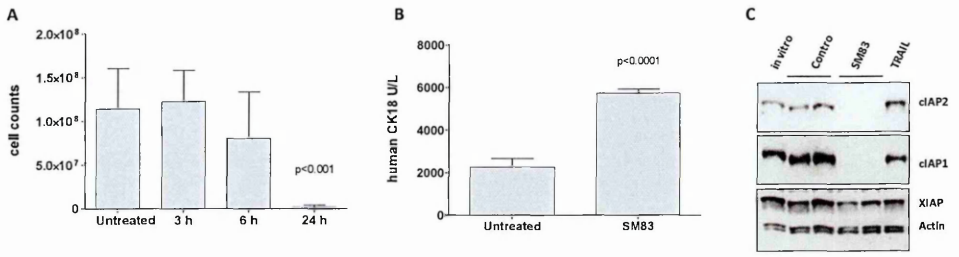

Figure 29. SM83 rapidly kills the IGROV-1 cells floating in mouse ascites. (A) The ascitic fluids were collected from nude mice injected with IGROV-1 cells and left untreated or treated with a single injection of SM83 (5 mg/kg). The graph shows the number of tumor cells within the ascites of untreated animals (n=11) or of animals treated for 3 h (n=4), 6 h (n=4) and 24 h (n=9). Data are mean and SD. (B) Levels of human cytokeratin-18 in the serum collected 24 h after a single dose of SM83 (5 mg/kg) or after no treatment. (C) Western blot of the SM targets in IGROV-1 cells cultured *in vitro* or recovered from the ascites of control mice (n=2) or mice treated with SM83 (n=2) or TRAIL for 24 h. Actin is shown as the loading control.

To investigate the mechanism responsible for cancer cell killing, the tumor cells present in the ascites were lysed and used in western blot analysis that confirmed the capacity of SM83 to trigger, also *in vivo*, the degradation of cIAP1 and cIAP2. As expected, XIAP was only slightly affected by the treatment (Figure 29C).

Moreover, in an attempt to understand the cell death mechanisms responsible for the rapid decrease of floating tumor cells, we detected the markers of activated apoptosis at different time points. At 24 h, SM83 treatment led to a faint increase of cleaved PARP, there was no evidence of cleaved, active caspase-8 and only a modest effect on cleavage of caspase-3 (Figure 30A). As control, we also detected these apoptotic markers in ascites cells treated with TRAIL, which, despite being ineffective in reducing the ascitic cell number, still showed a greater activation of apoptosis (compare figure 30A

and B).

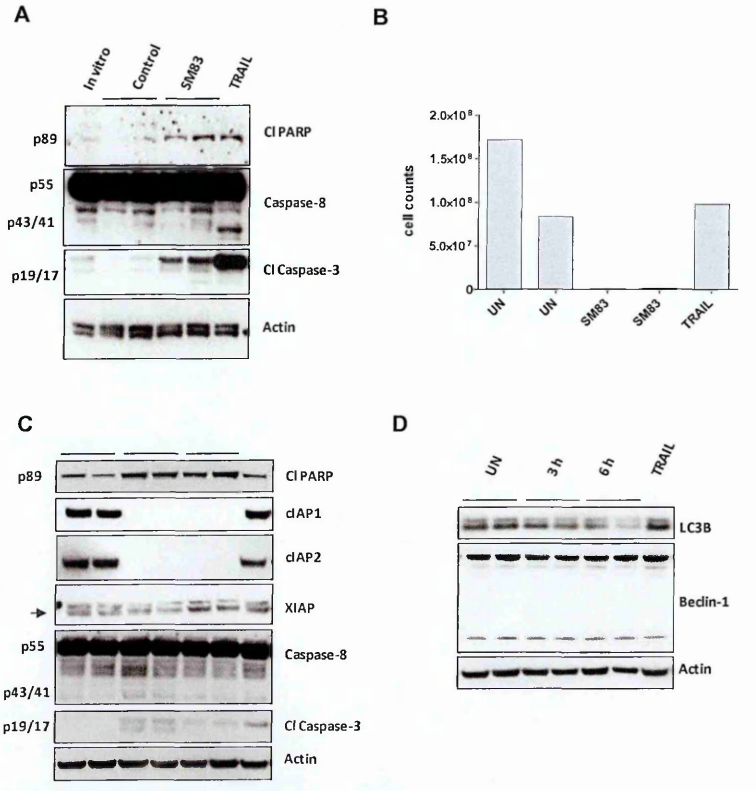

Figure 30. SM83 kills the cancer cells within the ascites mainly by a non-apoptotic mechanism. (A) Western blot showing the activated apoptosis markers cleaved PARP (p89), caspase-8 (precursor p55 and cleaved form p43/41) and cleaved caspase-3 (p19/p17) in IGROV-1 cells cultured *in vitro* or recovered from the ascites (24 h) of control mice (n=2) and of mice treated with 5 mg/kg SM83 (n=2) or 10 mg/kg TRAIL. Actin is shown as a loading control. (B) Tumor cell counts from ascites of untreated nude mice (2 mice, UN) or treated with 5 mg/kg SM83 (2) or 2.5 mg/kg TRAIL for 24 h. (C) Western blot of apoptotic markers in tumor cells collected from the ascites of untreated mice (n=2) or from mice treated for 3 or 6 h with SM83 (n=2 for both) or with TRAIL for 24 h. Arrow, specific band for XIAP. (D) Western blot to detect the autophagy mediators LC3B and beclin-1 in IGROV-1 cells harvested from the ascites of mice untreated (UN) or treated with a single dose of 5 mg/kg SM83 and collected at the indicated times, or treated with 2.5 mg/kg TRAIL and collected 24 h later. Actin is the loading control.

In an attempt to detect the apoptotic events, western blot analysis was performed with cells collected after 3 and 6 hours of treatment. Also in this case, SM83 caused the complete degradation of cIAP1 and cIAP2, but only a faint accumulation of the active forms of PARP, caspase-8 and caspase-3 (Figure 30C). The low activation of the apoptotic cascade suggested that the cause of tumor cell death was not mainly apoptotic. To test the possibility that autophagy was responsible for the loss of ascites tumor cells, we measured the levels of beclin-1 and of cleaved LC3B. Autophagy in fact is usually considered a protective cell mechanism to environmental insults but, when abnormally and continuously activated, it can also lead to cell death. Nonetheless, as SM83 treatment did not increase the levels of these proteins (Figure 30D), we concluded that autophagy was not involved in SM83-induced tumor cell death, strongly suggesting that the death was more likely to be necrotic.

5.3.4. SM83 triggers the secretion of pro-inflammatory cytokines *in vivo*

Since SM83 cell killing in monotherapy is known to be dependent on autocrine TNF secretion of sensitive cancer cells, we measured the levels of inflammatory cytokines in the ascites. There was a basal level of murine TNF in the ascites of untreated mice that significantly increased after SM83 treatment at 3 and 6 h, but not at 24 h (Figure 31A). Conversely, human TNF was at first not affected by SM83 treatment, but increased after 6 h probably stimulated also by murine TNF (Figure 31B).

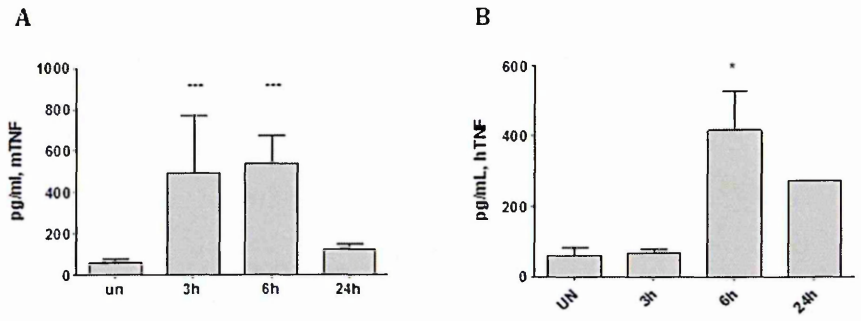

Figure 31. SM83 rapidly induces the secretion of mouse TNF, which also stimulates the production of cancer cell TNF. Nude mice were injected ip with IGROV-1 cells and treated or not treated with a single dose of 5 mg/kg SM83; ascites was collected 3, 6 and 24 h after SM83 administration. (A) SM83 transiently increased the level of murine TNF measured by ELISA. (B) Levels of human TNF in ascites of untreated nude mice or after 3 h of treatment with a single injection of 5 mg/kg SM83. * $P < 0.05$, *** $P < 0.001$

To test the relevance of TNF in this model, mice were then pre-treated with two inhibitors of TNF, Etanercept and Infliximab. High doses of Etanercept completely prevented the cytotoxic effect of SM83 (Figure 32A). Importantly, Etanercept did not affect SM83-triggered degradation of cIAPs (Figure 32B). This demonstrates that the production of TNF is the determining factor responsible for SM-mediated toxicity, while the down-regulation of the cIAPs is a direct effect of SM83 administration. However, it is not sufficient to kill cancer cells on its own. Overall, these data suggest that SM83 *in vivo* cytotoxic activity stems from the stimulation and secretion of murine TNF, which rapidly kills the detached cancer cells within the ascitic fluid. Also human TNF, produced by IGROV-1 cells in response to mouse TNF, might play a role in cancer cell killing. Of note, Infliximab, which is more specific for human than mouse TNF, failed to rescue cells (data not shown), contrary to Enbrel (a much broader TNF blocker). However, we cannot exclude the fact that the different outcome observed is only due to the doses used and

not to a different role played by human and mouse TNF.

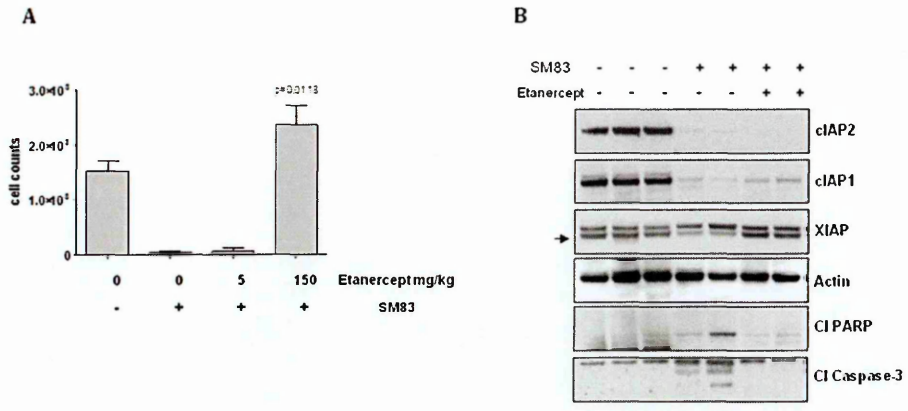

Figure 32. SM83-mediated killing of cancer cells within ascites is TNF-dependent. (A) SM83 treatment reduces the number of cancer ascites cells, but this effect is prevented when TNF is blocked with high doses of Etanercept. (B) Western blots of ascites tumor cell protein from untreated mice and mice treated with SM83 alone or in combination with 150 mg/kg Etanercept. Arrows indicate the specific band for XIAP.

As TNF is a pro-inflammatory cytokine, we checked whether the SM83-dependent secretion of TNF was indeed stimulating a pro-inflammatory environment and therefore tested murine cytokines IL-1β and IFN-γ levels in the ascitic fluid. Interestingly, we found that they were all up-regulated in response to SM83 administration (Figure 33A and B). In clear contrast, the levels of some immunosuppressive cytokines, such as IL-10, TGF-β and IL-4, remained mostly unchanged, with the exception of IL-4, which significantly increased at 24 h, most likely secreted to restrain the strong inflammation in process (Figure 33C, D and E).

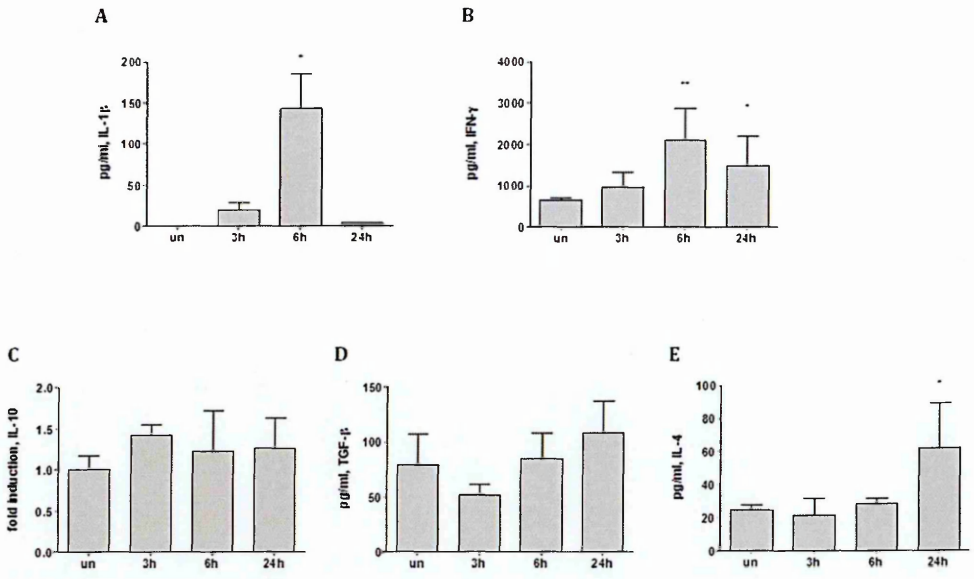

Figure 33. SM83 triggers the secretion of pro-inflammatory cytokines *in vivo*. Nude mice bearing IGROV-1 cancer ascites were treated or not treated with a single dose of 5 mg/kg SM83; ascites was collected 3, 6 and 24 h after SM83 administration. ELISA results for IL-1β (A), IFN-γ (B), IL-10 (C), TGF-β (D) and IL-4 (E) in the ascitic fluid of mice treated as above. Results for IL-10 are shown as fold induction due to the lack of recombinant protein standard.

5.3.5. SM83 is toxic for macrophages and stimulates their cytokine secretion

To test if the pro-inflammatory effect of SM83 relied on the activation of macrophages, BMDMs from BALB/c mice were treated *in vitro* with SM83 and the cell supernatants assayed for TNF and IL-1β levels. As expected, SM83-stimulated macrophages secreted TNF and also IL-1β at later time points (Figure 34A and B). Moreover, as macrophage activation depends on the NF-κB pathway, we checked whether SM83 modulated this pathway. For this purpose, we employed a macrophage cell line stably transfected with a luciferase reporter gene under the control of the NF-κB response element. NF-κB activation was rapidly detectable after SM83 administration but returned to basal levels after 24 h (Figure 34C).

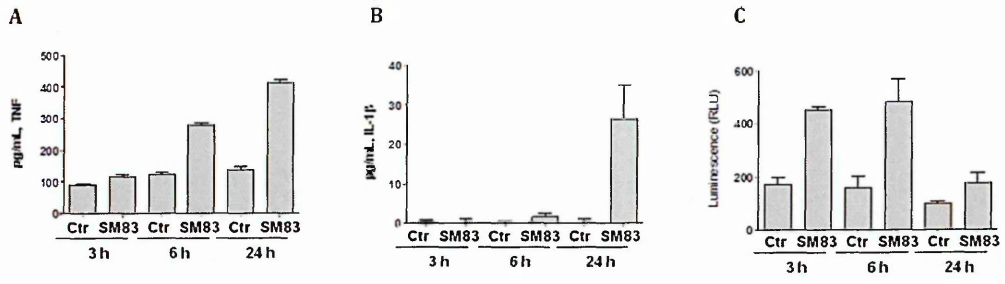

Figure 34. SM83 stimulates macrophage TNF, IL-1β secretion and NF-kB activation. BALB/c BMDMs were treated or not treated with 1 µM SM83 for up to 24 h. SM83 treatment promoted the secretion of the pro-inflammatory cytokines TNF (A) and IL-1β (B). (C) NF-kB activation by SM83 evaluated in the macrophage cell line RAW stably transfected with a NF-kB luciferase reporter gene.

Moreover, SM83 treatment also killed the BMDM through a necroptotic mechanism, which was evident after 24 h of treatment both by morphology and viability tests (Figure 35). In fact, the cytotoxicity could be prevented by pre-treatment with the necroptosis inhibitor necrostatin-1, but not by the pan-caspase inhibitor z-vad-fmk, which actually increased BMDM death (Figure 35B). Our data suggest that macrophages could be the first target of SM83. Macrophages are then stimulated and secrete various pro-inflammatory cytokines such as TNF and IL-1β, which favor the formation of an anti-tumor pro-inflammatory environment.

Importantly, to exclude the possibility that SM83-dependent activation of macrophages and IL-1β production could be due to a contamination of LPS, via the stimulation of TLR-4, we also employed BMDM from TLR4-KO mice and found that IL-1β was secreted to a similar extent as it was from BALB/c cells (Figure 36).

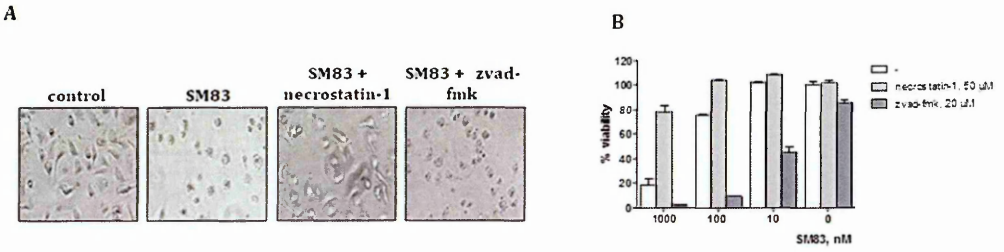

Figure 35. SM83 kills BMDM by necroptosis. BALB/c BMDMs were treated with serial dilutions of SM83 in the absence or presence of Necrostatin-1 or z-vad-fmk to inhibit necroptosis or apoptosis, respectively. (A) Representative images showing cell morphology after 24 h of treatment. (B) Cell viability after SM83 treatment evaluated using the CellTiter-Glo assay.

Furthermore, SM83 preparations for injection were analyzed by the Endosafe-PTS (Charles River Laboratories) test. The test was negative, confirming that, if present, lipopolysaccharides (LPS) levels were under detectable levels.

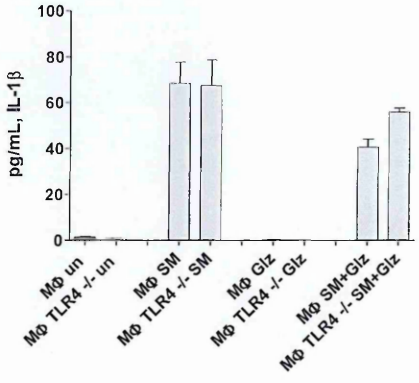

Figure 36. SM83-mediated secretion of IL-1β is not due to LPS contamination. Levels of mouse IL-1β secreted in the culture medium by wild-type or TLR4-/- BMDM, untreated or treated for 24 h with 1 μM SM83, in the absence or presence of 100 μM glycyrrhizin (Glz).

5.3.6. SM83 treatment causes the recruitment of neutrophils *in vivo*

After having investigated the pro-inflammatory effect of SM83 in the tumor microenvironment, we next evaluated whether this resulted in a modification of the

innate immune cells infiltrating the ascites. By IF, we identified both monocytes/macrophages (CD11b^{+} Gr-1^{-}, Figure 37A) and granulocytes (CD11b^{+} Gr-1^{+}, Figure 37A and B in mice that were either untreated or treated for 3 and 6 h, without noticeable differences in cell density. However, after 24 h of treatment, neutrophils massively accumulated both in the ascitic fluid (Figure 37A and B) and in the tumor nodules (Figure 38).

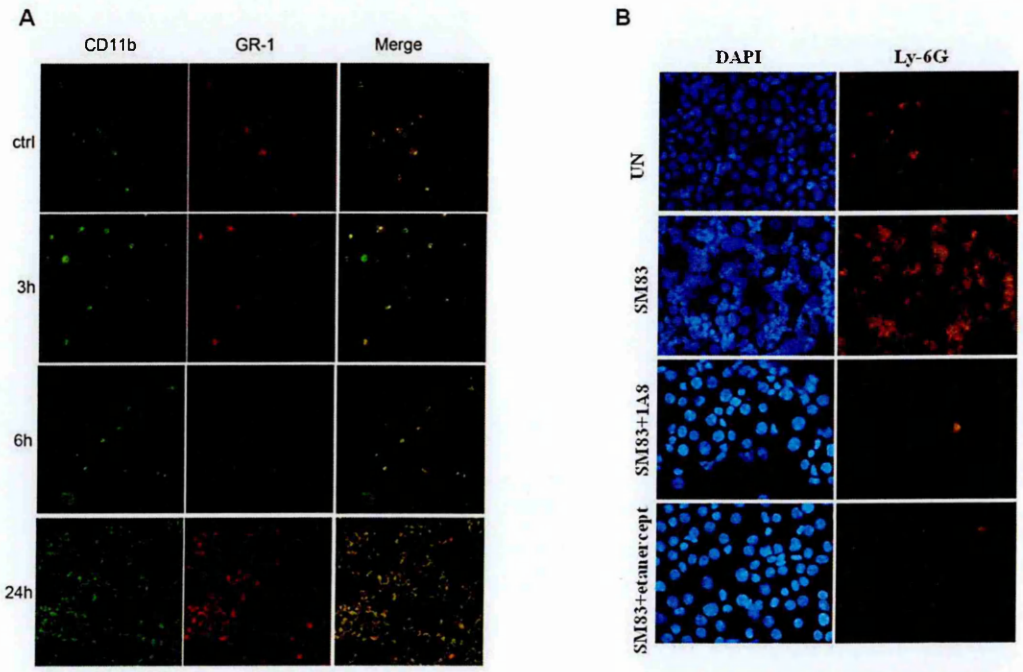

Figure 37. SM83 promotes peritoneal recruitment of neutrophils while TNF-blockers prevent this effect. (A) Cells were harvested from the ascitic fluid of mice treated with 5 mg/kg SM83 and immunofluorescence for CD11b (green) and Gr-1 (red) was performed on cytospin cell preparations. SM83 treatment induced a massive recruitment of neutrophils (CD11b^{+} Gr-1^{+}) at 24 h but not at earlier time points. (B) DAPI nuclear stain and anti-Ly-6G immunofluorescence of cells collected from ascites of nude mice left untreated (UN), treated with 5 mg/kg SM83 alone, with SM83 and 150 mg/kg Etanercept, or with SM83 24 h after neutrophil depletion by injection of the mAb 1A8.

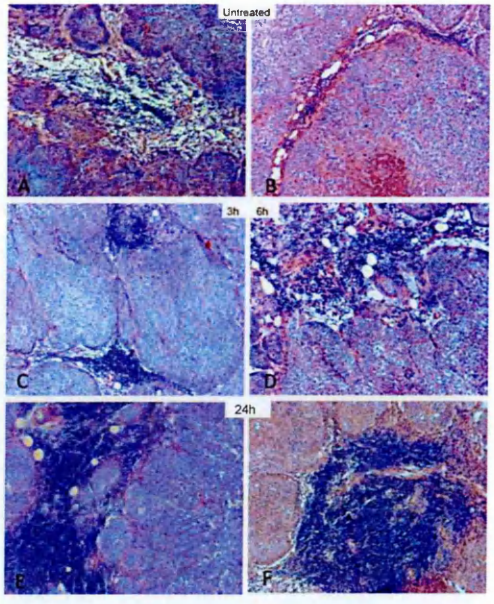

Figure 38. SM83 also stimulates neutrophil accumulation in the solid tumors attached to the peritoneal wall. Histology (H&E stain) of IGROV-1 solid tumors from mice injected ip with IGROV-1 cells and treated or not with a single dose of 5 mg/kg SM83. Solid tumors were recovered from untreated animals (A-B) or from treated animals after 3 h (C), 6 h (D) and 24 h (E-F). SM83 treatment increased the amount of infiltrating leukocytes mainly after 24 h of treatment.

In an attempt to explain the massive neutrophil recruitment, we detected by dot blot the presence of HMGB-1 in the ascites (Figure 39A and B). This "alarmin" is in fact released during necrosis and immunogenic cell death and, together with TNF, attracts and activates neutrophils. We therefore checked whether this was true also in our model and, according to our hypothesis, we found that HMGB-1 accumulated in the ascitic fluid starting 6 h after SM83 treatment (Figure 39A) and was located within the cytoplasm of dying tumor cells (Figure 39B).

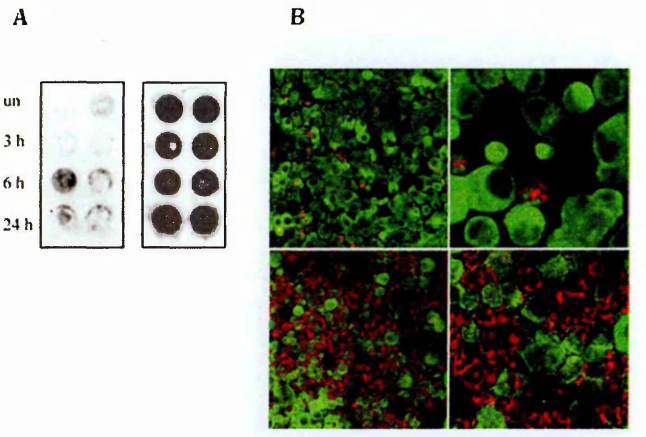

Figure 39. Treatment with SM83 causes the release of HMGB-1 into the ascitic fluid. (A) Dot blot of HMGB-1 (left panel) was performed on cleared ascitic fluids collected from untreated (un) or treated mice at 3, 6 and 24 h after a single injection of 5 mg/kg SM83. Right panel, loading control. (B) Infiltration of neutrophils (Gr-1; red) and HMGB-1 expression in dying tumor cells (green) in ascites untreated (upper row) and treated for 24 h (lower row) with a single injection of SM83. Left and right panels show two different magnifications (10x and 40x).

To confirm that neutrophils can be recruited by HMGB-1 and TNF, we isolated the neutrophils from spleens of BALB/c (wild-type) and TNF-R1-deficient mice. In Transwell assays, the migration of wild-type neutrophils towards ascites from SM83-treated mice was greater than that from untreated mice. The HMGB-1 inhibitor partially reduced the migration, while neutrophils from TNFR-1-deficient mice did not migrate in response to ascites from SM83-treated mice (Figure 40). These findings suggest that neutrophil migration in the presence of ascites from SM83-treated mice is stimulated mainly by TNF. These *in vitro* data recapitulated the *in vivo* observations where TNF-inhibitor Etanercept blocked the recruitment of these cells into the ascites (Figure 37B).

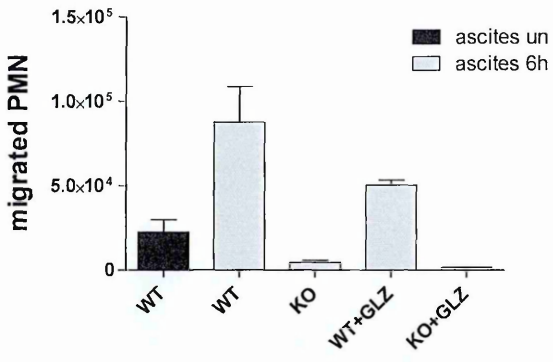

Figure 40. Neutrophils are recruited in a TNF-dependent manner. PMN migration assessed by Transwell assay. Wild type PMN from BALB/c mice (WT) or TNFR-1-deficient PMN from TNFR-KO mice (KO) were seeded into the upper chamber in the absence or presence of the HMGB-1 inhibitor glycyrrhizin (GLZ), whereas the ascitic fluid of mice untreated or treated for 6 h (1:20 in medium) was added to the lower chamber of the Transwell insert. PMN were left to migrate overnight, harvested and counted.

5.3.7. The recruitment of neutrophils is a by-stander effect of the treatment

Knowing that, in certain conditions, neutrophils can be responsible for tumor cell killing, we depleted the neutrophils of ascites-bearing mice prior to SM83 treatment. In *nude* mice, this depletion did not impede the ability of SM83 to reduce the number of floating tumor cells in the ascites (Figure 41A and B). Furthermore, in immunocompetent BALB/c mice bearing Meth A ascites, depletion of neutrophils did not prevent SM83 from prolonging survival, even though these mice have $CD8^+$ T cells that are known to support the activity of neutrophils. On the contrary, neutrophil depletion improved the efficacy of SM83 treatment by a significant increase of the overall survival of mice treated with SM83 ($p=0.0458$ vs 1A8 alone; figure 41C). These results support the notion that, in our models, neutrophils recruitment plays no role in SM-dependent cancer cell killing but rather, at least in the Meth A model, could be in some way detrimental for the host.

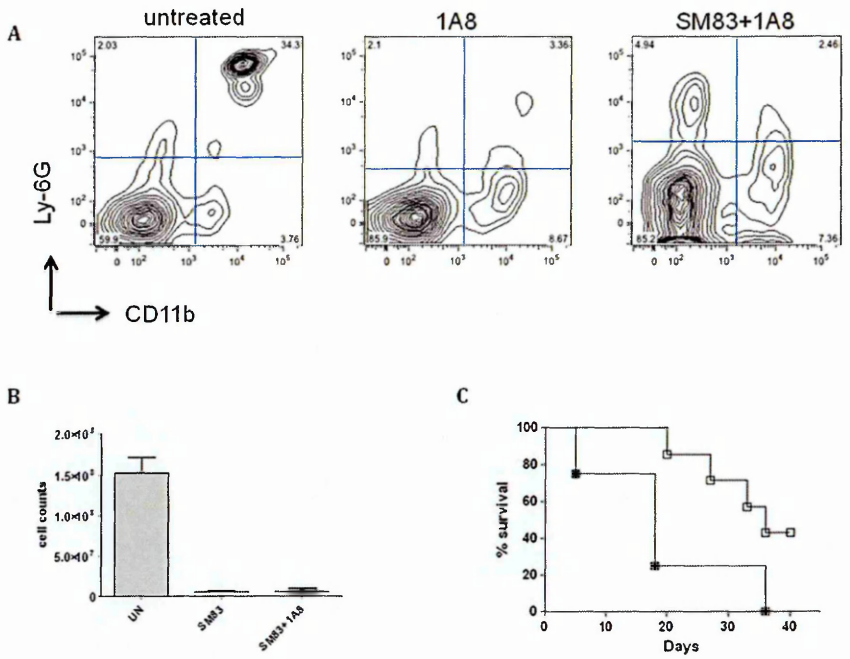

Figure 41. Neutrophils are not responsible for SM83-mediated depletion of ascitic IGROV-1. (A) Neutrophil depletion was checked in mice untreated, treated with 1 injection of 1A8, and in mice injected with both SM83 and 1A8. Flow cytometry of peripheral blood mononuclear cells (PBMCs) shows a reduction in circulating $Ly6G^+$ $CD11b^+$ neutrophils in 1A8-treated mice. (B) Tumor cell counts in the ascites of untreated mice (UN), mice treated with a single injection of SM83 alone, or mice treated with SM83 24 h after depletion of neutrophils by injection with the 1A8 mAb. (C) BALB/c mice were injected ip with Meth A cells and treated with 1A8 alone (■) or in combination with 5 mg/kg SM83 (□), starting from day 7.

5.3.8. Proposed model for SM activity in cancer ascites

In conclusion, our work shows that SM83 acts *in vivo* in cancer ascites by targeting macrophages associated with tumor and most likely by causing their skewing from an M2-like phenotype, which supports the tumor, to an M1-like phenotype, endowed with anti-tumor activity. As a result, macrophages secrete cytokines such as TNF, IL-1β and IFNγ that cause a rapid TNF-dependent necrotic death of the ascites cancer cells;

subsequently, the dying cells release HMGB-1, which, together with TNF, stimulates a massive infiltration of neutrophils (Figure 42).

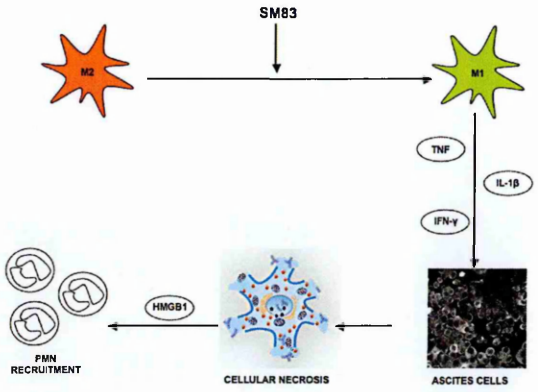

Figure 42. Mechanism of SM83 activity in the ovarian cancer ascites. SM83 stimulates the reversal of macrophages from M2 to M1 phenotype. TNF secreted by M1 macrophages trigger necrotic death of the cancer cells within the ascitic fluid; the dying cells release HMGB-1, which, together with TNF, recruits neutrophils.

5.4. Looking for synthetic lethality: oncogenic KRAS

After having demonstrated that SM83 is endowed with anti-tumor activity and can be effective both *in vitro* and *in vivo*, we looked for genetic settings in which SM83 could be more active. SM83 was therefore tested alone, in combination with TRAIL and in association to several other pharmacological compounds.

5.4.1. Oncogenic KRAS sensitizes cells to drug treatment

As already mentioned, TRAIL is considered an attractive compound in cancer treatment, because its toxicity is highly specific for transformed cells while being almost completely ineffective against normal tissues. On the other hand, SMs display a poor anti-

tumor efficacy as standalones, but can powerfully enhance the efficacy of other compounds in combined treatments. To identify novel compounds that can increase the effectiveness of TRAIL/SM administration, in 2010, a screening was performed at The Institute of Cancer Research, London, in which HeLa cells were treated with SM83 and izTRAIL, in addition to 3 libraries of FDA-approved drugs. SM83/TRAIL was therefore combined with about 3000 drugs (2309 unique compounds screened). Interestingly, the best hits, which efficiently improved the cytotoxicity of the treatment, were topoisomerase inhibitors (Table 6), in agreement with several other studies.

Compound	P-value
10-hydroxycamptothecin	0,000103319
Camptothecin	0,000040974
Camptothecine (S,+)	0,001697753
AMSACRINE	0,000274229
FLUOROURACIL	0,000537959
Aminacrine hydrochloride	0,015471379
Decitabine	0,000022640
MEFLOQUINE	0,000168791
Sutent	0,000444038
NETILMICIN SULFATE	0,005887782

Table 6. Drugs that enhance the activity of SM83 plus izTRAIL. Using a high-throughput approach we treated HeLa with SM83, izTRAIL and a library of about 3000 FDA-approved drugs. The best 10 hits, capable of increasing the cytotoxic activity of the treatment, are shown.

Hits were then validated using the same cell line employed in the screening and in a panel of cancer cell lines (data not shown). Moreover, a number of cancer and normal immortalized cells bearing knock-in and knock-out mutations in genes frequently associated to cancer were also treated. With this approach, we observed that G13D-

mutated KRAS sensitizes human mammary epithelial (HME) cells to TRAIL and SM83/CPT treatment (Figure 43A-D).

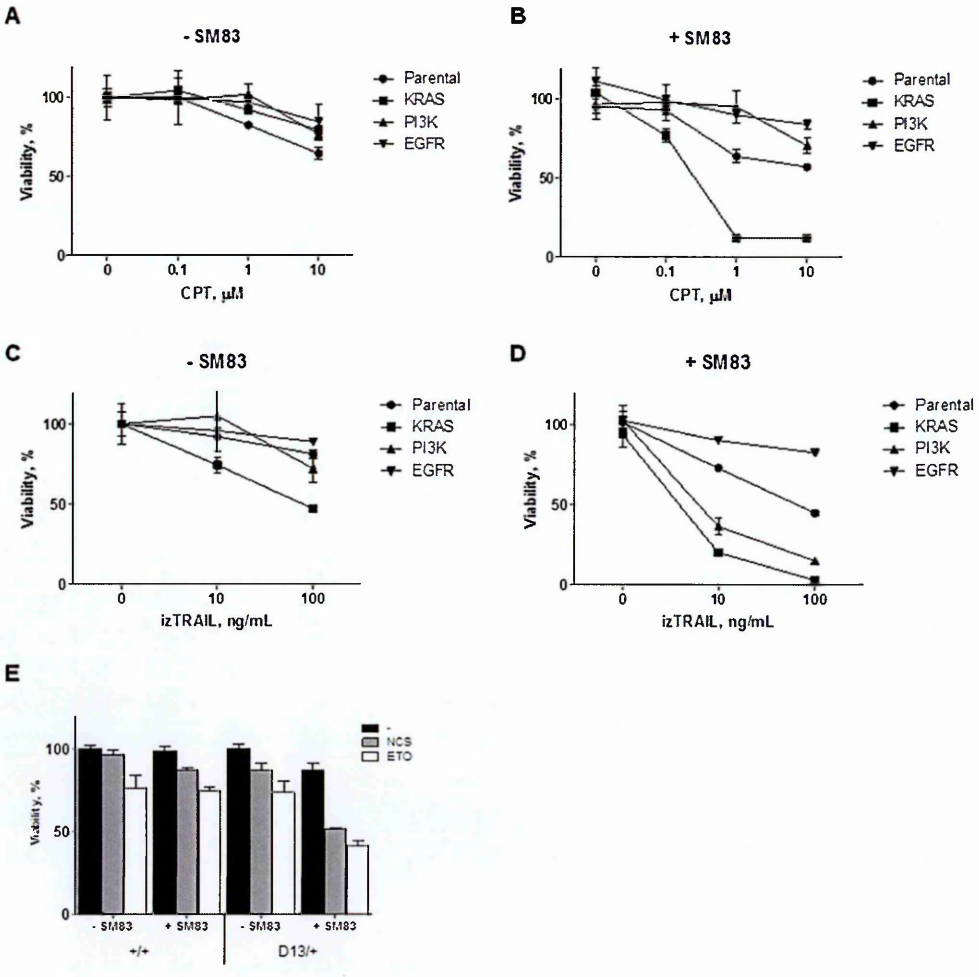

Figure 43. Oncogenic KRAS increases sensitivity of HME cells to DNA-damaging agents and TRAIL. (A) The parental human mammary epithelial (HME) cell line and the isogenic cell lines with knock-in mutations in KRAS (G13D), PI3K (H1047R) and EGFR (delE746A750) were treated with the indicated doses of CPT alone (A) or in combination with 100 nM SM83 (B). The parental human mammary epithelial (HME) cell line and the isogenic cell lines with knock-in mutations in KRAS (G13D), PI3K (H1047R) and EGFR (delE746A750) were treated with the indicated doses of izTRAIL alone (C) or in combination with 100 nM SM83 (D) and (E) with 8.8 nM NCS and 1 μM ETO, with or without 100 nM SM83 (lower panel). Viabilities are shown after 24 h of treatment.

To test whether this effect was specific to topoisomerase I inhibitors or a more

general sensitiveness to cytotoxic compounds, the same cells were treated also with topoisomerase II inhibitor etoposide (ETO) and the DNA double strand maker neocarzinostatin (NCS) both in the presence of SM83 and not (Figure 43E). Our viability tests suggest that the presence of oncogenic KRAS generally sensitizes cells to death inducers and is not specific to a particular compound such as CPT.

5.4.2. Ectopic expression of G13D KRAS sensitizes cells to SM83/CPT treatment

To further assess whether the presence of oncogenic KRAS is indeed responsible for the increased sensitivity to treatment, we silenced KRAS and treated cells with CPT observing a notable reduction of sensitivity (Figure 44A). Moreover, we cloned G13D KRAS in an inducible lentiviral expression vector (Figure 44B) and transduced both HME and MCF10A cells in which we stimulated the over-expression with doxocyclin. Over-expression was confirmed by western blot, detecting the phosphorylation of ERK (Figure 44C), which is a downstream substrate of KRAS activation and by pull-down experiments with the Raf-1 RBD (Figure 44D).

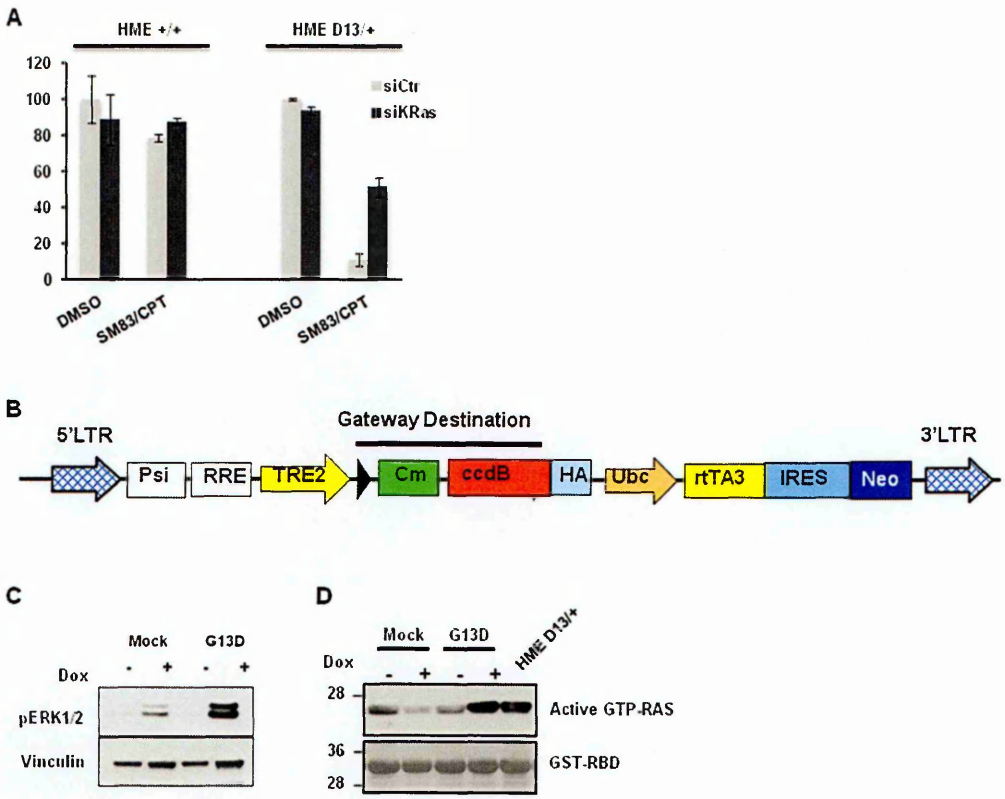

Figure 44. KRAS is responsible for increased sensitivity of HME to SM83/CPT treatment. (A) HME +/+ and HME D13/+ were transfected with siRNA targeting KRAS for 48 h and subsequently treated with 100 nM SM83 and 1 μM CPT. Cell viability was determined after 24 h of treatment. (B) pINDUCER20 used to transduce HME for transient expression of mutated KRAS. (C) HME pINDUCER20-Mock (Mock) and HME pINDUCER20-KRAS G13D (G13D) were incubated with Dox (250 ng/ml) for 48 h, lysed and western blot performed. The presence of activated KRAS was determined by detection of phosphorylated ERK. (D) Active GTP-RAS was purified in cells stimulated as in (C) by pull-down assay using the recombinant RBD domain of Raf-1; HME D13/+ are shown as a positive control for activated KRAS.

We then treated both HME with SM83/CPT (Figure 45A) and TRAIL (Figure 45B), observing an increased sensitivity in the presence of induced G13D KRAS in line with what was observed employing knock-in cell lines (Figure 44A). Oncogenic KRAS was induced also in MCF10A to exclude that the observed sensitization was a cell line-dependent

effect. Mutated KRAS induced the phosphorylation of ERK also in these cells (Figure 45C) and this was associated to increased sensitivity to SM83/CPT treatment (Figure 45D).

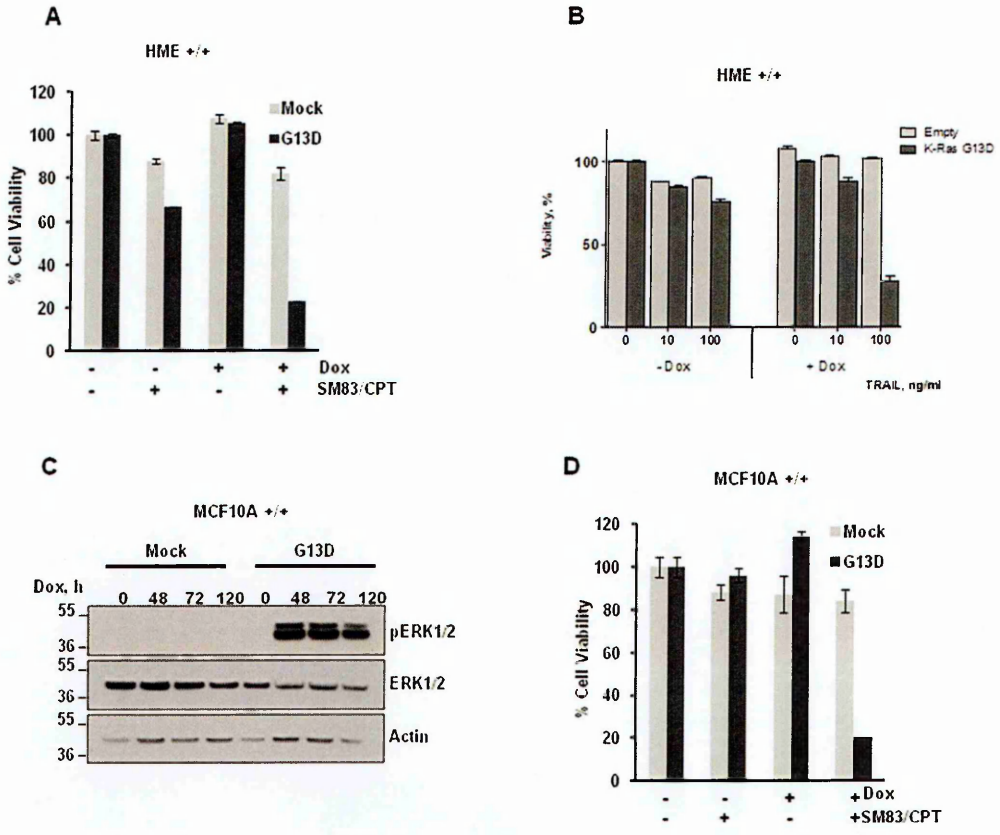

Figure 45. Ectopic oncogenic KRAS sensitize different epithelial cells to SM83/CPT and TRAIL treatment. (A) HME pINDUCER-Mock and HME pINDUCER-KRAS G13D were incubated with Dox (250 ng/ml) for 48 h and treated with 100 nM SM83 and 1 μM CPT, or (B) izTRAIL. Cell viability was determined after 24 h. (C) MCF10A pINDUCER-Mock and MCF10A pINDUCER-KRAS G13D were incubated with Dox (250 ng/ml) for the indicated time, lysed and analyzed by western blot for the detection of ERK and phosphorylated ERK. Actin is shown as loading control. (D) MCF10A pINDUCER-Mock and MCF10A pINDUCER KRAS G13D were incubated with Dox (250 ng/ml) for 48 h and treated with 100 nM SM83 and 0.1 μM CPT. Cell viability was determined after 24 h.

5.4.3. KRAS G13D-expressing cells treated with SM83/CPT die by apoptosis

Parental and KRAS G13D cells were then treated with CPT and SM83 (Figure 46A and

B). As expected, cIAPs were depleted by SM83 in both cell lines (Figure 46B), but only HME KRAS G13D-bearing cells treated with the combination of SM83 plus CPT underwent apoptosis, revealed by cleavage of PARP, caspase-3 and caspase-8 (Figure 46A). As the latter caspase is responsible for the activation of the extrinsic pathway and SM cytotoxicity is often associated with TNF increased expression or sensitivity to it, we investigated a potential role of this cytokine in cell killing.

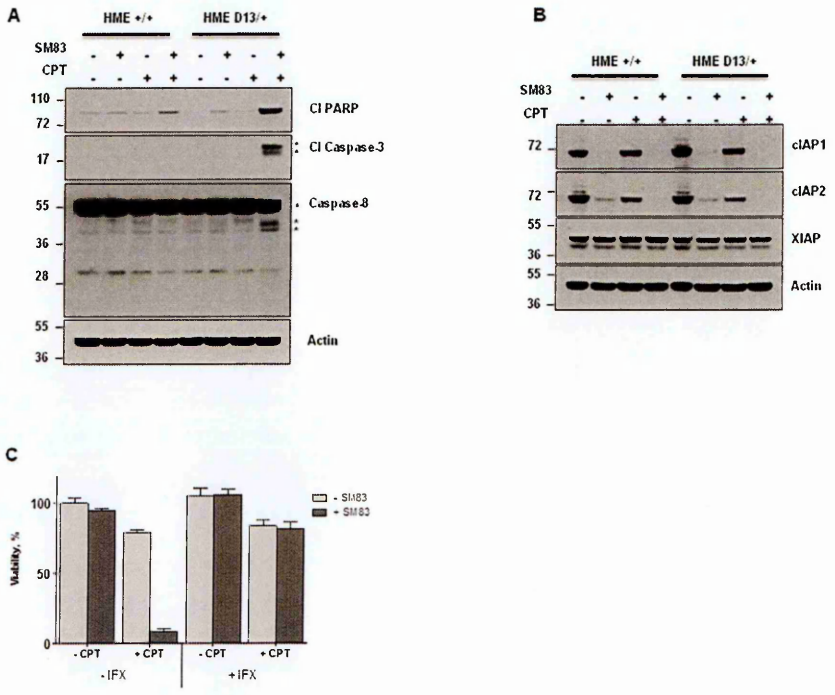

Figure 46. SM83/CPT treatment activates a TNF-dependent apoptotic event in epithelial cells bearing oncogenic KRAS. (A, B) HME +/+ and HME D13/+ cells were mock treated and treated with 100 nM SM83, 1 μM CPT alone and in combination for 6 h. Cells were lysed and subjected to western blot to detect the apoptosis markers cleaved PARP, caspase-3 and caspase-8 (A) and the SM targets cIAP1, cIAP2 and XIAP (B). Actin is the loading control; asterisks show the cleaved forms p17/p19 of caspase-3 and the pro-caspase p55/p57 forms of caspase-8, together with its cleaved forms p41/p43. (C) Before SM83/CPT treatment, HME D13/+ cells were pre-treated with the neutralizing antibody IFX. Viability was measured after a 24 h treatment by CellTiter-Glo.

For this reason, we pre-treated cells with the TNF-neutralizing antibody, Infliximab and then treated HME with the SM83/CPT combination. In line with our hypothesis, we prevented CPT/SM83 toxicity and rescued cells from the treatment (Figure 46C), strongly supporting the notion that oncogenic KRAS-bearing cells are killed by the treatment via a TNF-dependent mechanism.

5.4.4. NOXA is at least in part responsible for KRAS G13D-dependent sensitivity to death

To understand the mechanisms that are responsible for the increased sensitivity of HME KRAS G13D cells to treatment compared to parental cells, we characterized both cell lines by western blot, detecting several proteins involved in the apoptotic pathway (Figure 47 and data not shown). The most striking difference between the two cell lines was represented by the over-expression of NOXA in the presence of mutated KRAS even in untreated cells. In fact, while wild type cells display very low levels of NOXA that can barely be detected in untreated cells, but increase after treatment, on the other hand, KRAS G13D cells show high basal levels of this pro-apoptotic protein in untreated cells, too (Figure 47A). Simultaneously, NOXA antagonist, the anti-apoptotic Mcl1, is depleted more efficiently by the treatment in the presence of oncogenic KRAS (Figure 47A). The capability of mutated KRAS to increase the expression levels of NOXA was further investigated in HME and MCF10A transduced with the inducible KRAS G13D. In line with the G13D knock-in mutation of KRAS, time-course stimulation of ectopic G13D KRAS with doxocyclin also stimulated NOXA expression in these models (Figure 47B). Finally, to assess whether the increased levels of NOXA were indeed responsible for the enhanced sensitivity to treatment, cells with knock-in KRAS G13D mutation were transfected with siRNAs targeting NOXA and viability tested after SM83 and CPT treatment. Down-

regulation of NOXA enhanced resistance to treatment even if it did not completely rescue cells, strongly supporting the notion that NOXA plays an important role in the increased responsiveness to treatment (Figure 47C), but it is not the only protein involved. Importantly, silencing of KRAS decreased NOXA levels, suggesting that KRAS sustains high levels of NOXA (Figure 47D).

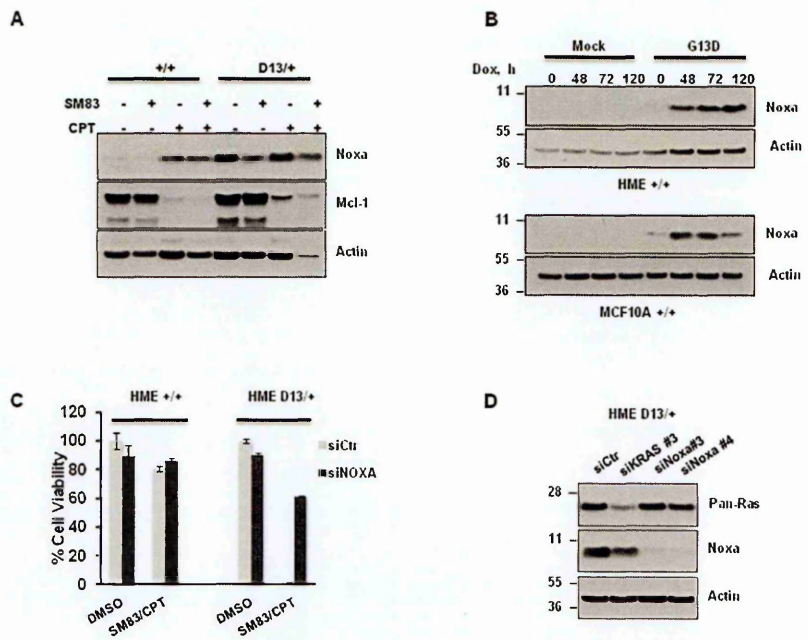

Figure 47. Oncogenic KRAS-dependent up-regulation of NOXA is responsible for the increased sensitivity to treatment. (A) HME +/+ and HME D13/+ cells were treated with 100 nM SM83 and 1 μM CPT for 6 h, lysed and subjected to western blot to detect NOXA and Mcl1 levels. (B) HME (upper panel) and MCF10A (lower panel) transduced with pINDUCER20-Mock and pINDUCER20-KRAS G13D lentiviruses were incubated with Dox (250 ng/ml) for the indicated time points and subjected to western blot to detect NOXA levels. (C) HME +/+ and HME D13/+ were transiently transfected with siRNA targeting NOXA for 48 h and subsequently treated with 100 nM SM83 and 1 μM CPT. Cell viability was determined after 24 h. (D) HME cells bearing the G13D knock-in mutation were transfected with siRNAs targeting KRAS and NOXA for 72 h. Western blot was performed to evaluate NOXA and RAS levels. Actin is shown as a loading control.

5.4.5. Increased sensitivity to treatment stems from KRAS-dependent MAPK activation

We next investigated the mechanisms that are responsible for this acquired sensitivity of KRAS-mutated HME to cell death. Hence, both parental and G13D HME cells were treated with CPT and SM83 in the presence of various inhibitors of MAPK, AKT and PI3K kinases which can be activated by mutated RAS and transmit its signaling. In parental cells, the administration of MEK1/2 inhibitors PD98059 and UO126, AKT inhibitor triciribine or PI3K inhibitor LY294002 did not significantly affect the toxicity of SM83/CPT treatment (Figure 48A). In clear contrast, both MEK1/2 inhibitors partially protected D13/+ HME cells from SM83/CPT treatment and conferred resistance to the same extent as parental cells (Figure 48A). Having found that NOXA is a pivotal mediator of KRAS-dependent increased sensitivity to the combination (Figure 47C), we evaluated whether the MAPK pathway was responsible for the increased levels of NOXA and found, as expected, that both MEK inhibitors reduced the levels of phosphorylated ERK1 and ERK2, and also concurrently reduced the levels of NOXA (Figure 48B). Importantly, MEK inhibition slightly reduced NOXA basal levels also in parental HME (left panel) suggesting that the MAPK pathway stimulates NOXA in physiological conditions as well. To understand whether MEK targets ERK1 and ERK2 both contribute the NOXA regulation, we silenced each of them in G13D HME cells thereby finding that only ERK2 down-regulation results in reduced NOXA levels, while ERK1 silencing has an even opposite effect causing a faint accumulation of NOXA (Figure 48C). In line with these findings, ERK1 silencing slightly enhances the sensitivity of D13/+ HME cells to SM83/CPT treatment, while ERK2 results in an opposite effect (Figure 48D).

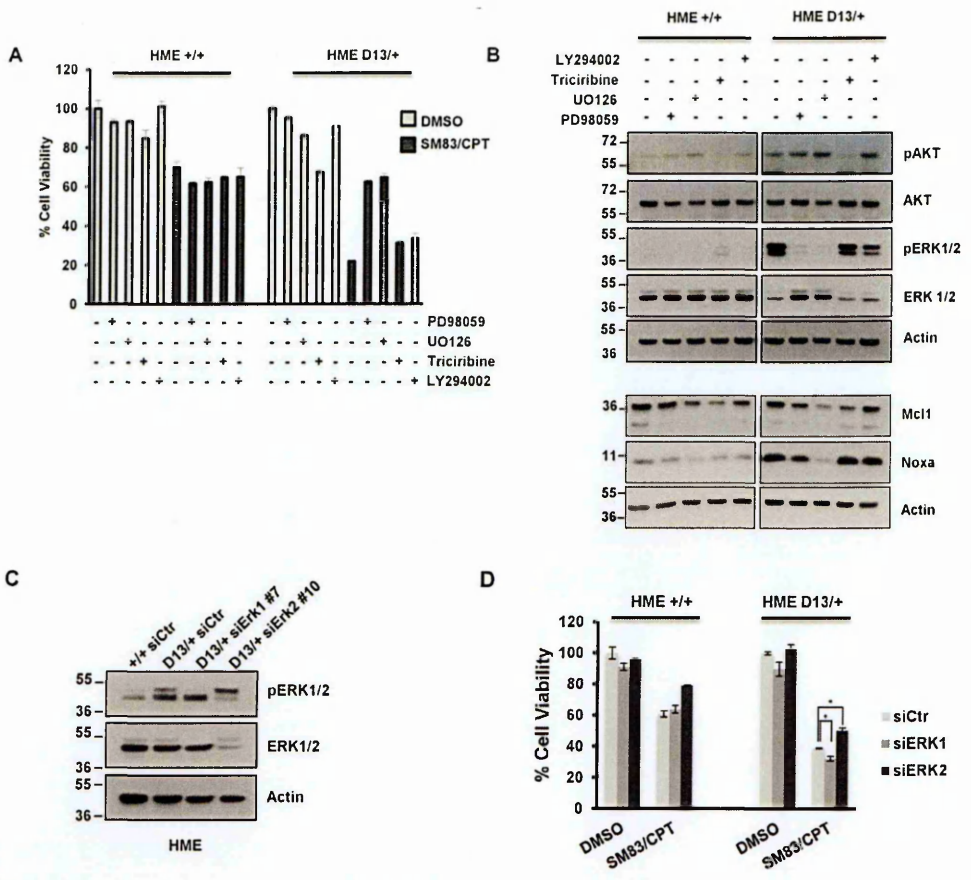

Figure 48. ERK2, but not ERK1 is responsible for KRAS-dependent NOXA-induction. (A) HME +/+ and HME D13/+ cell lines were pre-incubated 2 h with 50 μM PD98059, 25 μM UO126, 20 μM Triciribine and 20 μM LY294002, and then treated with 100 nM SM83 and 1 μM CPT. Cell viability was quantified after 24 h. (B) HME +/+ (left panel) and HME D13/+ (right panel) cell lines were treated 2 h with 50 μM PD98059, 25 nM UO126, 20 μM Triciribine and 20 μM LY294002 and subsequently analyzed by western blot to detect NOXA and the phosphorylated forms of AKT, ERK1 and ERK2, and their total levels. Actin is shown as a loading control. (C) HME +/+ and HME D13/+ were transiently transfected with the indicated siRNAs for 72 hours and subsequently analyzed by western blot to detect phosphorylated ERK1 and ERK2, and their total levels, NOXA and Actin as the loading control. (D) Parental HME +/+ and HME D13/+ cells were silenced for 48 h and then treated with DMSO and 100 nM SM83 plus 1 μM CPT for a further 24 h. Statistical analysis was performed with GraphPad Prism 5.02 using the two-tailed unpaired t-test * $P < 0.05$ vs siCtr.

5.4.6. Cancer cells are not sensitized to treatment by KRAS G13D mutations

Having shown that normal immortalized epithelial cells are sensitized to treatment by the presence of oncogenic KRAS, the next question was whether this effect was also true in tumor cells. For this purpose, a panel of colorectal cancer (CRC) cells with knock-in and knock-out KRAS G13D was used. Surprisingly and contrary to what had observed with HME, SW48, DLD-1, HCT-116 and Lim1215 displayed the same sensitivity to treatment in the presence of both wild type or mutated KRAS (Figure 49A-D). Moreover, SM83 administration made little, if any, difference, again in opposition to what had been observed with the treatment of HME KRAS G13D.

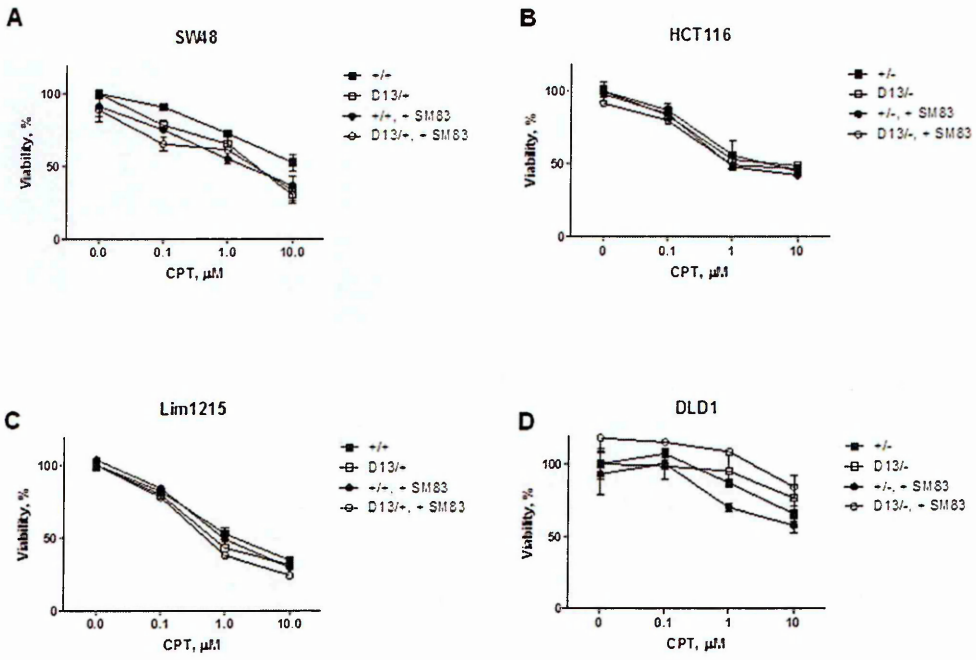

Figure 49. Oncogenic KRAS does not confer sensitivity to combined SM83/CPT treatment in CRC cell lines. SW48 +/+ and SW48 D13/+ (A), HCT116 +/- and HCT116 D13/- (B), Lim1215 +/+ and Lim1215 D13/+ (C), DLD1 D13/- and DLD1 +/- (D) cell lines were treated with DMSO and the combination of SM83 and CPT at the indicated concentrations. Cell viability was evaluated after 24 h.

5.4.7. KRAS G13D does not stimulate NOXA levels in cancer cells

Having previously shown that HME cells are more sensitive to treatment due to a KRAS-dependent increase of NOXA levels, we investigated the levels of NOXA in the panel of CRC cell lines. Interestingly, almost all cell lines have increased basal level of NOXA compared to HME (data not shown), but the presence of wild type or mutated KRAS did not affect its levels (Figure 50A-D). This observation could explain why each couple of isogenic cells with knock-in or knock-out KRAS G13D exhibited the same sensitivity to CPT/SM83 treatment (Figure 49A-D).

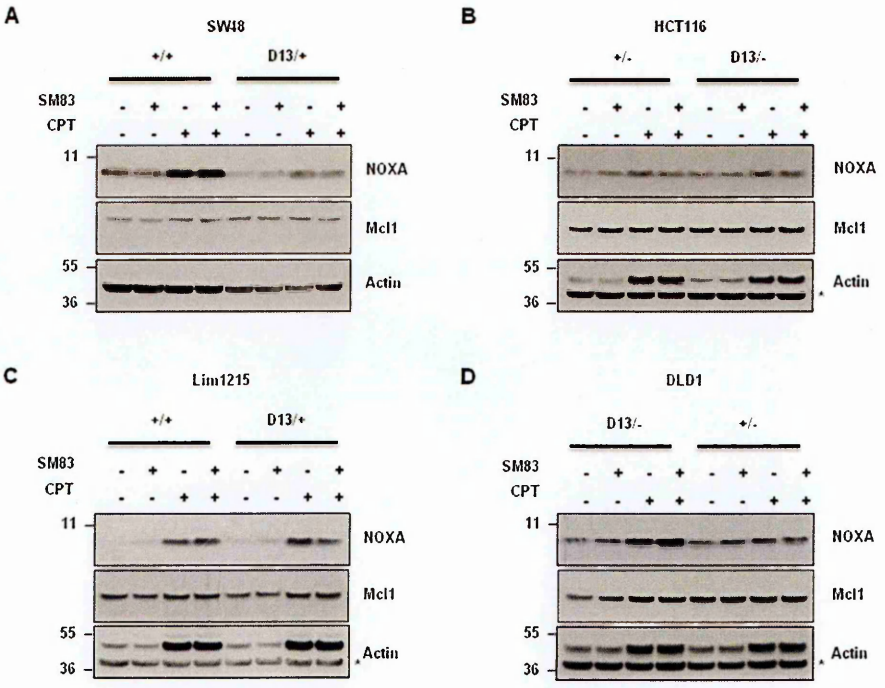

Figure 50. Oncogenic KRAS does not stimulate NOXA up-regulation in cancer cells. SW48 +/+ and SW48 D13/+ (A), HCT116 +/- and HCT116 D13/- (B), Lim1215 +/+ and Lim1215 D13/+ (C), DLD1 D13/- and DLD1 +/- (D) cell lines were treated with DMSO and 100 nM SM83, 0.1 μM CPT in monotherapy and in combination for 6 h. Cells were lysed and analyzed by western blotting for NOXA and Mcl1 levels. Asterisk indicates the specific band of Actin that is shown as a loading control.

As NOXA levels are not affected by the presence of oncogenic KRAS in this panel of cancer cells, we also checked whether its antagonist, Mcl1, is depleted by CPT treatment with the same kinetic found in HME cells. Dose-response experiments show that Mcl1 is slightly more stable in cancer cells compared to normal epithelial cells and its degradation occurs at higher CPT doses compared to HME (Figure 51).

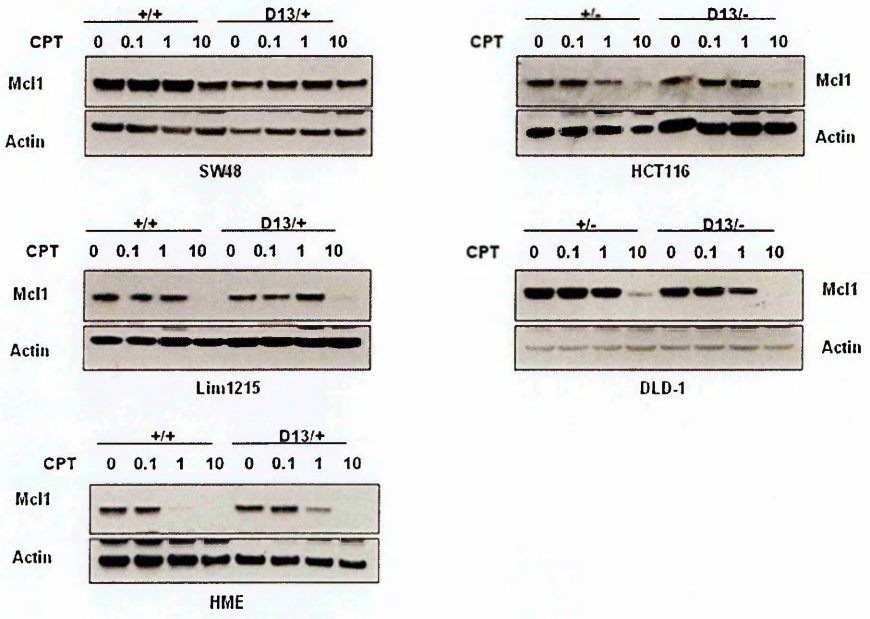

Figure 51. NOXA antagonist Mcl1 is more stable in colorectal cancer cells treated with CPT, compared to HME cells. SW48, HCT116, Lim1215, DLD1 colorectal and mammary epithelial HME cell lines were treated with increased concentrations of CPT for 6 h. Western blots were performed to detect Mcl1 levels. Actin is shown as a loading control.

5.4.8. Aberrant activation of AKT counterbalances the KRAS-mediated pro-apoptotic scenario in colorectal cancer cell lines

Despite the presence of mutant KRAS, our findings suggest that cancer cells are not sensitized to SM83/CPT treatment. Therefore, we hypothesized that malignant progression might have caused the deregulation of other pathways that can

counterbalance the potential apoptotic effect of oncogenic KRAS. Interestingly, HCT116 and DLD1 cells bear mutated PI3K, which results in hyper-activation of the PI3K/AKT pathway, a signaling cascade known to promote cell survival. For this reason, we treated HCT116 bearing mutated and wild type KRAS with SM83/CPT after pre-treatment with inhibitors of MEK1/2, AKT and PI3K.

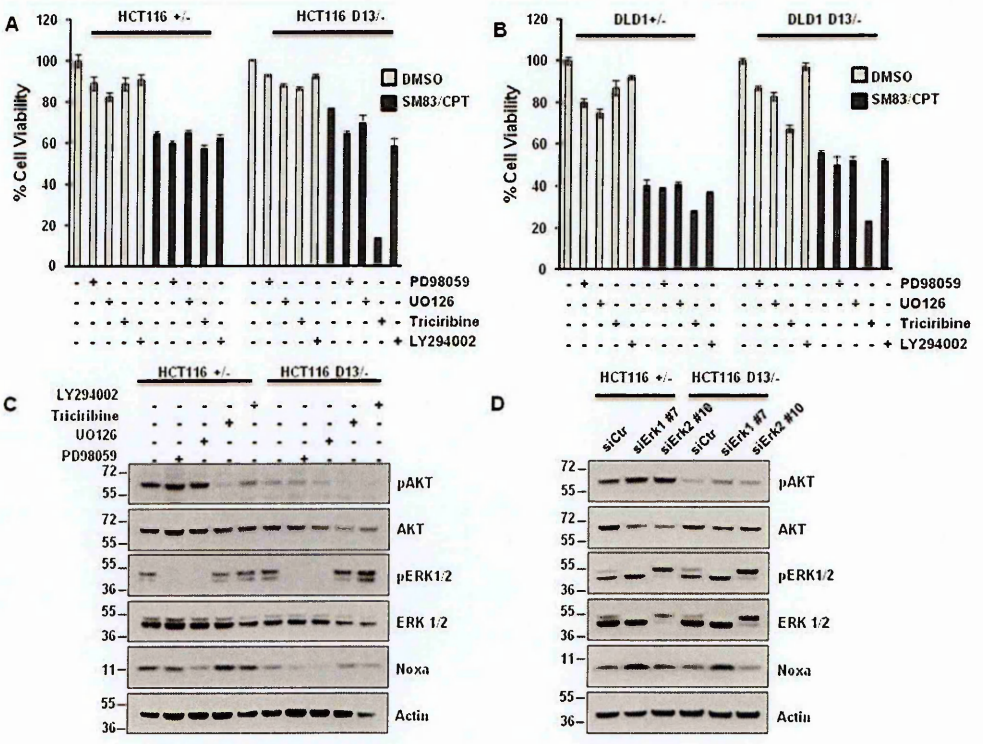

Figure 52. Aberrant AKT activation protects HCT116 cells from the pro-death effect of oncogenic KRAS. (A) HCT116 and (B) DLD1 cells were pre-incubated 2 h with 50 μM PD98059, 25 μM UO126, 20 μM Triciribine and 20 μM LY294002, and then mock-treated or treated with 100 nM SM83 and 1 μM CPT. Cell viability was quantified after 24 h. (C) HCT116 cells were treated for 2 h with the indicated inhibitors as in (A) and then analyzed by western blot to detect the NOXA levels and the phosphorylated and total levels of AKT and ERK. Actin is shown as loading control. (D) HCT116 cells were transfected with siRNAs targeting ERK1 and ERK2, after 72 h cells were collected and analyzed by western blot to detect NOXA and the total and phosphorylated levels of AKT and ERK. Actin is shown as loading control.

Interestingly, and concordant with our hypothesis, AKT inhibition restored sensitivity to the treatment only in the presence of mutant KRAS (Figure 52A and B). NOXA levels were lowered by MAPK blocking (Figure 52C) as already observed in HME cells (Figure 48B), but were not affected by AKT inhibition, suggesting that the AKT pathway blocks the pro-death effect triggered by oncogenic KRAS in an independent fashion. We further investigated the mechanisms by which NOXA levels are controlled in HCT116 cells and demonstrated that the findings described for HME are true also in this cancer cell line. In fact, the targeting of ERK1 by silencing enhanced the levels of NOXA, while a specific siRNA targeting ERK2 slightly reduced its expression (Figure 52D).

5.4.9. AKT counterbalances the KRAS-mediated pro-apoptotic effect also in the absence of mutations activating the PI3K/AKT pathway

The observation that AKT inhibition specifically sensitizes oncogenic KRAS-bearing CRC cells to treatment in the presence of mutated PI3K stimulated us to check whether this was true also in PI3K wild type cells. We then treated Lim1215 and SW48, in which PI3k is not mutated and bearing wild-type or mutated KRAS, with SM83/CPT after pre-treatment with AKT inhibitors. Confirming the previous observations, AKT blocking sensitized Lim1215 bearing G13D KRAS to the treatment (Figure 53, left). Importantly, a similar effect was shown also in the SW48 cell line that was already particularly sensitive to AKT inhibition, independently of KRAS status (Figure 53, right).

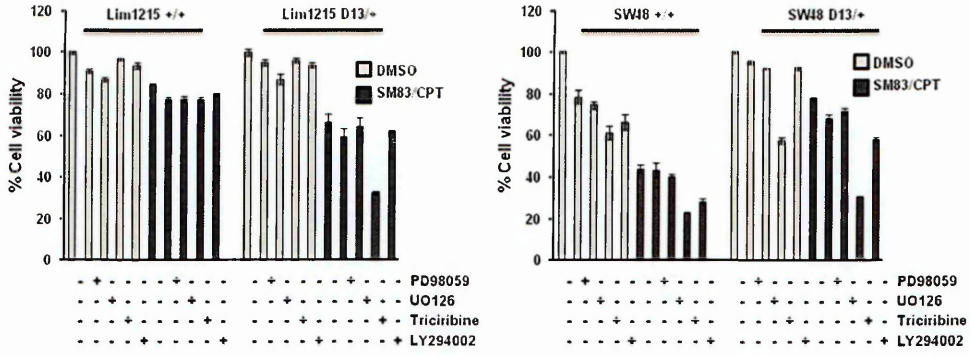

Figure 53. Aberrant AKT activation protects HCT116 cells from the pro-death effect of oncogenic KRAS also in the presence of wild type PI3K. (Left) Lim1215 and (right) SW48 cells were pre-incubated 2 h with 50 μM PD98059, 25 μM UO126, 20 μM Triciribine and 20 μM LY294002, and then mock-treated or treated with 100 nM SM83 and 1 μM CPT. Cell viability was quantified after 24 h.

6. DISCUSSION

In these last few years, the focus of our attention has been on a class of compounds, called SMs, which were described and proposed for cancer therapy about 10 years ago (Li *et al*, 2004). The aim of our work has therefore been to design new molecules in order to increase their cytotoxic activity, modifying their pharmacokinetic features, the affinity for the known targets and introducing novel modifications also on the basis of the most recent findings. In fact, SMs were initially considered only XIAP inhibitors (Sun *et al*, 2007). Nowadays, however, they are known to target other members of the IAP family, such as cIAP1, cIAP2 and ML-IAP (Condon *et al*, 2014; Cossu *et al*, 2009a). Consequently different affinities for these proteins result in diverse activities and treatment outcome.

The initial discovery of the SMs immediately generated great interest, because their targets, the IAPs, are considered pivotal players in the acquired cancer cell resistance to death and this is a major issue in cancer therapy (Fulda, 2014b). Accordingly, several groups have generated thousands of modified molecules and a few of these compounds are currently being tested in clinical trials (Fulda, 2014b). Nevertheless, the latest findings have somewhat dampened the initial enthusiasm showing a limited efficacy in cancer healing and highlighting a few side-effects (Wong *et al*, 2014). These results have significantly changed the concept of SM activity. For example, it has been suggested that SM XIAP inhibition could even be detrimental and could result in excessive cytokine-related inflammation. For this reason, a few new SMs have been designed to reduce the affinity for XIAP (Condon *et al*, 2014), which was the original target of this class of compounds, and specifically deplete cIAP1 and cIAP2.

Although many works have been published to date, it is still however necessary to

fully comprehend the mechanisms of SM activity in order to avoid the negative side-effects and to identify the ideal settings in which to employ these compounds successfully. To this end, in collaboration with the University of Milan, we have built a library of about 140 SMs and have characterized their affinity for cIAP1, cIAP2 and XIAP, together with their cytotoxic activity as standalones and in combination with other compounds. Thanks to the data obtained in this multi-laboratory project, we selected SM83, a compound with nanomolar affinities for the IAP BIR domains, extremely cytotoxic for sensitive cancer cells, capable of enhancing the activity of other compounds and employable both *in vitro* and *in vivo* (Lecis *et al*, 2012). Thus, almost all my PhD work focuses on the use of this SM.

So far, SMs have been tested in many different tumors and their efficacy has not been correlated to the cancer type studied. Hence, in our work, diverse tumor models were exploited focusing on breast cancer triple negative carcinoma and ovarian cancer ascites. Finally, in an attempt to identify the genetic lesions that enhance the sensitivity to SM/TRAIL treatment, we investigated the effect of KRAS mutations and consequently employed CRC cells, which are often characterized by this type of genetic lesion.

6.1. The anti-metastatic effect of SM83 in triple negative breast cancer

Triple negative breast carcinomas are intensively studied, because they represent one of the most aggressive subtypes of breast tumors and there is the need for new therapeutic approaches. Furthermore, the MDA-MB231 cell line is probably the most characterized in SM-related works, because it is one of the few cell lines to be killed by SM treatment in monotherapy (Varfolomeev *et al*, 2007). It thus offers a standardized

model for comparing SM efficacy and to identify the mechanisms that are responsible for responsiveness to SMs. Accordingly, along with Kym, SKOV3 and A2058 cell lines, the MDA-MB231 cell line was used in the papers which demonstrated for the first time that SM cytotoxic activity stems from cIAP1 depletion and is triggered by autocrine TNF secretion (Varfolomeev *et al*, 2007; Vince *et al*, 2007). The effect on XIAP is therefore surprisingly dispensable for SM toxicity in monotherapy (Sun *et al*, 2014). Finally, MDA-MB231 cells easily engraft immunosuppressed mice and are extremely prone to forming spontaneous metastasis not only in lungs, but also in bones and the brain (Bos *et al*, 2009; Kang *et al*, 2003; Minn *et al*, 2005). As a result, they are therefore intensively used for the study of the metastasizing process and to identify the compounds that could prevent or reduce metastasis formation.

In our work, the capability of SM83 to reduce the growth of triple negative breast cancers both *in vitro* and *in vivo* was tested. SM83 was administered both as a standalone and in combination with other compounds, and especially in association with TRAIL. This ligand was proposed for cancer therapy in the late 90s because of its capability to selectively kill transformed cells without affecting normal tissues (Walczak *et al*, 1999). Moreover, genetic *in vivo* studies employing transgenic mice with depleted TRAIL-Rs suggested a natural anti-cancer role of TRAIL (Finnberg *et al*, 2008; Grosse-Wilde *et al*, 2008) and generated great enthusiasm regarding its employment in medical treatment. Although pre-clinical data were extremely promising and supported the testing of a number of TRAIL agonist compounds, the clinical trial results betrayed the expectations (Yang *et al*, 2010). The reasons for the *in vivo* ineffectiveness have not been fully understood, but it is speculated that TRAIL short half-life, together with its inability to stimulate both TRAIL-R1 and R2, and the intrinsic mechanisms of cancer cell resistance

impede its efficacy (Falschlehner *et al*, 2009). Several approaches have therefore been suggested to increase TRAIL efficacy, modifying its molecule to increase the stability and capability to trimerize (Ganten *et al*, 2006), and to improve its pharmacokinetic profile. Interestingly, SMs were shown to represent the ideal compound for combination with TRAIL and the other ligands of the TNF family (Li *et al*, 2004). XIAP, in fact, plays a crucial role in protecting from TRAIL-mediated cytotoxic activity (Cummins *et al*, 2004). Moreover, the other SM targets, cIAP1 and cIAP2, are components of the TNF-RS complexes (Emmerich *et al*, 2011; Gerlach *et al*, 2011; Lu *et al*, 2011), where, upon the stimulation of the cognate ligand, they regulate the switch from a pro-death to a pro-survival signaling.

In our work, we tried to increase the *in vivo* efficacy of TRAIL by means of a genetic approach, employing $CD34^+$ cells transduced with adenoviruses that allow the expression of TRAIL bound to the membrane. This technique allows the expression of mTRAIL, which is more stable and it is continually expressed by engineered cells, at least for 3-4 days. This approach has already been employed successfully in models of lymphomas and multiple myeloma (Carlo-Stella *et al*, 2006; Lavazza *et al*, 2010). TRAIL-armed $CD34^+$ cells were shown to accumulate in the tumors and increase mice survival by reducing the number of cancer cells. Interestingly, even though TRAIL-armed CD34 cells were shown to poorly inhibit the growth of the solid primary tumors, they caused the formation of large necrotic areas within the tumors and this effect was caused by the destruction of the tumor-associated vasculature (Lavazza *et al*, 2010).

In accordance with previous literature, our SM83 synergized with sTRAIL *in vitro* using both the SM-sensitive MDA-MB231 and the SM-resistant MDA-MB468. Moreover, co-

culture experiments of these breast cancer cells with TRAIL-armed CD34 cells showed that SM83 favors the activation of apoptosis, in these settings also. Nonetheless, several experiments failed to confirm an improvement of TRAIL-armed CD34 cell *in vivo* activity in combination with SM83. Primary MDA-MB231 and MDA-MB468 tumors were both reduced by SM83 administration by about 50%. This is surprising as only MDA-MB231 are intrinsically sensitive to SMs suggesting that SM83 interacts *in vivo* with something present in the micro-environment which enhances its activity. TNF produced by the host (Probst *et al*, 2010), the cytokines (Beug *et al*, 2014) or other factors could be responsible for the enhanced sensitivity to SM83, but another hypothesis is that SMs might also affect other processes, such as angiogenesis, and consequently could indirectly delay the primary tumor growth. This idea seems to be supported by recent findings in transgenic mice which reported that the triple targeting of cIAP1, cIAP2 and XIAP, by knock-out, is lethal due to damaged vasculature endothelium (Moulin *et al*, 2012).

As previously mentioned, SM83 did not enhance the efficacy of TRAIL-expressing CD34 cells in our experiments and mTRAIL had only a negligible effect both alone and in combination therapy. A number of reasons may have contributed to this limited-efficacy result. However, most probably, 4 injections of 10^6 cells are not sufficient to eradicate or significantly reduce the volume of already established and developed tumors. Furthermore, the presence of large necrotic areas also in untreated tumors, which is a common feature of triple negative breast cancers, may have impeded us from appreciating a potential effect in killing restricted areas of the primary tumors. Nonetheless, we demonstrated that SM83 depletes the cIAPs *in vivo* and reduces XIAP levels. The latter effect might stem from cIAP1 down-regulation as it is also observable *in vitro* in cells silenced for cIAP1. This strongly supports the notion that the levels of the

diverse IAPs are interlinked (Silke *et al*, 2005) and some can affect the levels of the others by increasing the protein stability or the gene expression.

Of note, as MDA-MB231 form lung metastases *in vivo* (Minn *et al*, 2005), we investigated whether SM83 could have a role in this process and noticed a significant reduction of the size and number of MDA-MB231 colonies in the lungs of treated animals. Having shown that SM83 treatment kills by apoptosis only a small portion of cancer cells, we speculated that the anti-metastasis effect could have been caused by another mechanism. As cIAP1 and cIAP2 are apical regulators of several signaling cascades that eventually control gene trans-activation (Varfolomeev *et al*, 2012), we analyzed by GEP the primary tumors collected from mice. According to our hypothesis, the analysis of treated tumors revealed that 15 genes were significantly down-regulated and 50 up-regulated. The down-regulated genes were all tested in wound-healing assays using an unbiased approach. Cancer motility is an important feature for metastasizing cancer cells (Reymond *et al*, 2013), in particular in the first steps of dissemination. We therefore silenced the selected genes and found that Snai2, RNF144B and BDNF, 3 of the 15 genes down-regulated *in vivo* by SM83 treatment, down-regulation prevented cancer motility and could most probably be responsible for the reduced number of metastases. We then focused our attention on Snai2 because it is a mediator of the EMT process (Villarejo *et al*, 2014) and it is known to play a role in metastasis formation (Kim *et al*, 2014).

Further work confirmed that Snai2 is inhibited by SM83 through the depletion of cIAP1. We also demonstrated that Snai2 down-regulation parallels the activation of the non-canonical NF-kB pathway in cells treated with SM83 or TWEAK, whilst it is stimulated by TNF administration. The down-regulation of Snai2 could therefore depend on multiple

effects triggered by SM83 such as the non-canonical NF-kB pathway activation or the simultaneous canonical NF-kB pathway inhibition. These mechanisms are difficult to investigate because they are strictly interlinked. Consequently, the modification of one pathway inevitably results in the variation of the other.

The analysis of a panel of breast cancer cell lines belonging to different subtypes showed that the triple negative breast cancer cells usually express higher Snai2 levels compared to other cells. Importantly, SM83 treatment broadly reduces its expression, excluding a cell line-specific effect. Our work therefore suggests that cIAP1 might concur with cancer cell aggressiveness by supporting the high levels of the metastasis-favoring gene Snai2. This evidence is in accordance with previous works by others that demonstrate a pro-metastasis effect of IAPs independently of their capability to control apoptosis (Mehrotra *et al*, 2010). In conclusion, SM adjuvant treatment could represent a possible approach for reducing the formation of metastasis in Snai2-positive cells. Moreover, the observation that cIAP1 plays a role in controlling this process supports the investigation of the signaling controlled by this IAP in order to identify new targets for anti-metastasis treatment.

6.2. Affecting the cross-talk between tumor and micro-environment: SM83 efficacy in ovarian cancer ascites

Ascites formation is a feature of the ovarian cancer and of the advanced tumors arising from other organs. Ascites are caused by the cancer cell obstruction that results in the accumulation of the ascitic fluid. Ovarian carcinomas rarely form metastasis outside the peritoneum (Lengyel, 2010), therefore the ascites themselves are responsible for

cancer deaths. Cancer ascites are characterized by the massive accumulation of liquid in which detached cancer cells can grow in close contact to the cells of the immune system. Despite the fact that this environment is extremely infiltrated with immune cells, such as macrophages, these are often anergic and do not display anti-cancer cell activity. On the contrary, they stimulate the tumor by secretion of several cytokines and chemokines. Macrophages are numerous in the cancer ascites, but instead of protecting from the tumor, they are polarized in a particular state, termed M2, which, in contrast, favor cancer growth (Sica *et al*, 2006; Sica and Mantovani, 2012). For this reason, a possible approach to treating tumors could be represented by the targeting of the immune system in order to inhibit the support received by the micro-environment. Importantly, macrophage skewing is controlled by the NF-kB pathway (Hagemann *et al*, 2008), which could therefore represent a potential target for therapy directed against cancer-associated immunity.

An opportunity to study the efficacy of SMs in the treatment of ovarian carcinomas is constituted by the IGROV-1 cells, which can grow *in vitro*, both attached to a cell culture surface and in suspension, and *in vivo*. In immunosuppressed mice, they can form solid tumors when engrafted subcutaneously, but also cancer ascites if injected in the peritoneum (De Cesare *et al*, 2010). Of note, IGROV-1 cells are completely resistant *in vitro* to SM83 treatment even though this compound completely depletes the levels of cIAP1 and cIAP2. As already noted in SM-resistant breast cancer models, SM83 can nevertheless enhance the activity of TRAIL in combination therapy and trigger an apoptotic event in IGROV-1 cells, but does not affect their growth when administered as a standalone. Nonetheless, the efficacy of SM83 changes *in vivo* and, in accordance to what was observed in the MDA-MB468 xenografts, SM83 treatment inhibits *in vivo* the growth

of cancer cells intrinsically resistant *in vitro*.

Our data therefore suggested that SM83 exploits the tumor micro-environment to be effective in the ovarian model as well. In particular, our data revealed that continued treatments significantly increased mice survival, while one single injection dramatically depleted the detached cancer cells floating in the ascitic fluid. It is known that the cells killed by SMs in monotherapy secrete high levels of TNF and this becomes toxic when the IAPs are inhibited (Varfolomeev *et al*, 2007; Vince *et al*, 2007). Thus, we first studied the levels of diverse cytokines after SM83 administration. This can be easily studied in the case of the IGROV-1 ascites model because the tumor environment is constituted by the ascitic fluid that can simply be collected by syringe and analyzed in ELISA assays. After one single injection of SM83, we noticed that the TNF levels rapidly increased and, importantly, mouse TNF was produced before human TNF, suggesting that SM83 administration was acting on the host before being effective on the tumor cells. TNF was indeed responsible for cancer cell killing, because its blocking by means of Enbrel prevented cancer cell depletion. We can therefore conclude that SM83 caused the secretion of TNF from mouse cells and this was then responsible for the establishment of an inflammatory environment. Accordingly, other pro-inflammatory cytokines such as IFNγ and IL-1β were induced 6 h after the injection, whereas the immunosuppressive TGFβ, IL-4 and IL-10 were not affected by the treatment.

In these experiments, we used immunosuppressed nude mice. These animals are athymic and therefore lack T cells, resulting in severe impairment of the adaptive immune compartment. To investigate the mechanisms by which SM83 rapidly kills the detached cancer cells within the ascites, induces a rapid inflammatory event and delays cancer

growth prolonging engrafted animals, we therefore focused on the innate immunity. In particular, we studied the role of macrophages because they are known to produce the studied cytokines (Hagemann *et al*, 2008; Heusinkveld *et al*, 2011), are numerous in the ascites and play a role in cancer-supporting when skewed in the M2 state. *In vitro* experiments employing BMDMs showed that SM83 stimulates their rapid TNF secretion together with the activation of the NF-kB pathway. Furthermore, in accordance with other previous reports (Muller-Sienerth *et al*, 2011), we demonstrated that SMs kill macrophages via a necroptotic, but not apoptotic, mechanism. Treatment with the RIP1 kinase inhibitor Necrostatin-1, in fact, prevented the toxicity, while the pan caspase inhibitor event enhanced BMDM death.

The analysis of the immune cell populations that infiltrate the IGROV-1 ascites revealed that SM83 causes an enormous recruitment of neutrophils 24 hours after the treatment. This was evident both in the ascitic fluid and in the solid nodules attached to the peritoneum wall. We then investigated whether these cells also played a role in cancer cell killing. We employed various approaches, including *in vitro* co-culture of spleen-derived neutrophils and IGROV-1 cells, and arrays to measure neutrophil activation (data not shown), migration assays and *in vivo* depletion. Our experiments strongly support the idea that the neutrophils are recruited in response to the SM83-dependent inflammatory event, which is caused also by the rapid death of millions of cancer cells that most likely release numerous immunogenic factors, but do not play a role in IGROV-1 cell killing. Neutrophil depletion before SM83 treatment did not prevent its efficacy, but on the contrary prolonged mouse survival. This demonstrates that neutrophils are not necessary for SM83 activity and are even detrimental, either supporting tumor growth or causing excessive inflammation that becomes toxic for

animals already weakened by the tumor. Further experiments confirmed that ascites derived by animals treated with SM83 significantly attract neutrophils in migration assays and this is TNF dependent, but HMGB-1 independent. This protein is known to be released by dying cells and is responsible for immunogenic death (Sims *et al*, 2010). In our models, we found a relevant release of HMGB-1 in the ascitic fluid, which nevertheless was not responsible for neutrophil recruitment. HMGB-1 and ATP release are considered markers of immunogenic death (Kepp *et al*, 2011), a type of cell death often considered desirable in cancer therapy because it could direct the immune system against the cancer cells, further increasing the efficacy of traditional chemotherapy. Of note, SMAC-triggered cell death has recently been shown to be inflammation-related (Emeagi *et al*, 2012) and our work demonstrated that SMs could also produce a similar cytotoxic effect.

As the immune system plays a fundamental role in the activity of SM83 in cancer ascites, we decided to further study the efficacy of this compound in immunocompetent mice. We therefore engrafted BALB/c mice with syngeneic sarcoma Meth A cells, which rapidly evolve into cancer ascites and kill the mice (Watanabe *et al*, 1986). Also in this case, SM83 significantly prolonged mouse survival, in a few cases being also curative, further demonstrating that SM treatment can be effective in cancer ascites treatment. Preliminary experiments were also performed to check whether SM treatment might also stimulate an immune memory, supported by the observation that mice cured though the administration of SM83 did not develop ascites even if re-challenged with further Meth A injections.

Of note, in both the ascites model used, the concomitant administration of TRAIL did not improve the efficacy of SM83 treatment, again supporting the notion that the *in*

vivo employment of TRAIL needs to be carefully planned in terms of doses, schedule and the cancer model used. Nonetheless, our *in vitro* data still support the idea that the SM/TRAIL combination could be extremely effective in cancer cell killing.

6.3. Enhancing SM83 efficacy through novel drug combinations and genetic interactions

As previously mentioned, SMs are unlikely to be effective in cancer treatment as standalones. In fact, very few cells are killed by SMs *in vitro* in monotherapy (Petersen *et al*, 2007) and these cells can acquire resistance *in vivo* (Bai *et al*, 2012). Nevertheless, SMs could be successfully employed in combination therapies and, confirming this, several works have reported a plethora of drugs that synergize with different SMs (Lecis *et al*, 2010; Probst *et al*, 2010; Servida *et al*, 2010; Steinhart *et al*, 2013; Wagner *et al*, 2012). Keeping this in mind, in 2010, we performed a high-throughput screening at the Institute of Cancer Research (ICR) in London, looking for FDA-approved drugs whose cytotoxic activity could be enhanced by simultaneous administration of SM83 and/or TRAIL. Traditional chemotherapeutic drugs commonly used in cancer treatment and already known to enhance SM and TRAIL activity represented the best hits of the screening. In fact, we identified the topoisomerase I inhibitor camptothecin (Singh *et al*, 2003), and decitarabine and fluorouracil.

Whether a specific genetic lesion could render the cancer cells more prone to cell death was our next question. Therefore, we exploited a panel of isogenic cell lines bearing mutations frequently associated to tumors. The use of isogenic cells with KI and KO mutations, in fact, allows the investigation of the effect of a single gene, but avoiding

the genetic variability that affects the results when comparing two different cell lines (Arena *et al*, 2007). Furthermore, the introduction of KI and KO mutations by-passes the artefacts introduced by the ectopic expression of transgenes, thus producing non-physiological protein levels due to the presence of several copies of the transgenes, the absence of transcription regulation due to the use of strong constitutive promoters and unnatural post-transcription maturation of the mRNA, because transgenes are usually constituted by cDNAs. On the contrary, isogenic cell lines can be used to identify oncogene and non-oncogene addiction, and to study synthetic lethality (Roulston *et al*, 2013; Steckel *et al*, 2012).

In our work, a panel of CRC and human mammary epithelial cell lines with mutations in the PI3K, EGFR, BRAF and KRAS genes was used. Viability tests showed that normal cells with G13D mutations in the KRAS gene are more prone to cell death when treated with several compounds such as camptothecin, neocarzinostatin, etoposide and TRAIL. The increased death was mediated by the pro-apoptotic protein NOXA, whose basal levels were over-expressed in an ERK2-dependent manner. In fact, oncogenic KRAS stimulates the MEK/ERK pathway and this results in NOXA up-regulation in agreement with previous works (Elgendy *et al*, 2011). Other groups, in fact, showed that mutated KRAS stimulates NOXA-dependent autophagic cell death in human ovarian surface epithelial (HOSE) cell line or sensitizes cancer cells to cisplatin-mediated apoptosis (de Bruijn *et al*, 2010). Importantly, mutated KRAS has also shown to induce senescence in primary cells (Serrano *et al*, 1997; Vizioli *et al*, 2014), further supporting the notion that activated oncogenes could sensitize cells to death, at least when cells are not fully transformed and represent a premalignant lesion. This increased proneness to death in the presence of mutated oncogenes could derive from a protective mechanism of the

cells from oncogenic transformation. Normal cells might therefore sense a genetic lesion, become more sensitive to cells and easily be removed by the organism before forming a possible tumor. In accordance to this hypothesis, treatment of our premalignant models – HME cells with KI G13D mutations of KRAS and ectopic expression of oncogenic KRAS in HME and MCF10A cells – with SM83 and CPT caused the activation of an apoptotic cascade.

Interestingly, ERK2 and not ERK1 is responsible for NOXA up-regulation suggesting that, even if extremely conserved and activated by the same up-stream stimuli, these two kinases display peculiar and even opposite functions. Nonetheless, MEK chemical inhibition, which switch off the activation of both ERK1 and ERK2, resulted in NOXA down-regulation and cell protection from the treatment.

In our work, we demonstrated that NOXA enhanced the sensitivity to the treatment, but we did not fully comprehend the mechanisms that were responsible for the killing. Again, we focused on the TNF and saw that TNF blocking by means of Infliximab and Enbrel, and silencing of TNF and TNF-R1, but not TNF-R2 (data not shown), rescued treated cells. As in preliminary experiments, we did not observe an increased release of TNF in the medium of treated cells. As a result, we can conclude that TNF becomes toxic upon CPT/SM83 treatment most likely by increase of TNF-R1 exposure or by removal of factors that usually protect from TNF.

Because the epithelial cells bearing KRAS mutations only represent a premalignant model, we then considered whether our observations were true in transformed cells also. For this reason, we treated a panel of CRC bearing KI and KO KRAS mutations with SM83/CPT. In clear contrast to what had been observed in HME and MCF10A cells, CRC

sensitivity to the treatment was completely independent from KRAS status. Moreover, NOXA levels were not up-regulated in the presence of G13D KRAS despite the fact that ERK2 was still controlling its expression. We then speculated that another parallel pathway was protecting cancer cells from the pro-death stimulus deriving from oncogenic KRAS. As HCT116 and DLD1 cells bear activating mutations of PI3K, which is the up-stream activator of AKT, we inhibited both these kinases in combination to SM83/CPT. Interestingly, we observed that AKT suppression sensitized cancer cells to treatment, especially in cells KRAS mutated. These results were further confirmed in the Lim1215 cell line in which AKT inhibition still sensitized oncogenic KRAS-bearing cells to treatment, despite the fact that these cells bear wild-type PI3K. On the contrary, SW48 were particularly sensitive to the treatment and therefore we did not observe a specific sensitization to treatment in the presence of mutated KRAS. Altogether, these data support the notion that mutated KRAS has the potential of sensitizing cancer cells to death, but its effect is prevented by AKT.

Therefore, our findings present two main implications. First, it is possible to increase sensitivity to cancer cells bearing mutated KRAS by simultaneous inhibition of the AKT pathway. Second, the inhibition of the pathway directly activated by KRAS, such as the MAPK pathway, might even result in an immediate anti-proliferative effect, but could also switch off the potentially pro-death stimuli arising from oncogenic KRAS.

6.4. Conclusions and future research

In conclusion, our work shows that SMs, and, in particular, our SM83, can be successfully employed to target the IAPs both *in vitro* and *in vivo* as tools to study IAP

functions, and potentially as adjuvant therapy in cancer treatment. SM83, in fact, can enhance the cytotoxic activity of other compounds, but can also target the tumor micro-environment and affect the immune system associated to the tumors. Nonetheless, much work is still required in order to eliminate the side-effect deriving from excessive cytokine production and to identify precise settings in which SM therapy could be more effective. In line with this, we showed that KRAS mutations have the potential to increase sensitivity to treatment, but further studies will permit understanding as to how AKT protects from this stimulus and therefore determining the best combination approach to enhance the efficacy of the therapy.

Finally, our work proposed an anti-metastasis effect of SM83 due to its capability to modulate gene expression. In particular, we showed that cIAP1 promotes high levels of Snai2 and, as a result, SM83 treatment significantly reduces the levels of this mediator of the EMT process. Our work in progress is therefore focused on the comprehension of the mechanisms by which cIAP1 up-regulates Snai2 expression in order to identify other target-specific compounds that could reduce its levels without preventing IAP activity that, as we have shown, produces many side-effects.

LIST OF ABBREVIATIONS

5-FU	Fluorouracil
ATP	Adenosine triphosphate
AVPI	Alanine-Valine-Proline-Isoleucine
BAFF	B cell activating factor
Bak	Bcl-2 homologous antagonist/killer
Bax	Bcl-2-associated X protein
BCA	Bicinchonic acid
BDNF	Brain-derived neurotrophic factor
BH3	Bcl-2 homology domain 3
Bid	BH3 interacting-domain death agonist
BIR	Baculoviral IAP repeat
BM	Bone marrow
BMDM	Bone marrow-derived macrophages
BRCA	Breast cancer susceptibility genes
BSA	Bovine serum albumin
CARD	Caspase recruitment domain
Caspases	Cysteine-dependent aspartate-directed proteases
cDNA	Complementary DNA
cFLIP	Cellular FLICE (FADD-like IL-1β-converting enzyme)-inhibitory protein
CHX	Cycloheximide
cIAP	Cellular IAP
CK	Cytokeratin
CPT	Camptothecin
CRC	Colorectal cancer
DAPI	4',6-Diamidino-2-phenylindole dihydrochloride
DcR	Decoy receptor
DD	Death domains
DISC	Death inducing signaling complex
DMEM	Dulbecco's Modified Eagle's medium
DMSO	Dimethylsulfoxide
DNA	Deoxyribonucleic acid
Dox	Doxycicline
DR	Death receptor
DTT	Dithiothreitol
EGF	Epidermal growth factor
EGFR	Epidermal growth factor receptor
ELISA	Enzyme-linked immunosorbent assay
EMT	Epithelial to mesenchymal transition
ER	Estrogen Receptor
ERK	Extracellular signal-regulated kinase
ETO	Etoposide
FAK	Focal adhesion kinase
FBS	Fetal bovine serum
FDA	Food and Drug Administration
FITC	Fluorescein isothiocyanate
GDP	Guanosine diphosphate
GEP	Gene expression profiling
GTP	Guanosine triphosphate
H&E	Hematoxylin and eosin
HER2	Human epidermal growth factor receptor 2

HME	Human mammary epithelial
HMGB-1	High mobility group box 1
IAP	Inhibitor of apoptosis protein
IBM	IAP binding motif
IF	Immunofluorescence
IFN	Interferon
IHC	Immunohistochemistry
IkB	Inhibitor of NF-kB
IKK	Inhibitor of NF-kB kinase
IL	Interleukin
ILP2	Insulin-like peptide 2
IMDM	Iscove's modified Dulbecco's medium
ip	Intraperitoneal
IPTG	Isopropyl-b-D-thiogalactopyranoside
iv	Intravenous
izTRAIL	Isoleucine zipper TRAIL
KI	Knock-in
KO	Knock-out
LRIG-1	Leucine-rich repeats and immunoglobulin-like domains protein 1
LUBAC	Linear ubiquitin chain assembly complex
MALT	Mucosa-associated lymphoid tissue
MAPK	Mitogen-activated protein kinases
Mcl1	Induced myeloid leukemia cell differentiation protein
MEK	MAPK/ERK kinase
ML-IAP	Melanoma-IAP
MOMP	Mitochondrial outer membrane permeabilization
mP	Millipolarization units
mRNA	Messenger RNA
mTRAIL	Membrane TRAIL
NCS	Neocarzinostatin
NEMO	NF-kB essential modulator
NF-kB	Nuclear factor kappa-light-chain-enhancer of activated B cells
NIK	NF-kB inducing kinase
NOD	Nucleotide-binding oligomerization domain-containing protein
NOD/SCID	Non-obese diabetic/severe combined immunodeficiency disease
PARP	Poly-ADP ribose polymerase
PBS	Phosphate-buffered saline
PBS-T	PBS-Tween
PI	Propidium iodide
PI3K	Phosphatidylinositol 4,5-bisphosphate 3-kinase
PMN	Polymorphonuclear leucocytes
PR	Progesterone receptor
PUMA	p53 up-regulated modulator of apoptosis
Rac1	Ras related C3 botulinum toxin substrate
RBD	Ras binding domain
RING	Really interesting new gene
RIP1	Receptor interacting protein 1
RNA	Ribonucleic acid
RNF144	RING finger protein 144B
RPMI-1640	Roswell Park Memorial Institute-1640
RT	Room temperature
sc	Subcutaneous
SDS	Sodium dodecyl sulfate

siRNA	Short interfering (siRNA)
SMAC	Second mitochondria-derived activator of caspases
SM	Smac mimetic
sTRAIL	Soluble TRAIL
TAB	TGF-beta-activated kinase 1-binding protein 3
TAK	TNF-associated kinase
TGF-β	Transforming growth factor
TLR	Toll-like receptors
TNF	Tumor necrosis factor
TNF-R	TNF-receptor
TNF-RS	TNF-R superfamily
TRADD	TNF-R1-associated death domain
TRAF	TNF-R-associated factor
TRAIL	TNF-related apoptosis-inducing ligand
TRAIL-R	TRAIL-receptor
TWEAK	TNF-related weak inducer of apoptosis
XIAP	X-linked IAP

LIST OF FIGURES

LIST OF TABLES

PUBLICATIONS (2011-2015)

Specifically related to the PhD project:

1. Conti A, Majorini MT, Elliott R, Ashworth A, Lord C, Cancelliere C, Bardelli A, Seneci P, Walczak H, Delia D, **Lecis D**. Oncogenic KRAS sensitizes premalignant, but not malignant cells, to Noxa-dependent apoptosis through the activation of the MEK/ERK pathway. *Oncotarget*. Accepted

2. **Lecis D**, De Cesare M, Perego P, Conti A, Corna E, Drago C, Seneci P, Walczak H, Colombo MP, Delia D and Sangaletti S. Smac mimetics induce inflammation and necrotic tumour cell death by modulating macrophage activity. *Cell Death and Disease*. 2013 Nov 14;4:e920

3. **Lecis D**, Mastrangelo E, Belvisi L, Bolognesi M, Civera M, Cossu F, De Cesare M, Delia D, Drago C, Manenti G, Manzoni L, Milani M, Moroni E, Perego P, Potenza D, Rizzo V, Scavullo C, Scolastico C, Servida F, Vasile F and Seneci P. Dimeric Smac mimetics/IAP inhibitors as *in vivo*-active pro-apoptotic agents. Part II: Structural and biological characterization. *Bioorg Med Chem*. 2012 Nov 15;20(22):6709-23

4. Cossu F, Milani M, Vachette P, Malvezzi F, Grassi S, **Lecis D**, Delia D, Drago C, Seneci P, Bolognesi M and Mastrangelo E. Structural insight into inhibitor of apoptosis proteins recognition by a potent divalent smac-mimetic. *PLoS One*. 2012 7(11):e49527

Not related to the PhD project:

1. Raulf N, El-Attar R, Kulms D, **Lecis D**, Delia D, Walczak H, Papenfuss K, Odell E, and Tavassoli M. Differential response of head and neck cancer cell lines to TRAIL or Smac mimetics is associated with the cellular levels and activity of caspase-8 and caspase-10. *Br J Cancer.* 2014 Nov 11;111(10):1955-64.

2. Möller Y, Siegemund M, Beyes S, Herr R, **Lecis D**, Delia D, Kontermann R, Brummer T, Pfizenmaier K, Olayioye MA. EGFR-Targeted TRAIL and a Smac Mimetic Synergize to Overcome Apoptosis Resistance in KRAS Mutant Colorectal Cancer Cells. *PLoS One.* 2014 Sep 8;9(9):e107165.

3. Carlessi L, Poli EF, Bechi G, Mantegazza M, Pascucci B, Narciso L, Dogliotti E, Sala C, Verpelli C, **Lecis D**, Delia D. Functional and molecular defects of hiPSC-derived neurons from patients with ATM deficiency. *Cell Death Dis.* 2014 Jul 17;5:e1342.

4. Mingozzi M, Manzoni L, Arosio D, Dal Corso A, Manzotti M, Innamorati F, Pignataro L, **Lecis D**, Delia D, Seneci P, Gennari C. Synthesis and biological evaluation of dual action cyclo-RGD/SMAC mimetic conjugates targeting αvβ3/αvβ5 integrins and IAP proteins. *Org Biomol Chem*. 2014 May 28;12(20):3288-302

5. Seneci P, Rizzi M, Ballabio L, **Lecis D**, Conti A, Carrara C, Licandro E.SPION-Smac mimetic nano-conjugates: Putative pro-apoptotic agents in oncology. *Bioorg Med Chem Lett*. 2014 Mar 25. pii: S0960-894X(14)00275-3.

6. Gatti L, De Cesare M, Ciusani E, Corna E, Arrighetti N, Cominetti D, Belvisi L, Potenza D, Moroni E, Vasile F, **Lecis D**, Delia D, Castiglioni V, Scanziani E, Seneci P, Zaffaroni N, Perego P. Antitumor activity of a novel homodimeric SMAC mimetic in ovarian

carcinoma. *Mol Pharm*. 2014 Jan 6;11(1):283-93

7. Scavullo C, Servida F, **Lecis D**, Onida F, Drago C, Ferrante L, Seneci P, Barcellini W, Lionetti M, Todoerti K, Neri A, Cortelezzi A, Delia D and Lambertenghi Deliliers G. Single-agent Smac-mimetic compounds induce apoptosis in B chronic lymphocytic leukaemia (B-CLL). *Leuk Res.* 2013 Jul;37(7):809-15

8. Bianchi A, Ugazzi M, Ferrante L, **Lecis D**, Scavullo C, Mastrangelo E and Seneci P. Rational design, synthesis and characterization of potent, drug-like monomeric Smac mimics as pro-apoptotic anticancer agents. *Bioorg Med Chem Lett.* 2012 Mar;22(6):2204-8

ACKNOWLEDGMENTS

No work can be done by a single person, and this thesis makes no exception. During my PhD period, many people contributed to this project and it is almost impossible to mention all of them here. Nonetheless, I would like first of all to thank my Director of Studies, Dr. Domenico Delia, not only for the supervision of my PhD project, but also for the opportunity to work in the research field for so many years. I am also extremely grateful to my External Supervisor, Prof. Henning Walczak, for his help before and during my PhD studies and for hosting me in his lab at Imperial College, London.

This thesis just could not be possible without the continuous work and effort of my colleagues working on the "SM project" and especially of Annalisa Conti, Maria Teresa Majorini and Enrico Fontanella. I thank also many other people from different labs of our institute for providing reagents, information and for always helping me. I would like to mention in particular Maria Chiara Anania and Paola Romeo, and Giacomo Manenti for helping me with the in vivo experiments. The SMs were designed and synthesized in collaboration with the University of Milan and in particular with Prof. Pierfausto Seneci, Carmelo Drago and the members of Prof. Martino Bolognesi's group Federica Cossu, Eloise Mastrangelo and Mario Milani. I'm also grateful to Antonella Montinaro and Silvia Von Karstedt for their suggestions for my thesis.

Finally, I would like to thank my parents and in particular my mother for editing all my writings, and Federica for being so patient during all the hours that I spent in front of this computer, writing my thesis! All my work, efforts and this thesis are dedicated to my beloved son, Tom, wishing him a great future and never-ending happiness.

REFERENCES

Acloque H, Thiery JP, Nieto MA (2008) The physiology and pathology of the EMT. Meeting on the epithelial-mesenchymal transition. *EMBO Rep* **9**: 322-326, doi:10.1038/embor.2008.30 [doi]

Allensworth JL, Sauer SJ, Lyerly HK, Morse MA, Devi GR (2013) Smac mimetic Birinapant induces apoptosis and enhances TRAIL potency in inflammatory breast cancer cells in an IAP-dependent and TNF-alpha-independent mechanism. *Breast Cancer Res Treat* **137**: 359-371, doi:10.1007/s10549-012-2352-6 [doi]

Amaravadi R, Schilder R, Dy G, Ma W, Fetterly G, Weng D, Graham A, Burns J, Chunduru S, Condon S (2011) Phase 1 study of the Smac mimetic TL32711 in adult subjects with advanced solid tumors and lymphoma to evaluate safety, pharmacokinetics, pharmacodynamics and antitumor activity.

Annunziata CM, Davis RE, Demchenko Y, Bellamy W, Gabrea A, Zhan F, Lenz G, Hanamura I, Wright G, Xiao W, Dave S, Hurt EM, Tan B, Zhao H, Stephens O, Santra M, Williams DR, Dang L, Barlogie B, Shaughnessy JD,Jr, Kuehl WM, Staudt LM (2007) Frequent engagement of the classical and alternative NF-kappaB pathways by diverse genetic abnormalities in multiple myeloma. *Cancer Cell* **12**: 115-130, doi:10.1016/j.ccr.2007.07.004

Arena S, Isella C, Martini M, de Marco A, Medico E, Bardelli A (2007) Knock-in of oncogenic Kras does not transform mouse somatic cells but triggers a transcriptional response that classifies human cancers. *Cancer Res* **67**: 8468-8476, doi:67/18/8468 [pii]

Arnt CR, Chiorean MV, Heldebrant MP, Gores GJ, Kaufmann SH (2002) Synthetic Smac/DIABLO peptides enhance the effects of chemotherapeutic agents by binding XIAP and cIAP1 in situ. *J Biol Chem* **277**: 44236-44243, doi:10.1074/jbc.M207578200 [doi]

Au PY, Martin N, Chau H, Moemeni B, Chia M, Liu FF, Minden M, Yeh WC (2005) The oncogene PDGF-B provides a key switch from cell death to survival induced by TNF. *Oncogene* **24**: 3196-3205, doi:1208516 [pii]

Autelli R, Crepaldi S, De Stefanis D, Parola M, Bonelli G, Baccino FM (2005) Intracellular free iron and acidic pathways mediate TNF-induced death of rat hepatoma cells. *Apoptosis* **10**: 777-786, doi:10.1007/s10495-005-2944-2 [doi]

Bai L, McEachern D, Yang CY, Lu J, Sun H, Wang S (2012) LRIG1 modulates cancer cell sensitivity to Smac mimetics by regulating TNFalpha expression and receptor tyrosine kinase signaling. *Cancer Res*, doi:10.1158/0008-5472.CAN-11-2428

Barnhart BC, Alappat EC, Peter ME (2003) The CD95 type I/type II model. *Semin Immunol* **15**: 185-193

Berger R, Jennewein C, Marschall V, Karl S, Cristofanon S, Vellanki SH, Hehlgans S, Rodel F, Ludolph A, Fulda S (2011) NF-{kappa}B is required for Smac mimetic-mediated sensitization of glioblastoma cells for {gamma}-irradiation-induced apoptosis. *Mol Cancer Ther*, doi:10.1158/1535-7163.MCT-11-0218

Bertrand MJM, Milutinovic S, Dickson KM, Ho WC, Boudreault A, Durkin J, Gillard JW, Jaquith JB, Morris SJ, Barker PA (2008) cIAP1 and cIAP2 Facilitate Cancer Cell Survival by Functioning as E3 Ligases that Promote RIP1 Ubiquitination. *Molecular Cell* **30**: 689-700,

doi:10.1016/j.molcel.2008.05.014

Beug ST, Tang VA, Lacasse EC, Cheung HH, Beauregard CE, Brun J, Nuyens JP, Earl N, St-Jean M, Holbrook J, Dastidar H, Mahoney DJ, Ilkow C, Le Boeuf F, Bell JC, Korneluk RG (2014) Smac mimetics and innate immune stimuli synergize to promote tumor death. *Nat Biotechnol* **32**: 182-190, doi:10.1038/nbt.2806; 10.1038/nbt.2806

Bishop AJ, Barlow C, Wynshaw-Boris AJ, Schiestl RH (2000) Atm deficiency causes an increased frequency of intrachromosomal homologous recombination in mice. *Cancer Res* **60**: 395-399

Bos PD, Zhang XH, Nadal C, Shu W, Gomis RR, Nguyen DX, Minn AJ, van de Vijver MJ, Gerald WL, Foekens JA, Massague J (2009) Genes that mediate breast cancer metastasis to the brain. *Nature* **459**: 1005-1009, doi:10.1038/nature08021 [doi]

Branschadel M, Aird A, Zappe A, Tietz C, Krippner-Heidenreich A, Scheurich P (2010) Dual function of cysteine rich domain (CRD) 1 of TNF receptor type 1: conformational stabilization of CRD2 and control of receptor responsiveness. *Cell Signal* **22**: 404-414, doi:10.1016/j.cellsig.2009.10.011 [doi]

Bunting K, Rao S, Hardy K, Woltring D, Denyer GS, Wang J, Gerondakis S, Shannon MF (2007) Genome-wide analysis of gene expression in T cells to identify targets of the NF-kappa B transcription factor c-Rel. *J Immunol* **178**: 7097-7109, doi:178/11/7097 [pii]

Cancer Genome Atlas Network (2012) Comprehensive molecular characterization of human colon and rectal cancer. *Nature* **487**: 330-337, doi:10.1038/nature11252 [doi]

Carlo-Stella C, Lavazza C, Di Nicola M, Cleris L, Longoni P, Milanesi M, Magni M, Morelli D,

Gloghini A, Carbone A, Gianni AM (2006) Antitumor activity of human CD34+ cells expressing membrane-bound tumor necrosis factor-related apoptosis-inducing ligand. *Hum Gene Ther* **17**: 1225-1240, doi:10.1089/hum.2006.17.1225

Carter BZ, Kornblau SM, Tsao T, Wang RY, Schober WD, Milella M, Sung HG, Reed JC, Andreeff M (2003) Caspase-independent cell death in AML: caspase inhibition in vitro with pan-caspase inhibitors or in vivo by XIAP or Survivin does not affect cell survival or prognosis. *Blood* **102**: 4179-4186, doi:10.1182/blood-2003-03-0960 [doi]

Chai J, Shiozaki E, Srinivasula SM, Wu Q, Dataa P, Alnemri ES, Shi Y (2001) Structural Basis of Caspase-7 Inhibition by XIAP. **104**: 769-780

Chaturvedi MM, Sung B, Yadav VR, Kannappan R, Aggarwal BB (2011) NF-kappaB addiction and its role in cancer: 'one size does not fit all'. *Oncogene* **30**: 1615-1630, doi:10.1038/onc.2010.566

Che X, Yang D, Zong H, Wang J, Li X, Chen F, Chen X, Song X (2012) Nuclear cIAP1 overexpression is a tumor stage- and grade-independent predictor of poor prognosis in human bladder cancer patients. *Urol Oncol* **30**: 450-456, doi:10.1016/j.urolonc.2010.12.016 [doi]

Cheung HH, Plenchette S, Kern CJ, Mahoney DJ, Korneluk RG (2008) The RING Domain of cIAP1 Mediates the Degradation of RING-bearing Inhibitor of Apoptosis Proteins by Distinct Pathways. *Mol Biol Cell* **19**: 2729-2740, doi:10.1091/mbc.E08-01-0107

Chiang AC and Massague J (2008) Molecular basis of metastasis. *N Engl J Med* **359**: 2814-2823, doi:10.1056/NEJMra0805239 [doi]

Choi YE, Butterworth M, Malladi S, Duckett CS, Cohen GM, Bratton SB (2009) The E3 ubiquitin ligase cIAP1 binds and ubiquitinates caspase-3 and -7 via unique mechanisms at distinct steps in their processing. *J Biol Chem* **284**: 12772-12782, doi:10.1074/jbc.M807550200 [doi]

Chopra M, Riedel SS, Biehl M, Krieger S, von Krosigk V, Bauerlein CA, Brede C, Jordan Garrote AL, Kraus S, Schafer V, Ritz M, Mattenheimer K, Degla A, Mottok A, Einsele H, Wajant H, Beilhack A (2013) Tumor necrosis factor receptor 2-dependent homeostasis of regulatory T cells as a player in TNF-induced experimental metastasis. *Carcinogenesis* **34**: 1296-1303, doi:10.1093/carcin/bgt038 [doi]

Clarke PG (1990) Developmental cell death: morphological diversity and multiple mechanisms. *Anat Embryol (Berl)* **181**: 195-213

Condon SM, Mitsuuchi Y, Deng Y, LaPorte MG, Rippin SR, Haimowitz T, Alexander MD, Kumar PT, Hendi MS, Lee YH, Benetatos CA, Yu G, Kapoor GS, Neiman E, Seipel ME, Burns JM, Graham MA, McKinlay MA, Li X, Wang J, Shi Y, Feltham R, Bettjeman B, Cumming MH, Vince JE, Khan N, Silke J, Day CL, Chunduru SK (2014) Birinapant, a smac-mimetic with improved tolerability for the treatment of solid tumors and hematological malignancies. *J Med Chem* **57**: 3666-3677, doi:10.1021/jm500176w [doi]

Corcoran RB, Cheng KA, Hata AN, Faber AC, Ebi H, Coffee EM, Greninger P, Brown RD, Godfrey JT, Cohoon TJ, Song Y, Lifshits E, Hung KE, Shioda T, Dias-Santagata D, Singh A, Settleman J, Benes CH, Mino-Kenudson M, Wong KK, Engelman JA (2013) Synthetic lethal interaction of combined BCL-XL and MEK inhibition promotes tumor regressions in KRAS mutant cancer models. *Cancer Cell* **23**: 121-128, doi:10.1016/j.ccr.2012.11.007 [doi]

Cossu F, Mastrangelo E, Milani M, Sorrentino G, Lecis D, Delia D, Manzoni L, Seneci P, Scolastico C, Bolognesi M (2009a) Designing Smac-mimetics as antagonists of XIAP, cIAP1, and cIAP2. *Biochem Biophys Res Commun* **378**: 162-167, doi:10.1016/j.bbrc.2008.10.139

Cossu F, Milani M, Mastrangelo E, Vachette P, Servida F, Lecis D, Canevari G, Delia D, Drago C, Rizzo V, Manzoni L, Seneci P, Scolastico C, Bolognesi M (2009b) Structural Basis for Bivalent Smac-Mimetics Recognition in the IAP Protein Family. *J Mol Biol* **392**: 630-644, doi:10.1016/j.jmb.2009.04.033

Cossu F, Milani M, Vachette P, Malvezzi F, Grassi S, Lecis D, Delia D, Drago C, Seneci P, Bolognesi M, Mastrangelo E (2012) Structural insight into inhibitor of apoptosis proteins recognition by a potent divalent smac-mimetic. *PLoS One* **7**: e49527, doi:10.1371/journal.pone.0049527; 10.1371/journal.pone.0049527

Cretney E, Takeda K, Yagita H, Glaccum M, Peschon JJ, Smyth MJ (2002) Increased susceptibility to tumor initiation and metastasis in TNF-related apoptosis-inducing ligand-deficient mice. *J Immunol* **168**: 1356-1361

Crook NE, Clem RJ, Miller LK (1993) An apoptosis-inhibiting baculovirus gene with a zinc finger-like motif. *J Virol* **67**: 2168-2174

Cummins JM, Kohli M, Rago C, Kinzler KW, Vogelstein B, Bunz F (2004) X-Linked Inhibitor of Apoptosis Protein (XIAP) Is a Nonredundant Modulator of Tumor Necrosis Factor-Related Apoptosis-Inducing Ligand (TRAIL)- Mediated Apoptosis in Human Cancer Cells. *Cancer Res* **64**: 3006-3008, doi:10.1158/0008-5472.CAN-04-0046

Dai Y, Liu M, Tang W, Li Y, Lian J, Lawrence TS, Xu L (2009) A Smac-mimetic sensitizes

prostate cancer cells to TRAIL-induced apoptosis via modulating both IAPs and NF-kappaB. *BMC Cancer* **9**: 392, doi:10.1186/1471-2407-9-392

Darding M, Feltham R, Tenev T, Bianchi K, Benetatos C, Silke J, Meier P (2011) Molecular determinants of Smac mimetic induced degradation of cIAP1 and cIAP2. *Cell Death Differ* **18**: 1376-1386, doi:10.1038/cdd.2011.10

Datta R, Oki E, Endo K, Biedermann V, Ren J, Kufe D (2000) XIAP Regulates DNA Damage-induced Apoptosis Downstream of Caspase-9 Cleavage. *J Biol Chem ; J Biol Chem* **275**: 31733-31738, doi:10.1074/jbc.M910231199

de Bruijn MT, Raats DA, Hoogwater FJ, van Houdt WJ, Cameron K, Medema JP, Borel Rinkes IH, Kranenburg O (2010) Oncogenic KRAS sensitises colorectal tumour cells to chemotherapy by p53-dependent induction of Noxa. *Br J Cancer* **102**: 1254-1264, doi:10.1038/sj.bjc.6605633 [doi]

De Cesare M, Sfondrini L, Campiglio M, Sommariva M, Bianchi F, Perego P, van Rooijen N, Supino R, Rumio C, Zunino F, Pratesi G, Tagliabue E, Balsari A (2010) Ascites regression and survival increase in mice bearing advanced-stage human ovarian carcinomas and repeatedly treated intraperitoneally with CpG-ODN. *J Immunother* **33**: 8-15, doi:10.1097/CJI.0b013e3181affaa7

Degterev A and Yuan J (2008) Expansion and evolution of cell death programmes. *Nat Rev Mol Cell Biol* **9**: 378-390, doi:10.1038/nrm2393 [doi]

Demchenko YN, Glebov OK, Zingone A, Keats JJ, Bergsagel PL, Kuehl WM (2010) Classical and/or alternative NF-kappaB pathway activation in multiple myeloma. *Blood* **115**: 3541-

3552, doi:10.1182/blood-2009-09-243535

Di Nicolantonio F, Arena S, Gallicchio M, Zecchin D, Martini M, Flonta SE, Stella GM, Lamba S, Cancelliere C, Russo M, Geuna M, Appendino G, Fantozzi R, Medico E, Bardelli A (2008) Replacement of normal with mutant alleles in the genome of normal human cells unveils mutation-specific drug responses. *Proc Natl Acad Sci U S A* **105**: 20864-20869, doi:10.1073/pnas.0808757105 [doi]

Di Nicolantonio F, Arena S, Tabernero J, Grosso S, Molinari F, Macarulla T, Russo M, Cancelliere C, Zecchin D, Mazzucchelli L, Sasazuki T, Shirasawa S, Geuna M, Frattini M, Baselga J, Gallicchio M, Biffo S, Bardelli A (2010) Deregulation of the PI3K and KRAS signaling pathways in human cancer cells determines their response to everolimus. *J Clin Invest* **120**: 2858-2866, doi:10.1172/JCI37539 [doi]

Dickens LS, Boyd RS, Jukes-Jones R, Hughes MA, Robinson GL, Fairall L, Schwabe JW, Cain K, Macfarlane M (2012a) A death effector domain chain DISC model reveals a crucial role for caspase-8 chain assembly in mediating apoptotic cell death. *Mol Cell* **47**: 291-305, doi:10.1016/j.molcel.2012.05.004 [doi]

Dickens LS, Powley IR, Hughes MA, MacFarlane M (2012b) The 'complexities' of life and death: death receptor signalling platforms. *Exp Cell Res* **318**: 1269-1277, doi:10.1016/j.yexcr.2012.04.005 [doi]

Dillon CP, Weinlich R, Rodriguez DA, Cripps JG, Quarato G, Gurung P, Verbist KC, Brewer TL, Llambi F, Gong YN, Janke LJ, Kelliher MA, Kanneganti TD, Green DR (2014) RIPK1 blocks early postnatal lethality mediated by caspase-8 and RIPK3. *Cell* **157**: 1189-1202,

doi:10.1016/j.cell.2014.04.018 [doi]

Dogan T, Harms GS, Hekman M, Karreman C, Oberoi TK, Alnemri ES, Rapp UR, Rajalingam K (2008) X-linked and cellular IAPs modulate the stability of C-RAF kinase and cell motility. *Nat Cell Biol* **10**: 1447-1455, doi:10.1038/ncb1804

Du C, Fang M, Li Y, Li L, Wang X (2000) Smac, a Mitochondrial Protein that Promotes Cytochrome cDependent Caspase Activation by Eliminating IAP Inhibition. *Cell* **102**: 33-42

Duckett CS, Nava VE, Gedrich RW, Clem RJ, Van Dongen JL, Gilfillan MC, Shiels H, Hardwick JM, Thompson CB (1996) A conserved family of cellular genes related to the baculovirus iap gene and encoding apoptosis inhibitors. *EMBO J* **15**: 2685-2694

Dueber EC, Schoeffler AJ, Lingel A, Elliott JM, Fedorova AV, Giannetti AM, Zobel K, Maurer B, Varfolomeev E, Wu P, Wallweber HJ, Hymowitz SG, Deshayes K, Vucic D, Fairbrother WJ (2011) Antagonists induce a conformational change in cIAP1 that promotes autoubiquitination. *Science* **334**: 376-380, doi:10.1126/science.1207862 [doi]

Eckelman BP, Salvesen GS, Scott FL (2006) Human inhibitor of apoptosis proteins: why XIAP is the black sheep of the family. *EMBO Rep* **7**: 988-994, doi:10.1038/sj.embor.7400795

Elgendy M, Sheridan C, Brumatti G, Martin SJ (2011) Oncogenic Ras-induced expression of Noxa and Beclin-1 promotes autophagic cell death and limits clonogenic survival. *Mol Cell* **42**: 23-35, doi:10.1016/j.molcel.2011.02.009 [doi]

Emeagi PU, Van Lint S, Goyvaerts C, Maenhout S, Cauwels A, McNeish IA, Bos T, Heirman C, Thielemans K, Aerts JL, Breckpot K (2012) Proinflammatory characteristics of

SMAC/DIABLO-induced cell death in antitumor therapy. *Cancer Res* **72**: 1342-1352, doi:10.1158/0008-5472.CAN-11-2400

Emmerich CH, Schmukle AC, Haas TL, Gerlach B, Cordier SM, Rieser E, Walczak H (2011) The linear ubiquitin chain assembly complex forms part of the TNF-R1 signalling complex and is required for effective TNF-induced gene induction and prevents TNF-induced apoptosis. *Adv Exp Med Biol* **691**: 115-126, doi:10.1007/978-1-4419-6612-4_12 [doi]

Eschenburg G, Eggert A, Schramm A, Lode HN, Hundsdoerfer P (2012) Smac mimetic LBW242 sensitizes XIAP-overexpressing neuroblastoma cells for TNF-alpha independent apoptosis. *Cancer Res*, doi:10.1158/0008-5472.CAN-11-4072

Eser S, Schnieke A, Schneider G, Saur D (2014) Oncogenic KRAS signalling in pancreatic cancer. *Br J Cancer* **111**: 817-822, doi:10.1038/bjc.2014.215 [doi]

Estornes Y and Bertrand MJ (2014) IAPs, regulators of innate immunity and inflammation. *Semin Cell Dev Biol*, doi:S1084-9521(14)00073-1 [pii]

Falschlehner C, Ganten TM, Koschny R, Schaefer U, Walczak H (2009) TRAIL and other TRAIL receptor agonists as novel cancer therapeutics. *Adv Exp Med Biol* **647**: 195-206, doi:10.1007/978-0-387-89520-8_14 [doi]

Farmer H, McCabe N, Lord CJ, Tutt AN, Johnson DA, Richardson TB, Santarosa M, Dillon KJ, Hickson I, Knights C, Martin NM, Jackson SP, Smith GC, Ashworth A (2005) Targeting the DNA repair defect in BRCA mutant cells as a therapeutic strategy. *Nature* **434**: 917-921, doi:nature03445 [pii]

Favaloro B, Allocati N, Graziano V, Di Ilio C, De Laurenzi V (2012) Role of apoptosis in

disease. *Aging (Albany NY)* **4**: 330-349, doi:100459 [pii]

Feltham R, Bettjeman B, Budhidarmo R, Mace PD, Shirley S, Condon SM, Chunduru SK, McKinlay MA, Vaux DL, Silke J, Day CL (2011) SMAC-mimetics activate the E3 ligase activity of cIAP1 by promoting RING dimerisation. *J Biol Chem* **286**: 17015-17028, doi:10.1074/jbc.M111.222919

Feoktistova M, Geserick P, Kellert B, Dimitrova DP, Langlais C, Hupe M, Cain K, Macfarlane M, Hacker G, Leverkus M (2011) cIAPs Block Ripoptosome Formation, a RIP1/Caspase-8 Containing Intracellular Cell Death Complex Differentially Regulated by cFLIP Isoforms. *Mol Cell* **43**: 449-463, doi:10.1016/j.molcel.2011.06.011

Fernandez Y, Espana L, Manas S, Fabra A, Sierra A (2000) Bcl-xL promotes metastasis of breast cancer cells by induction of cytokines resistance. *Cell Death Differ* **7**: 350-359, doi:10.1038/sj.cdd.4400662 [doi]

Fingas CD, Blechacz BR, Smoot RL, Guicciardi ME, Mott J, Bronk SF, Werneburg NW, Sirica AE, Gores GJ (2010) A smac mimetic reduces TNF related apoptosis inducing ligand (TRAIL)-induced invasion and metastasis of cholangiocarcinoma cells. *Hepatology* **52**: 550-561, doi:10.1002/hep.23729

Finnberg N, Klein-Szanto AJ, El-Deiry WS (2008) TRAIL-R deficiency in mice promotes susceptibility to chronic inflammation and tumorigenesis. *J Clin Invest* **118**: 111-123, doi:10.1172/JCI29900 [doi]

Foster F, Owens T, Tanianis-Hughes J, Clarke R, Brennan K, Bundred N, Streuli C (2009) Targeting inhibitor of apoptosis proteins in combination with ErbB antagonists in breast

cancer. **11**: R41

Friedl P and Gilmour D (2009) Collective cell migration in morphogenesis, regeneration and cancer. *Nat Rev Mol Cell Biol* **10**: 445-457, doi:10.1038/nrm2720 [doi]

Fulda S (2014a) Inhibitor of Apoptosis (IAP) proteins in hematological malignancies: molecular mechanisms and therapeutic opportunities. *Leukemia* **28**: 1414-1422, doi:10.1038/leu.2014.56 [doi]

Fulda S (2014b) Molecular pathways: targeting inhibitor of apoptosis proteins in cancer--from molecular mechanism to therapeutic application. *Clin Cancer Res* **20**: 289-295, doi:10.1158/1078-0432.CCR-13-0227; 10.1158/1078-0432.CCR-13-0227

Fulda S and Debatin KM (2006) Extrinsic versus intrinsic apoptosis pathways in anticancer chemotherapy. *Oncogene* **25**: 4798-4811, doi:1209608 [pii]

Fulda S and Vucic D (2012) Targeting IAP proteins for therapeutic intervention in cancer. *Nat Rev Drug Discov* **11**: 109-124, doi:10.1038/nrd3627; 10.1038/nrd3627

Fulda S, Wick W, Weller M, Debatin KM (2002) Smac agonists sensitize for Apo2L/TRAIL- or anticancer drug-induced apoptosis and induce regression of malignant glioma in vivo. *Nat Med* **8**: 808-815, doi:10.1038/nm735

Gaither A, Porter D, Yao Y, Borawski J, Yang G, Donovan J, Sage D, Slisz J, Tran M, Straub C, Ramsey T, Iourgenko V, Huang A, Chen Y, Schlegel R, Labow M, Fawell S, Sellers WR, Zawel L (2007) A Smac Mimetic Rescue Screen Reveals Roles for Inhibitor of Apoptosis Proteins in Tumor Necrosis Factor-{alpha} Signaling. *Cancer Res* **67**: 11493-11498,

doi:10.1158/0008-5472.CAN-07-5173

Galluzzi L, Bravo-San Pedro JM, Vitale I, Aaronson SA, Abrams JM, Adam D, Alnemri ES, Altucci L, Andrews D, Annicchiarico-Petruzzelli M, Baehrecke EH, Bazan NG, Bertrand MJ, Bianchi K, Blagosklonny MV, Blomgren K, Borner C, Bredesen DE, Brenner C, Campanella M, Candi E, Cecconi F, Chan FK, Chandel NS, Cheng EH, Chipuk JE, Cidlowski JA, Ciechanover A, Dawson TM, Dawson VL, De Laurenzi V, De Maria R, Debatin KM, Di Daniele N, Dixit VM, Dynlacht BD, El-Deiry WS, Fimia GM, Flavell RA, Fulda S, Garrido C, Gougeon ML, Green DR, Gronemeyer H, Hajnoczky G, Hardwick JM, Hengartner MO, Ichijo H, Joseph B, Jost PJ, Kaufmann T, Kepp O, Klionsky DJ, Knight RA, Kumar S, Lemasters JJ, Levine B, Linkermann A, Lipton SA, Lockshin RA, Lopez-Otin C, Lugli E, Madeo F, Malorni W, Marine JC, Martin SJ, Martinou JC, Medema JP, Meier P, Melino S, Mizushima N, Moll U, Munoz-Pinedo C, Nunez G, Oberst A, Panaretakis T, Penninger JM, Peter ME, Piacentini M, Pinton P, Prehn JH, Puthalakath H, Rabinovich GA, Ravichandran KS, Rizzuto R, Rodrigues CM, Rubinsztein DC, Rudel T, Shi Y, Simon HU, Stockwell BR, Szabadkai G, Tait SW, Tang HL, Tavernarakis N, Tsujimoto Y, Vanden Berghe T, Vandenabeele P, Villunger A, Wagner EF, Walczak H, White E, Wood WG, Yuan J, Zakeri Z, Zhivotovsky B, Melino G, Kroemer G (2015) Essential versus accessory aspects of cell death: recommendations of the NCCD 2015. *Cell Death Differ* **22**: 58-73, doi:10.1038/cdd.2014.137 [doi]

Galluzzi L, Kepp O, Kroemer G (2012) Mitochondria: master regulators of danger signalling. *Nat Rev Mol Cell Biol* **13**: 780-788, doi:10.1038/nrm3479 [doi]

Ganten TM, Haas TL, Sykora J, Stahl H, Sprick MR, Fas SC, Krueger A, Weigand MA, Grosse-Wilde A, Stremmel W, Krammer PH, Walczak H (2004) Enhanced caspase-8

recruitment to and activation at the DISC is critical for sensitisation of human hepatocellular carcinoma cells to TRAIL-induced apoptosis by chemotherapeutic drugs. *Cell Death Differ* **11**: S86-S96

Ganten TM, Koschny R, Sykora J, Schulze-Bergkamen H, Buchler P, Haas TL, Schader MB, Untergasser A, Stremmel W, Walczak H (2006) Preclinical Differentiation between Apparently Safe and Potentially Hepatotoxic Applications of TRAIL Either Alone or in Combination with Chemotherapeutic Drugs. *Clin Cancer Res* **12**: 2640-2646, doi:10.1158/1078-0432.CCR-05-2635

Garg G, Vangveravong S, Zeng C, Collins L, Hornick M, Hashim Y, Piwnica-Worms D, Powell MA, Mutch DG, Mach RH, Hawkins WG, Spitzer D (2014) Conjugation to a SMAC mimetic potentiates sigma-2 ligand induced tumor cell death in ovarian cancer. *Mol Cancer* **13**: 50-4598-13-50, doi:10.1186/1476-4598-13-50 [doi]

Gerlach B, Cordier SM, Schmukle AC, Emmerich CH, Rieser E, Haas TL, Webb AI, Rickard JA, Anderton H, Wong WW, Nachbur U, Gangoda L, Warnken U, Purcell AW, Silke J, Walczak H (2011) Linear ubiquitination prevents inflammation and regulates immune signalling. *Nature* **471**: 591-596, doi:10.1038/nature09816

Giampieri S, Manning C, Hooper S, Jones L, Hill CS, Sahai E (2009) Localized and reversible TGFbeta signalling switches breast cancer cells from cohesive to single cell motility. *Nat Cell Biol* **11**: 1287-1296, doi:10.1038/ncb1973 [doi]

Gillissen B, Richter A, Richter A, Overkamp T, Essmann F, Hemmati PG, Preissner R, Belka C, Daniel PT (2013) Targeted therapy of the XIAP/proteasome pathway overcomes TRAIL-resistance in carcinoma by switching apoptosis signaling to a Bax/Bak-independent 'type I'

mode. *Cell Death Dis* **4**: e643, doi:10.1038/cddis.2013.67 [doi]

Green DR and Kroemer G (2004) The pathophysiology of mitochondrial cell death. *Science* **305**: 626-629, doi:10.1126/science.1099320 [doi]

Greer RM, Peyton M, Larsen JE, Girard L, Xie Y, Gazdar AF, Harran P, Wang L, Brekken RA, Wang X, Minna JD (2011) SMAC mimetic (JP1201) sensitizes non-small cell lung cancers to multiple chemotherapy agents in an IAP-dependent but TNF-alpha-independent manner. *Cancer Res* **71**: 7640-7648, doi:10.1158/0008-5472.CAN-10-3947

Grosse-Wilde A, Voloshanenko O, Bailey SL, Longton GM, Schaefer U, Csernok AI, Schutz G, Greiner EF, Kemp CJ, Walczak H (2008) TRAIL-R deficiency in mice enhances lymph node metastasis without affecting primary tumor development. *J Clin Invest* **118**: 100-110, doi:10.1172/JCI33061 [doi]

Gyrd-Hansen M and Meier P (2010) IAPs: from caspase inhibitors to modulators of NF-kappaB, inflammation and cancer. *Nat Rev Cancer* **10**: 561-574, doi:10.1038/nrc2889

Haas TL, Emmerich CH, Gerlach B, Schmukle AC, Cordier SM, Rieser E, Feltham R, Vince J, Warnken U, Wenger T, Koschny R, Komander D, Silke J, Walczak H (2009) Recruitment of the Linear Ubiquitin Chain Assembly Complex Stabilizes the TNF-R1 Signaling Complex and Is Required for TNF-Mediated Gene Induction. *Mol Cell* **36**: 831-844, doi:DOI: 10.1016/j.molcel.2009.10.013

Hadj-Slimane R, Pamonsinlapatham P, Herbeuval JP, Garbay C, Lepelletier Y, Raynaud F (2010) RasV12 induces Survivin/AuroraB pathway conferring tumor cell apoptosis resistance. *Cell Signal* **22**: 1214-1221, doi:10.1016/j.cellsig.2010.03.013 [doi]

Hagemann T, Lawrence T, McNeish I, Charles KA, Kulbe H, Thompson RG, Robinson SC, Balkwill FR (2008) "Re-educating" tumor-associated macrophages by targeting NF-κB. *J Exp Med* **205**: 1261-1268

Hanahan D and Weinberg RA (2011) Hallmarks of cancer: the next generation. *Cell* **144**: 646-674, doi:10.1016/j.cell.2011.02.013

Hashim YM, Spitzer D, Vangveravong S, Hornick MC, Garg G, Hornick JR, Goedegebuure P, Mach RH, Hawkins WG (2014) Targeted pancreatic cancer therapy with the small molecule drug conjugate SW IV-134. *Mol Oncol* **8**: 956-967, doi:10.1016/j.molonc.2014.03.005 [doi]

Hata AN, Yeo A, Faber AC, Lifshits E, Chen Z, Cheng KA, Walton Z, Sarosiek KA, Letai A, Heist RS, Mino-Kenudson M, Wong KK, Engelman JA (2014) Failure to induce apoptosis via BCL-2 family proteins underlies lack of efficacy of combined MEK and PI3K inhibitors for KRAS-mutant lung cancers. *Cancer Res* **74**: 3146-3156, doi:10.1158/0008-5472.CAN-13-3728 [doi]

Heusinkveld M, de Vos van Steenwijk PJ, Goedemans R, Ramwadhdoebe TH, Gorter A, Welters MJ, van Hall T, van der Burg SH (2011) M2 macrophages induced by prostaglandin E2 and IL-6 from cervical carcinoma are switched to activated M1 macrophages by CD4+ Th1 cells. *J Immunol* **187**: 1157-1165, doi:10.4049/jimmunol.1100889

Hoogwater FJ, Nijkamp MW, Smakman N, Steller EJ, Emmink BL, Westendorp BF, Raats DA, Sprick MR, Schaefer U, Van Houdt WJ, De Bruijn MT, Schackmann RC, Derksen PW, Medema JP, Walczak H, Borel Rinkes IH, Kranenburg O (2010) Oncogenic K-Ras turns

death receptors into metastasis-promoting receptors in human and mouse colorectal cancer cells. *Gastroenterology* **138**: 2357-2367, doi:10.1053/j.gastro.2010.02.046

Huang S, Ren X, Wang L, Zhang L, Wu X (2011) Lung-cancer chemoprevention by induction of synthetic lethality in mutant KRAS premalignant cells in vitro and in vivo. *Cancer Prev Res (Phila)* **4**: 666-673, doi:10.1158/1940-6207.CAPR-10-0235 [doi]

Hundsdoerfer P, Dietrich I, Schmelz K, Eckert C, Henze G (2010) XIAP expression is post-transcriptionally upregulated in childhood ALL and is associated with glucocorticoid response in T-cell ALL. *Pediatr Blood Cancer* **55**: 260-266, doi:10.1002/pbc.22541

Ibrahim AM, Mansour IM, Wilson MM, Mokhtar DA, Helal AM, Al Wakeel HM (2012) Study of survivin and X-linked inhibitor of apoptosis protein (XIAP) genes in acute myeloid leukemia (AML). *Lab Hematol* **18**: 1-10, doi:10.1532/LH96.09013 [doi]

Igney FH and Krammer PH (2002) Death and anti-death: tumour resistance to apoptosis. *Nat Rev Cancer* **2**: 277-288, doi:10.1038/nrc776 [doi]

Ikeda F, Deribe YL, Skanland SS, Stieglitz B, Grabbe C, Franz-Wachtel M, van Wijk SJ, Goswami P, Nagy V, Terzic J, Tokunaga F, Androulidaki A, Nakagawa T, Pasparakis M, Iwai K, Sundberg JP, Schaefer L, Rittinger K, Macek B, Dikic I (2011) SHARPIN forms a linear ubiquitin ligase complex regulating NF-kappaB activity and apoptosis. *Nature* **471**: 637-641, doi:10.1038/nature09814; 10.1038/nature09814

Infante JR, Dees EC, Olszanski AJ, Dhuria SV, Sen S, Cameron S, Cohen RB (2014) Phase I dose-escalation study of LCL161, an oral inhibitor of apoptosis proteins inhibitor, in patients with advanced solid tumors. *J Clin Oncol* **32**: 3103-3110,

doi:10.1200/JCO.2013.52.3993 [doi]

Ishimura N, Isomoto H, Bronk SF, Gores GJ (2006) Trail induces cell migration and invasion in apoptosis-resistant cholangiocarcinoma cells. *Am J Physiol Gastrointest Liver Physiol* **290**: G129-36, doi:00242.2005 [pii]

Itoh Y, Ishikawa M, Kitaguchi R, Okuhira K, Naito M, Hashimoto Y (2012) Double protein knockdown of cIAP1 and CRABP-II using a hybrid molecule consisting of ATRA and IAPs antagonist. *Bioorg Med Chem Lett* **22**: 4453-4457, doi:10.1016/j.bmcl.2012.04.134 [doi]

Jinesh GG, Chunduru S, Kamat AM (2012) Smac mimetic enables the anticancer action of BCG-stimulated neutrophils through TNF-alpha but not through TRAIL and FasL. *J Leukoc Biol*, doi:10.1189/jlb.1211623

Jost PJ, Grabow S, Gray D, McKenzie MD, Nachbur U, Huang DCS, Bouillet P, Thomas HE, Borner C, Silke J, Strasser A, Kaufmann T (2009) XIAP discriminates between type I and type II FAS-induced apoptosis. *Nature* **460**: 1035-1039

Kaelin WG,Jr (2005) The concept of synthetic lethality in the context of anticancer therapy. *Nat Rev Cancer* **5**: 689-698, doi:nrc1691 [pii]

Kang Y, Siegel PM, Shu W, Drobnjak M, Kakonen SM, Cordon-Cardo C, Guise TA, Massague J (2003) A multigenic program mediating breast cancer metastasis to bone. *Cancer Cell* **3**: 537-549, doi:S1535610803001326 [pii]

Kantari C and Walczak H (2011) Caspase-8 and bid: caught in the act between death receptors and mitochondria. *Biochim Biophys Acta* **1813**: 558-563,

doi:10.1016/j.bbamcr.2011.01.026 [doi]

Keats JJ, Fonseca R, Chesi M, Schop R, Baker A, Chng WJ, Van Wier S, Tiedemann R, Shi CX, Sebag M, Braggio E, Henry T, Zhu YX, Fogle H, Price-Troska T, Ahmann G, Mancini C, Brents LA, Kumar S, Greipp P, Dispenzieri A, Bryant B, Mulligan G, Bruhn L, Barrett M, Valdez R, Trent J, Stewart AK, Carpten J, Bergsagel PL (2007) Promiscuous mutations activate the noncanonical NF-kappaB pathway in multiple myeloma. *Cancer Cell* **12**: 131-144, doi:10.1016/j.ccr.2007.07.003

Kepp O, Galluzzi L, Martins I, Schlemmer F, Adjemian S, Michaud M, Sukkurwala AQ, Menger L, Zitvogel L, Kroemer G (2011) Molecular determinants of immunogenic cell death elicited by anticancer chemotherapy. *Cancer Metastasis Rev* **30**: 61-69, doi:10.1007/s10555-011-9273-4 [doi]

Kim J, Ahn S, Ko YG, Boo YC, Chi SG, Ni CW, Go YM, Jo H, Park H (2010) X-linked inhibitor of apoptosis protein controls alpha5-integrin-mediated cell adhesion and migration. *Am J Physiol Heart Circ Physiol* **299**: H300-9, doi:10.1152/ajpheart.00180.2010 [doi]

Kim S, Yao J, Suyama K, Qian X, Qian BZ, Bandyopadhyay S, Loudig O, De Leon-Rodriguez C, Zhou ZN, Segall J, Macian F, Norton L, Hazan RB (2014) Slug promotes survival during metastasis through suppression of Puma-mediated apoptosis. *Cancer Res* **74**: 3695-3706, doi:10.1158/0008-5472.CAN-13-2591 [doi]

Kreuz S, Siegmund D, Scheurich P, Wajant H (2001) NF-kappaB inducers upregulate cFLIP, a cycloheximide-sensitive inhibitor of death receptor signaling. *Mol Cell Biol* **21**: 3964-3973, doi:10.1128/MCB.21.12.3964-3973.2001 [doi]

LaCasse EC, Mahoney DJ, Cheung HH, Plenchette S, Baird S, Korneluk RG (2008) IAP-targeted therapies for cancer. *Oncogene* **27**: 6252-6275, doi:10.1038/onc.2008.302

Lamba S, Russo M, Sun C, Lazzari L, Cancelliere C, Grernrum W, Lieftink C, Bernards R, Di Nicolantonio F, Bardelli A (2014) RAF suppression synergizes with MEK inhibition in KRAS mutant cancer cells. *Cell Rep* **8**: 1475-1483, doi:10.1016/j.celrep.2014.07.033 [doi]

Lamkanfi M (2011) Emerging inflammasome effector mechanisms. *Nat Rev Immunol* **11**: 213-220, doi:10.1038/nri2936 [doi]

Laukens B, Jennewein C, Schenk B, Vanlangenakker N, Schier A, Cristofanon S, Zobel K, Deshayes K, Vucic D, Jeremias I, Bertrand MJ, Vandenabeele P, Fulda S (2011) Smac mimetic bypasses apoptosis resistance in FADD- or caspase-8-deficient cells by priming for tumor necrosis factor alpha-induced necroptosis. *Neoplasia* **13**: 971-979

Lavazza C, Carlo-Stella C, Giacomini A, Cleris L, Righi M, Sia D, Di Nicola M, Magni M, Longoni P, Milanesi M, Francolini M, Gloghini A, Carbone A, Formelli F, Gianni AM (2010) Human CD34+ cells engineered to express membrane-bound tumor necrosis factor-related apoptosis-inducing ligand target both tumor cells and tumor vasculature. *Blood* **115**: 2231-2240, doi:10.1182/blood-2009-08-239632

Lavrik I, Golks A, Krammer PH (2005) Death receptor signaling. *J Cell Sci* **118**: 265-267, doi:118/2/265 [pii]

Lecis D, De Cesare M, Perego P, Conti A, Corna E, Drago C, Seneci P, Walczak H, Colombo MP, Delia D, Sangaletti S (2013) Smac mimetics induce inflammation and necrotic tumour cell death by modulating macrophage activity. *Cell Death Dis* **4**: e920,

doi:10.1038/cddis.2013.449; 10.1038/cddis.2013.449

Lecis D, Drago C, Manzoni L, Seneci P, Scolastico C, Mastrangelo E, Bolognesi M, Anichini A, Kashkar H, Walczak H, Delia D (2010) Novel SMAC-mimetics synergistically stimulate melanoma cell death in combination with TRAIL and Bortezomib. *Br J Cancer* **102**: 1707-1716

Lecis D, Mastrangelo E, Belvisi L, Bolognesi M, Civera M, Cossu F, De Cesare M, Delia D, Drago C, Manenti G, Manzoni L, Milani M, Moroni E, Perego P, Potenza D, Rizzo V, Scavullo C, Scolastico C, Servida F, Vasile F, Seneci P (2012) Dimeric Smac mimetics/IAP inhibitors as in vivo-active pro-apoptotic agents. Part II: Structural and biological characterization. *Bioorg Med Chem* **20**: 6709-6723, doi:10.1016/j.bmc.2012.09.041; 10.1016/j.bmc.2012.09.041

Lehman TA, Modali R, Boukamp P, Stanek J, Bennett WP, Welsh JA, Metcalf RA, Stampfer MR, Fusenig N, Rogan EM (1993) P53 Mutations in Human Immortalized Epithelial Cell Lines. *Carcinogenesis* **14**: 833-839

Lengyel E (2010) Ovarian cancer development and metastasis. *Am J Pathol* **177**: 1053-1064, doi:10.2353/ajpath.2010.100105

Li L, Thomas RM, Suzuki H, De Brabander JK, Wang X, Harran PG (2004) A Small Molecule Smac Mimic Potentiates TRAIL- and TNF{alpha}-Mediated Cell Death. *Science* **305**: 1471-1474

Li P, Nijhawan D, Budihardjo I, Srinivasula SM, Ahmad M, Alnemri ES, Wang X (1997) Cytochrome c and dATP-dependent formation of Apaf-1/caspase-9 complex initiates an

apoptotic protease cascade. *Cell* **91**: 479-489, doi:S0092-8674(00)80434-1 [pii]

Liu J, Zhang D, Luo W, Yu J, Li J, Yu Y, Zhang X, Chen J, Wu XR, Huang C (2012) E3 ligase activity of XIAP RING domain is required for XIAP-mediated cancer cell migration, but not for its RhoGDI binding activity. *PLoS One* **7**: e35682, doi:10.1371/journal.pone.0035682 [doi]

Liu Z, Li H, Wu X, Yoo BH, Yan SR, Stadnyk AW, Sasazuki T, Shirasawa S, LaCasse EC, Korneluk RG, Rosen KV (2006) Detachment-induced upregulation of XIAP and cIAP2 delays anoikis of intestinal epithelial cells. *Oncogene* **25**: 7680-7690, doi:1209753 [pii]

Liu Z, Sun C, Olejniczak ET, Meadows RP, Betz SF, Oost T, Herrmann J, Wu JC, Fesik SW (2000) Structural basis for binding of Smac/DIABLO to the XIAP BIR3 domain. *Nature* **408**: 1004-1008

Lomonosova E and Chinnadurai G (2008) BH3-only proteins in apoptosis and beyond: an overview. *Oncogene* **27 Suppl 1**: S2-19, doi:10.1038/onc.2009.39 [doi]

Lopez J, John SW, Tenev T, Rautureau GJ, Hinds MG, Francalanci F, Wilson R, Broemer M, Santoro MM, Day CL, Meier P (2011) CARD-mediated autoinhibition of cIAP1's E3 ligase activity suppresses cell proliferation and migration. *Mol Cell* **42**: 569-583, doi:10.1016/j.molcel.2011.04.008

Lu J, McEachern D, Sun H, Bai L, Peng Y, Qiu S, Miller R, Liao J, Yi H, Liu M, Bellail A, Hao C, Sun SY, Ting AT, Wang S (2011) Therapeutic potential and molecular mechanism of a novel, potent, nonpeptide, Smac mimetic SM-164 in combination with TRAIL for cancer treatment. *Mol Cancer Ther* **10**: 902-914, doi:10.1158/1535-7163.MCT-10-0864

Luetzkendorf J, Mueller LP, Mueller T, Caysa H, Nerger K, Schmoll HJ (2010) Growth inhibition of colorectal carcinoma by lentiviral TRAIL-transgenic human mesenchymal stem cells requires their substantial intratumoral presence. *J Cell Mol Med* **14**: 2292-2304, doi:10.1111/j.1582-4934.2009.00794.x [doi]

Maione F, Capano S, Regano D, Zentilin L, Giacca M, Casanovas O, Bussolino F, Serini G, Giraudo E (2012) Semaphorin 3A overcomes cancer hypoxia and metastatic dissemination induced by antiangiogenic treatment in mice. *J Clin Invest* **122**: 1832-1848, doi:10.1172/JCI58976 [doi]

Manzoni L, Belvisi L, Bianchi A, Conti A, Drago C, de Matteo M, Ferrante L, Mastrangelo E, Perego P, Potenza D, Scolastico C, Servida F, Timpano G, Vasile F, Rizzo V, Seneci P (2012) Homo- and heterodimeric Smac mimetics/IAP inhibitors as in vivo-active pro-apoptotic agents. Part I: Synthesis. *Bioorg Med Chem* **20**: 6687-6708, doi:10.1016/j.bmc.2012.09.020; 10.1016/j.bmc.2012.09.020

Mehrotra S, Languino LR, Raskett CM, Mercurio AM, Dohi T, Altieri DC (2010) IAP regulation of metastasis. *Cancer Cell* **17**: 53-64, doi:10.1016/j.ccr.2009.11.021 [doi]

Metwalli AR, Khanbolooki S, Jinesh G, Sundi D, Shah JB, Shrader M, Choi W, Lashinger LM, Chunduru S, McConkey DJ, McKinlay M, Kamat AM (2010) Smac mimetic reverses resistance to TRAIL and chemotherapy in human urothelial cancer cells. *Cancer Biol Ther* **10**: 885-892, doi:10.4161/cbt.10.9.13237

Meyerhardt JA and Mayer RJ (2005) Systemic therapy for colorectal cancer. *N Engl J Med* **352**: 476-487, doi:352/5/476 [pii]

Mingozzi M, Manzoni L, Arosio D, Dal Corso A, Manzotti M, Innamorati F, Pignataro L, Lecis D, Delia D, Seneci P, Gennari C (2014) Synthesis and biological evaluation of dual action cyclo-RGD/SMAC mimetic conjugates targeting alpha(v)beta(3)/alpha(v)beta(5) integrins and IAP proteins. *Org Biomol Chem* **12**: 3288-3302, doi:10.1039/c4ob00207e [doi]

Minn AJ, Gupta GP, Siegel PM, Bos PD, Shu W, Giri DD, Viale A, Olshen AB, Gerald WL, Massague J (2005) Genes that mediate breast cancer metastasis to lung. *Nature* **436**: 518-524, doi:nature03799 [pii]

Misale S, Yaeger R, Hobor S, Scala E, Janakiraman M, Liska D, Valtorta E, Schiavo R, Buscarino M, Siravegna G, Bencardino K, Cercek A, Chen CT, Veronese S, Zanon C, Sartore-Bianchi A, Gambacorta M, Gallicchio M, Vakiani E, Boscaro V, Medico E, Weiser M, Siena S, Di Nicolantonio F, Solit D, Bardelli A (2012) Emergence of KRAS mutations and acquired resistance to anti-EGFR therapy in colorectal cancer. *Nature* **486**: 532-536, doi:10.1038/nature11156 [doi]

Miura K, Fujibuchi W, Ishida K, Naitoh T, Ogawa H, Ando T, Yazaki N, Watanabe K, Haneda S, Shibata C, Sasaki I (2011) Inhibitor of apoptosis protein family as diagnostic markers and therapeutic targets of colorectal cancer. *Surg Today* **41**: 175-182, doi:10.1007/s00595-010-4390-1

Moller Y, Siegemund M, Beyes S, Herr R, Lecis D, Delia D, Kontermann R, Brummer T, Pfizenmaier K, Olayioye MA (2014) EGFR-Targeted TRAIL and a Smac Mimetic Synergize to Overcome Apoptosis Resistance in KRAS Mutant Colorectal Cancer Cells. *PLoS One* **9**: e107165, doi:10.1371/journal.pone.0107165 [doi]

Moulin M, Anderton H, Voss AK, Thomas T, Wong WW, Bankovacki A, Feltham R, Chau D, Cook WD, Silke J, Vaux DL (2012) IAPs limit activation of RIP kinases by TNF receptor 1 during development. *EMBO J* **31**: 1679-1691, doi:10.1038/emboj.2012.18; 10.1038/emboj.2012.18

Muhlenbeck F, Schneider P, Bodmer JL, Schwenzer R, Hauser A, Schubert G, Scheurich P, Moosmayer D, Tschopp J, Wajant H (2000) The tumor necrosis factor-related apoptosis-inducing ligand receptors TRAIL-R1 and TRAIL-R2 have distinct cross-linking requirements for initiation of apoptosis and are non-redundant in JNK activation. *J Biol Chem* **275**: 32208-32213, doi:10.1074/jbc.M000482200 [doi]

Muller-Sienerth N, Dietz L, Holtz P, Kapp M, Grigoleit GU, Schmuck C, Wajant H, Siegmund D (2011) SMAC mimetic BV6 induces cell death in monocytes and maturation of monocyte-derived dendritic cells. *PLoS One* **6**: e21556, doi:10.1371/journal.pone.0021556

Newsom-Davis T, Prieske S, Walczak H (2009) Is TRAIL the holy grail of cancer therapy? *Apoptosis* **14**: 607-623

Nikolovska-Coleska Z, Wang R, Fang X, Pan H, Tomita Y, Li P, Roller PP, Krajewski K, Saito NG, Stuckey JA, Wang S (2004) Development and optimization of a binding assay for the XIAP BIR3 domain using fluorescence polarization. *Anal Biochem* **332**: 261-273, doi:10.1016/j.ab.2004.05.055

Nosseri C, Coppola S, Ghibelli L (1994) Possible involvement of poly(ADP-ribosyl) polymerase in triggering stress-induced apoptosis. *Exp Cell Res* **212**: 367-373, doi:S0014-4827(84)71156-6 [pii]

Oberoi TK, Dogan T, Hocking JC, Scholz RP, Mooz J, Anderson CL, Karreman C, Meyer zu Heringdorf D, Schmidt G, Ruonala M, Namikawa K, Harms GS, Carpy A, Macek B, Koster RW, Rajalingam K (2011) IAPs regulate the plasticity of cell migration by directly targeting Rac1 for degradation. *EMBO J* **31**: 14-28, doi:10.1038/emboj.2011.423; 10.1038/emboj.2011.423

Oberst A, Dillon CP, Weinlich R, McCormick LL, Fitzgerald P, Pop C, Hakem R, Salvesen GS, Green DR (2011) Catalytic activity of the caspase-8-FLIP(L) complex inhibits RIPK3-dependent necrosis. *Nature* **471**: 363-367, doi:10.1038/nature09852 [doi]

Oost TK, Sun C, Armstrong RC, Al-Assaad A, Betz SF, Deckwerth TL, Ding H, Elmore SW, Meadows RP, Olejniczak ET, Oleksijew A, Oltersdorf T, Rosenberg SH, Shoemaker AR, Tomaselli KJ, Zou H, Fesik SW (2004) Discovery of Potent Antagonists of the Antiapoptotic Protein XIAP for the Treatment of Cancer. *J Med Chem* **47**: 4417-4426

Perkins ND (2007) Integrating cell-signalling pathways with NF-kappaB and IKK function. *Nat Rev Mol Cell Biol* **8**: 49-62, doi:nrm2083 [pii]

Petersen SL, Peyton M, Minna JD, Wang X (2010) Overcoming cancer cell resistance to Smac mimetic induced apoptosis by modulating cIAP-2 expression. **107**: 11936-11941

Petersen SL, Wang L, Yalcin-Chin A, Li L, Peyton M, Minna J, Harran P, Wang X (2007) Autocrine TNFα Signaling Renders Human Cancer Cells Susceptible to Smac-Mimetic-Induced Apoptosis. *Cancer Cell* **12**: 445-456, doi:10.1016/j.ccr.2007.08.029

Ploner C, Kofler R, Villunger A (2008) Noxa: at the tip of the balance between life and death. *Oncogene* **27 Suppl 1**: S84-92, doi:10.1038/onc.2009.46; 10.1038/onc.2009.46

Probst BL, Liu L, Ramesh V, Li L, Sun H, Minna JD, Wang L (2010) Smac mimetics increase cancer cell response to chemotherapeutics in a TNF-alpha-dependent manner. *Cell Death Differ* **17**: 1645-1654, doi:10.1038/cdd.2010.44

Pylayeva-Gupta Y, Grabocka E, Bar-Sagi D (2011) RAS oncogenes: weaving a tumorigenic web. *Nat Rev Cancer* **11**: 761-774, doi:10.1038/nrc3106 [doi]

Raulf N, El-Attar R, Kulms D, Lecis D, Delia D, Walczak H, Papenfuss K, Odell E, Tavassoli M (2014) Differential response of head and neck cancer cell lines to TRAIL or Smac mimetics is associated with the cellular levels and activity of caspase-8 and caspase-10. *Br J Cancer* **111**: 1955-1964, doi:10.1038/bjc.2014.521 [doi]

Razani B, Zarnegar B, Ytterberg AJ, Shiba T, Dempsey PW, Ware CF, Loo JA, Cheng G (2010) Negative feedback in noncanonical NF-kappaB signaling modulates NIK stability through IKKalpha-mediated phosphorylation. *Sci Signal* **3**: ra41, doi:10.1126/scisignal.2000778

Reubold TF and Eschenburg S (2012) A molecular view on signal transduction by the apoptosome. *Cell Signal* **24**: 1420-1425, doi:10.1016/j.cellsig.2012.03.007 [doi]

Reymond N, d'Agua BB, Ridley AJ (2013) Crossing the endothelial barrier during metastasis. *Nat Rev Cancer* **13**: 858-870, doi:10.1038/nrc3628 [doi]

Riccioni R, Pasquini L, Mariani G, Saulle E, Rossini A, Diverio D, Pelosi E, Vitale A, Chierichini A, Cedrone M, Foa R, Lo Coco F, Peschle C, Testa U (2005) TRAIL decoy receptors mediate resistance of acute myeloid leukemia cells to TRAIL. *Haematologica* **90**: 612-624

Riedl SJ and Shi Y (2004) Molecular mechanisms of caspase regulation during apoptosis. *Nat Rev Mol Cell Biol* **5**: 897-907, doi:nrm1496 [pii]

Riedl SJ, Renatus M, Schwarzenbacher R, Zhou Q, Sun C, Fesik SW, Liddington RC, Salvesen GS (2001) Structural Basis for the Inhibition of Caspase-3 by XIAP. *Cell* **104**: 791-800

Rosebeck S, Madden L, Jin X, Gu S, Apel IJ, Appert A, Hamoudi RA, Noels H, Sagaert X, Van Loo P, Baens M, Du MQ, Lucas PC, McAllister-Lucas LM (2011) Cleavage of NIK by the API2-MALT1 fusion oncoprotein leads to noncanonical NF-kappaB activation. *Science* **331**: 468-472, doi:10.1126/science.1198946

Rossini A, Giussani M, Giacomini A, Guarnotta C, Tagliabue E, Balsari A (2012) Surveillance of spontaneous breast cancer metastasis by TRAIL-expressing CD34(+) cells in a xenograft model. *Breast Cancer Res Treat* **136**: 457-467, doi:10.1007/s10549-012-2281-4 [doi]

Rothe M, Pan MG, Henzel WJ, Ayres TM, Goeddel DV (1995) The TNFR2-TRAF signaling complex contains two novel proteins related to baculoviral inhibitor of apoptosis proteins. *Cell* **83**: 1243-1252, doi:0092-8674(95)90149-3 [pii]

Roulston A, Muller WJ, Shore GC (2013) BIM, PUMA, and the achilles' heel of oncogene addiction. *Sci Signal* **6**: pe12, doi:10.1126/scisignal.2004113 [doi]

Saha RN, Liu X, Pahan K (2006) Up-regulation of BDNF in astrocytes by TNF-alpha: a case for the neuroprotective role of cytokine. *J Neuroimmune Pharmacol* **1**: 212-222, doi:10.1007/s11481-006-9020-8 [doi]

Sahai E and Marshall CJ (2003) Differing modes of tumour cell invasion have distinct

requirements for Rho/ROCK signalling and extracellular proteolysis. *Nat Cell Biol* **5**: 711-719, doi:10.1038/ncb1019 [doi]

Salzmann S, Lang I, Rosenthal A, Schafer V, Weisenberger D, Carmona Arana JA, Trebing J, Siegmund D, Neumann M, Wajant H (2013) TWEAK inhibits TRAF2-mediated CD40 signaling by destabilization of CD40 signaling complexes. *J Immunol* **191**: 2308-2318, doi:10.4049/jimmunol.1202899 [doi]

Scaffidi C, Fulda S, Srinivasan A, Friesen C, Li F, Tomaselli KJ, Debatin KM, Krammer PH, Peter ME (1998) Two CD95 (APO-1/Fas) signaling pathways. *EMBO J* **17**: 1675-1687, doi:10.1093/emboj/17.6.1675 [doi]

Schimmer AD, Welsh K, Pinilla C, Wang Z, Krajewska M, Bonneau MJ, Pedersen IM, Kitada S, Scott FL, Bailly-Maitre B, Glinsky G, Scudiero D, Sausville E, Salvesen G, Nefzi A, Ostresh JM, Houghten RA, Reed JC (2004) Small-molecule antagonists of apoptosis suppressor XIAP exhibit broad antitumor activity. *Cancer Cell* **5**: 25-35, doi:S1535610803003325 [pii]

Seneci P, Bianchi A, Battaglia C, Belvisi L, Bolognesi M, Caprini A, Cossu F, Franco ED, Matteo MD, Delia D, Drago C, Khaled A, Lecis D, Manzoni L, Marizzoni M, Mastrangelo E, Milani M, Motto I, Moroni E, Potenza D, Rizzo V, Servida F, Turlizzi E, Varrone M, Vasile F, Scolastico C (2009) Rational design, synthesis and characterization of potent, non-peptidic Smac mimics/XIAP inhibitors as proapoptotic agents for cancer therapy. *Bioorg Med Chem* **17**: 5834-5856, doi:10.1016/j.bmc.2009.07.009

Seneci P, Rizzi M, Ballabio L, Lecis D, Conti A, Carrara C, Licandro E (2014) SPION-Smac mimetic nano-conjugates: putative pro-apoptotic agents in oncology. *Bioorg Med Chem*

Lett **24**: 2374-2378, doi:10.1016/j.bmcl.2014.03.048 [doi]

Serrano M, Lin AW, McCurrach ME, Beach D, Lowe SW (1997) Oncogenic ras provokes premature cell senescence associated with accumulation of p53 and p16INK4a. *Cell* **88**: 593-602, doi:S0092-8674(00)81902-9 [pii]

Servida F, Lecis D, Scavullo C, Drago C, Seneci P, Carlo-Stella C, Manzoni L, Polli E, Lambertenghi Deliliers G, Delia D, Onida F (2010) Novel second mitochondria-derived activator of caspases (Smac) mimetic compounds sensitize human leukemic cell lines to conventional chemotherapeutic drug-induced and death receptor-mediated apoptosis. *Invest New Drugs*, doi:10.1007/s10637-010-9475-6

Shakhov AN, Collart MA, Vassalli P, Nedospasov SA, Jongeneel CV (1990) Kappa B-type enhancers are involved in lipopolysaccharide-mediated transcriptional activation of the tumor necrosis factor alpha gene in primary macrophages. *J Exp Med* **171**: 35-47

Sica A and Mantovani A (2012) Macrophage plasticity and polarization: in vivo veritas. *J Clin Invest* **122**: 787-795, doi:10.1172/JCI59643; 10.1172/JCI59643

Sica A, Schioppa T, Mantovani A, Allavena P (2006) Tumour-associated macrophages are a distinct M2 polarised population promoting tumour progression: potential targets of anti-cancer therapy. *Eur J Cancer* **42**: 717-727, doi:10.1016/j.ejca.2006.01.003

Sikic B, Eckhardt S, Gallant G, Burris H, Camidge D, Covelas A (2011) Safety, pharmocokinetics (PK), and pharmacodynamics (PD) of HGS1029, an inhibitor of apoptosis protein (IAP), in patients (Pts.) with advanced solid tumors: Results of a Phase I study.

Silke J, Kratina T, Chu D, Ekert PG, Day CL, Pakusch M, Huang DC, Vaux DL (2005) Determination of cell survival by RING-mediated regulation of inhibitor of apoptosis (IAP) protein abundance. *Proc Natl Acad Sci U S A* **102**: 16182-16187, doi:0502828102 [pii]

Sims GP, Rowe DC, Rietdijk ST, Herbst R, Coyle AJ (2010) HMGB1 and RAGE in inflammation and cancer. *Annu Rev Immunol* **28**: 367-388, doi:10.1146/annurev.immunol.021908.132603; 10.1146/annurev.immunol.021908.132603

Singh TR, Shankar S, Chen X, Asim M, Srivastava RK (2003) Synergistic interactions of chemotherapeutic drugs and tumor necrosis factor-related apoptosis-inducing ligand/Apo-2 ligand on apoptosis and on regression of breast carcinoma in vivo. *Cancer Res* **63**: 5390-5400

Sprick MR, Weigand MA, Rieser E, Rauch CT, Juo P, Blenis J, Krammer PH, Walczak H (2000) FADD/MORT1 and caspase-8 are recruited to TRAIL receptors 1 and 2 and are essential for apoptosis mediated by TRAIL receptor 2. *Immunity* **12**: 599-609, doi:S1074-7613(00)80211-3 [pii]

Srinivasula SM and Ashwell JD (2008) IAPs: what's in a name? *Mol Cell* **30**: 123-135, doi:10.1016/j.molcel.2008.03.008 [doi]

Srinivasula SM, Hegde R, Saleh A, Datta P, Shiozaki E, Chai J, Lee R, Robbins PD, Fernandes-Alnemri T, Shi Y, Alnemri ES (2001) A conserved XIAP-interaction motif in caspase-9 and Smac/DIABLO regulates caspase activity and apoptosis. *Nature* **410**: 112-116

Stadel D, Cristofanon S, Abhari BA, Deshayes K, Zobel K, Vucic D, Debatin KM, Fulda S (2011) Requirement of nuclear factor kappaB for Smac mimetic-mediated sensitization of pancreatic carcinoma cells for gemcitabine-induced apoptosis. *Neoplasia* **13**: 1162-1170

Steckel M, Molina-Arcas M, Weigelt B, Marani M, Warne PH, Kuznetsov H, Kelly G, Saunders B, Howell M, Downward J, Hancock DC (2012) Determination of synthetic lethal interactions in KRAS oncogene-dependent cancer cells reveals novel therapeutic targeting strategies. *Cell Res* **22**: 1227-1245, doi:10.1038/cr.2012.82 [doi]

Stehlik C, de Martin R, Kumabashiri I, Schmid JA, Binder BR, Lipp J (1998) Nuclear factor (NF)-kappaB-regulated X-chromosome-linked iap gene expression protects endothelial cells from tumor necrosis factor alpha-induced apoptosis. *J Exp Med* **188**: 211-216

Steinhart L, Belz K, Fulda S (2013) Smac mimetic and demethylating agents synergistically trigger cell death in acute myeloid leukemia cells and overcome apoptosis resistance by inducing necroptosis. *Cell Death Dis* **4**: e802, doi:10.1038/cddis.2013.320 [doi]

Sun H, Lu J, Liu L, Yang CY, Wang S (2014) Potent and selective small-molecule inhibitors of cIAP1/2 proteins reveal that the binding of Smac mimetics to XIAP BIR3 is not required for their effective induction of cell death in tumor cells. *ACS Chem Biol* **9**: 994-1002, doi:10.1021/cb400889a [doi]

Sun H, Nikolovska-Coleska Z, Lu J, Meagher JL, Yang CY, Qiu S, Tomita Y, Ueda Y, Jiang S, Krajewski K, Roller PP, Stuckey JA, Wang S (2007) Design, synthesis, and characterization of a potent, nonpeptide, cell-permeable, bivalent Smac mimetic that concurrently targets both the BIR2 and BIR3 domains in XIAP. *J Am Chem Soc* **129**: 15279-15294,

doi:10.1021/ja074725f

Sun H, Nikolovska-Coleska Z, Yang C, Xu L, Liu M, Tomita Y, Pan H, Yoshioka Y, Krajewski K, Roller PP, Wang S (2004) Structure-Based Design of Potent, Conformationally Constrained Smac Mimetics. *J Am Chem Soc* **126**: 16686-16687

Sun H, Nikolovska-Coleska Z, Lu J, Qiu S, Yang C, Gao W, Meagher J, Stuckey J, Wang S (2006) Design, Synthesis, and Evaluation of a Potent, Cell-Permeable, Conformationally Constrained Second Mitochondria Derived Activator of Caspase (Smac) Mimetic. *J Med Chem* **49**: 7916-7920

Suzuki Y, Nakabayashi Y, Takahashi R (2001) Ubiquitin-protein ligase activity of X-linked inhibitor of apoptosis protein promotes proteasomal degradation of caspase-3 and enhances its anti-apoptotic effect in Fas-induced cell death. *Proc Natl Acad Sci U S A* **98**: 8662-8667, doi:10.1073/pnas.161506698 [doi]

Tamm I, Kornblau SM, Segall H, Krajewski S, Welsh K, Kitada S, Scudiero DA, Tudor G, Qui YH, Monks A, Andreeff M, Reed JC (2000) Expression and prognostic significance of IAP-family genes in human cancers and myeloid leukemias. *Clin Cancer Res* **6**: 1796-1803

Tao S, Wang S, Moghaddam SJ, Ooi A, Chapman E, Wong PK, Zhang DD (2014) Oncogenic KRAS confers chemoresistance by upregulating NRF2. *Cancer Res*, doi:canres.1439.2014 [pii]

Taylor RC, Cullen SP, Martin SJ (2008) Apoptosis: controlled demolition at the cellular level. *Nat Rev Mol Cell Biol* **9**: 231-241, doi:nrm2312 [pii]

Tchoghandjian A, Jennewein C, Eckhardt I, Rajalingam K, Fulda S (2013) Identification of

non-canonical NF-kappaB signaling as a critical mediator of Smac mimetic-stimulated migration and invasion of glioblastoma cells. *Cell Death Dis* **4**: e564, doi:10.1038/cddis.2013.70; 10.1038/cddis.2013.70

Tekedereli I, Alpay SN, Akar U, Yuca E, Ayugo-Rodriguez C, Han HD, Sood AK, Lopez-Berestein G, Ozpolat B (2013) Therapeutic Silencing of Bcl-2 by Systemically Administered siRNA Nanotherapeutics Inhibits Tumor Growth by Autophagy and Apoptosis and Enhances the Efficacy of Chemotherapy in Orthotopic Xenograft Models of ER (-) and ER (+) Breast Cancer. *Mol Ther Nucleic Acids* **2**: e121, doi:10.1038/mtna.2013.45 [doi]

Tenev T, Bianchi K, Darding M, Broemer M, Langlais C, Wallberg F, Zachariou A, Lopez J, Macfarlane M, Cain K, Meier P (2011) The Ripoptosome, a Signaling Platform that Assembles in Response to Genotoxic Stress and Loss of IAPs. *Mol Cell* **43**: 432-448, doi:10.1016/j.molcel.2011.06.006

Thornburg NJ and Raab-Traub N (2007) Induction of epidermal growth factor receptor expression by Epstein-Barr virus latent membrane protein 1 C-terminal-activating region 1 is mediated by NF-kappaB p50 homodimer/Bcl-3 complexes. *J Virol* **81**: 12954-12961, doi:JVI.01601-07 [pii]

Tokunaga F, Nakagawa T, Nakahara M, Saeki Y, Taniguchi M, Sakata S, Tanaka K, Nakano H, Iwai K (2011) SHARPIN is a component of the NF-kappaB-activating linear ubiquitin chain assembly complex. *Nature* **471**: 633-636, doi:10.1038/nature09815; 10.1038/nature09815

Trauzold A, Siegmund D, Schniewind B, Sipos B, Egberts J, Zorenkov D, Emme D, Roder C, Kalthoff H, Wajant H (2006) TRAIL promotes metastasis of human pancreatic ductal

adenocarcinoma. *Oncogene* **25**: 7434-7439, doi:1209719 [pii]

Varfolomeev E, Goncharov T, Maecker H, Zobel K, Komuves LG, Deshayes K, Vucic D (2012) Cellular Inhibitors of Apoptosis Are Global Regulators of NF-kappaB and MAPK Activation by Members of the TNF Family of Receptors. *Sci Signal* **5**: ra22, doi:10.1126/scisignal.2001878

Varfolomeev E, Blankenship JW, Wayson SM, Fedorova AV, Kayagaki N, Garg P, Zobel K, Dynek JN, Elliott LO, Wallweber HJA, Flygare JA, Fairbrother WJ, Deshayes K, Dixit VM, Vucic D (2007) IAP Antagonists Induce Autoubiquitination of c-IAPs, NF-κB Activation, and TNFα-Dependent Apoptosis. *Cell* **131**: 669-681, doi:10.1016/j.cell.2007.10.030

Villarejo A, Cortes-Cabrera A, Molina-Ortiz P, Portillo F, Cano A (2014) Differential role of Snail1 and Snail2 zinc fingers in E-cadherin repression and epithelial to mesenchymal transition. *J Biol Chem* **289**: 930-941, doi:10.1074/jbc.M113.528026 [doi]

Vince JE, Wong WW, Gentle I, Lawlor KE, Allam R, O'Reilly L, Mason K, Gross O, Ma S, Guarda G, Anderton H, Castillo R, Hacker G, Silke J, Tschopp J (2012) Inhibitor of apoptosis proteins limit RIP3 kinase-dependent interleukin-1 activation. *Immunity* **36**: 215-227, doi:10.1016/j.immuni.2012.01.012

Vince JE, Wong WW, Khan N, Feltham R, Chau D, Ahmed AU, Benetatos CA, Chunduru SK, Condon SM, McKinlay M, Brink R, Leverkus M, Tergaonkar V, Schneider P, Callus BA, Koentgen F, Vaux DL, Silke J (2007) IAP Antagonists Target cIAP1 to Induce TNFα-Dependent Apoptosis. *Cell* **131**: 682-693, doi:10.1016/j.cell.2007.10.037

Vizioli MG, Santos J, Pilotti S, Mazzoni M, Anania MC, Miranda C, Pagliardini S, Pierotti

MA, Gil J, Greco A (2014) Oncogenic RAS-induced senescence in human primary thyrocytes: molecular effectors and inflammatory secretome involved. *Oncotarget* **5**: 8270-8283, doi:2013 [pii]

Vogler M, Walczak H, Stadel D, Haas TL, Genze F, Jovanovic M, Bhanot U, Hasel C, Moller P, Gschwend JE, Simmet T, Debatin K, Fulda S (2009) Small Molecule XIAP Inhibitors Enhance TRAIL-Induced Apoptosis and Antitumor Activity in Preclinical Models of Pancreatic Carcinoma. *Cancer Res* **69**: 2425-2434

Wagner L, Marschall V, Karl S, Cristofanon S, Zobel K, Deshayes K, Vucic D, Debatin KM, Fulda S (2012) Smac mimetic sensitizes glioblastoma cells to Temozolomide-induced apoptosis in a RIP1- and NF-kappaB-dependent manner. *Oncogene*, doi:10.1038/onc.2012.108; 10.1038/onc.2012.108

Wajant H, Pfizenmaier K, Scheurich P (2003) Tumor necrosis factor signaling. *Cell Death Differ* **10**: 45-65, doi:10.1038/sj.cdd.4401189 [doi]

Walczak H, Degli-Esposti MA, Johnson RS, Smolak PJ, Waugh JY, Boiani N, Timour MS, Gerhart MJ, Schooley KA, Smith CA, Goodwin RG, Rauch CT (1997) TRAIL-R2: a novel apoptosis-mediating receptor for TRAIL. *EMBO J* **16**: 5386-5397

Walczak H (2011) TNF and ubiquitin at the crossroads of gene activation, cell death, inflammation, and cancer. *Immunol Rev* **244**: 9-28, doi:10.1111/j.1600-065X.2011.01066.x [doi]

Walczak H, Miller RE, Ariail K, Gliniak B, Griffith TS, Kubin M, Chin W, Jones J, Woodward A, Le T, Smith C, Smolak P, Goodwin RG, Rauch CT, Schuh JCL, Lynch DH (1999)

Tumoricidal activity of tumor necrosis factor-related apoptosis-inducing ligand in vivo. *Nat Med* **5**: 157-163

Wang S (2008) The promise of cancer therapeutics targeting the TNF-related apoptosis-inducing ligand and TRAIL receptor pathway. *Oncogene* **27**: 6207-6215, doi:10.1038/onc.2008.298 [doi]

Watanabe N, Niitsu Y, Sone H, Neda H, Urushizaki I, Yamamoto A, Nagamuta M, Sugawara Y (1986) Therapeutic effect of endogenous tumor necrosis factor on ascites Meth A sarcoma. *J Immunopharmacol* **8**: 271-283

Weidle UH, Maisel D, Eick D (2011) Synthetic lethality-based targets for discovery of new cancer therapeutics. *Cancer Genomics Proteomics* **8**: 159-171, doi:8/4/159 [pii]

Wilson NS, Yang A, Yang B, Couto S, Stern H, Gogineni A, Pitti R, Marsters S, Weimer RM, Singh M, Ashkenazi A (2012) Proapoptotic activation of death receptor 5 on tumor endothelial cells disrupts the vasculature and reduces tumor growth. *Cancer Cell* **22**: 80-90, doi:10.1016/j.ccr.2012.05.014 [doi]

Wong RS (2011) Apoptosis in cancer: from pathogenesis to treatment. *J Exp Clin Cancer Res* **30**: 87-9966-30-87, doi:10.1186/1756-9966-30-87 [doi]

Wong WW, Vince JE, Lalaoui N, Lawlor KE, Chau D, Bankovacki A, Anderton H, Metcalf D, O'Reilly L, Jost PJ, Murphy JM, Alexander WS, Strasser A, Vaux DL, Silke J (2014) cIAPs and XIAP regulate myelopoiesis through cytokine production in a RIPK1 and RIPK3 dependent manner. *Blood* **123**: 2562-2572, doi:10.1182/blood-2013-06-510743

Wood LD, Parsons DW, Jones S, Lin J, Sjoblom T, Leary RJ, Shen D, Boca SM, Barber T, Ptak

J, Silliman N, Szabo S, Dezso Z, Ustyanksky V, Nikolskaya T, Nikolsky Y, Karchin R, Wilson PA, Kaminker JS, Zhang Z, Croshaw R, Willis J, Dawson D, Shipitsin M, Willson JK, Sukumar S, Polyak K, Park BH, Pethiyagoda CL, Pant PV, Ballinger DG, Sparks AB, Hartigan J, Smith DR, Suh E, Papadopoulos N, Buckhaults P, Markowitz SD, Parmigiani G, Kinzler KW, Velculescu VE, Vogelstein B (2007) The genomic landscapes of human breast and colorectal cancers. *Science* **318**: 1108-1113, doi:1145720 [pii]

Wu G, Chai J, Suber TL, Wu J, Du C, Wang X, Shi Y (2000) Structural basis of IAP recognition by Smac/DIABLO. *Nature* **408**: 1008-1012

Wu YT, Tan HL, Huang Q, Sun XJ, Zhu X, Shen HM (2011) zVAD-induced necroptosis in L929 cells depends on autocrine production of TNFalpha mediated by the PKC-MAPKs-AP-1 pathway. *Cell Death Differ* **18**: 26-37, doi:10.1038/cdd.2010.72 [doi]

Xiao C, Yang BF, Asadi N, Beguinot F, Hao C (2002) Tumor necrosis factor-related apoptosis-inducing ligand-induced death-inducing signaling complex and its modulation by c-FLIP and PED/PEA-15 in glioma cells. *J Biol Chem* **277**: 25020-25025, doi:10.1074/jbc.M202946200 [doi]

Xu Y, Fang F, Dhar SK, St Clair WH, Kasarskis EJ, St Clair DK (2007) The role of a single-stranded nucleotide loop in transcriptional regulation of the human sod2 gene. *J Biol Chem* **282**: 15981-15994, doi:M608979200 [pii]

Yang A, Wilson NS, Ashkenazi A (2010) Proapoptotic DR4 and DR5 signaling in cancer cells: toward clinical translation. *Curr Opin Cell Biol* **22**: 837-844, doi:10.1016/j.ceb.2010.08.001; 10.1016/j.ceb.2010.08.001

Yang L, Mashima T, Sato S, Mochizuki M, Sakamoto H, Yamori T, Oh-Hara T, Tsuruo T (2003) Predominant suppression of apoptosome by inhibitor of apoptosis protein in non-small cell lung cancer H460 cells: therapeutic effect of a novel polyarginine-conjugated Smac peptide. *Cancer Res* **63**: 831-837

Yang QH and Du C (2004) Smac/DIABLO selectively reduces the levels of c-IAP1 and c-IAP2 but not that of XIAP and livin in HeLa cells. *J Biol Chem* **279**: 16963-16970, doi:10.1074/jbc.M401253200 [doi]

Yang XH, Feng ZE, Yan M, Hanada S, Zuo H, Yang CZ, Han ZG, Guo W, Chen WT, Zhang P (2012) XIAP is a predictor of cisplatin-based chemotherapy response and prognosis for patients with advanced head and neck cancer. *PLoS One* **7**: e31601, doi:10.1371/journal.pone.0031601; 10.1371/journal.pone.0031601

Yarom N and Jonker DJ (2011) The role of the epidermal growth factor receptor in the mechanism and treatment of colorectal cancer. *Discov Med* **11**: 95-105

Yawata A, Adachi M, Okuda H, Naishiro Y, Takamura T, Hareyama M, Takayama S, Reed JC, Imai K (1998) Prolonged cell survival enhances peritoneal dissemination of gastric cancer cells. *Oncogene* **16**: 2681-2686, doi:10.1038/sj.onc.1201792 [doi]

Yersal O and Barutca S (2014) Biological subtypes of breast cancer: Prognostic and therapeutic implications. *World J Clin Oncol* **5**: 412-424, doi:10.5306/wjco.v5.i3.412 [doi]

You M, Ku PT, Hrdlickova R, Bose HR,Jr (1997) ch-IAP1, a member of the inhibitor-of-apoptosis protein family, is a mediator of the antiapoptotic activity of the v-Rel oncoprotein. *Mol Cell Biol* **17**: 7328-7341

Zarnegar BJ, Wang Y, Mahoney DJ, Dempsey PW, Cheung HH, He J, Shiba T, Yang X, Yeh WC, Mak TW, Korneluk RG, Cheng G (2008) Noncanonical NF-kappaB activation requires coordinated assembly of a regulatory complex of the adaptors cIAP1, cIAP2, TRAF2 and TRAF3 and the kinase NIK. *Nat Immunol* **9**: 1371-1378, doi:10.1038/ni.1676

Zeng C, Vangveravong S, McDunn JE, Hawkins WG, Mach RH (2013) Sigma-2 receptor ligand as a novel method for delivering a SMAC mimetic drug for treating ovarian cancer. *Br J Cancer* **109**: 2368-2377, doi:10.1038/bjc.2013.593 [doi]

Zou H, Henzel WJ, Liu X, Lutschg A, Wang X (1997) Apaf-1, a human protein homologous to C. elegans CED-4, participates in cytochrome c-dependent activation of caspase-3. *Cell* **90**: 405-413, doi:S0092-8674(00)80501-2 [pii]